EBC

Energy in Buildings and Communities Programme

International Energy Agency

Experimental facilities and methods for assessing energy flexibility in buildings

Energy in Buildings and Communities Programme

Annex 67 Energy Flexible Buildings

June 2019

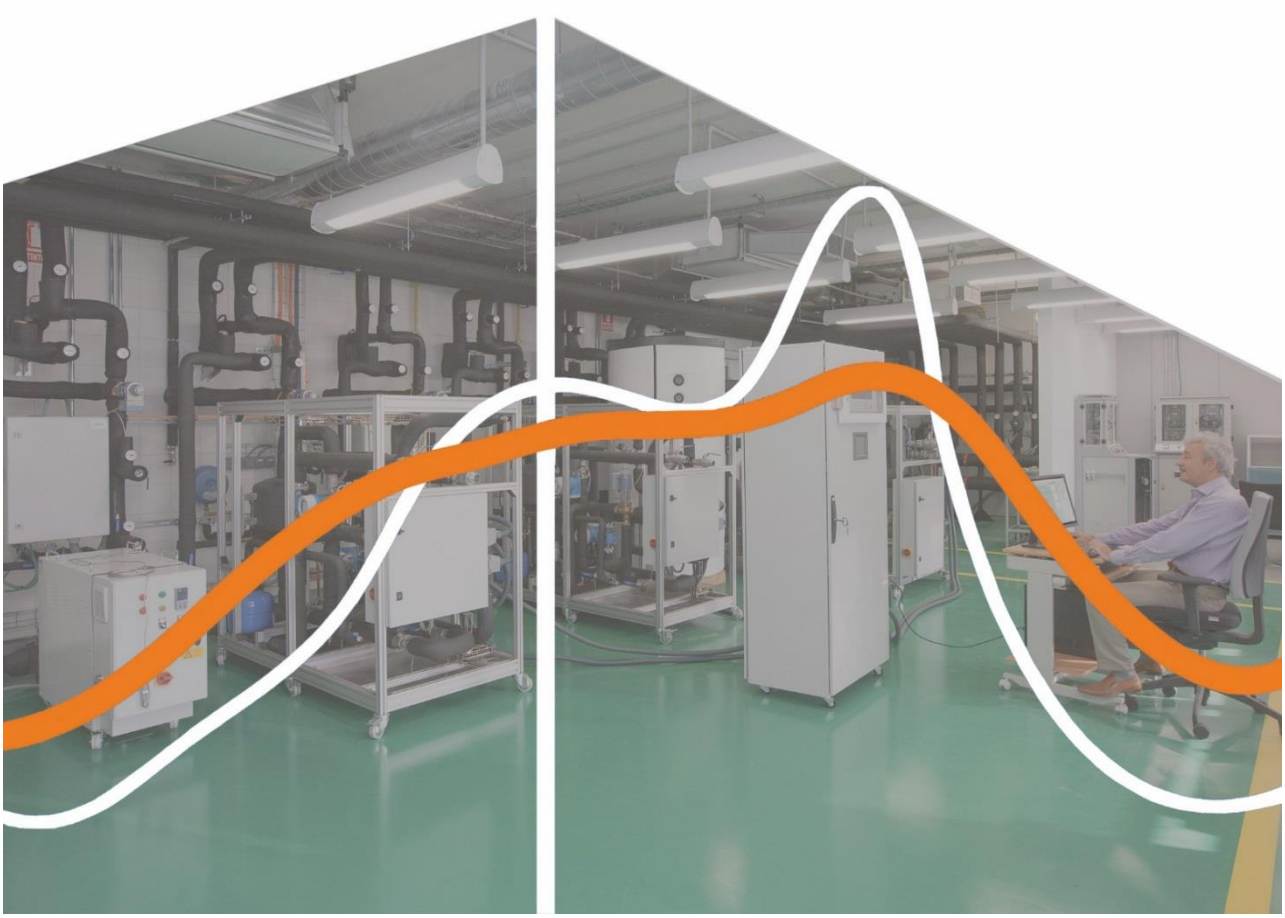

EBC
Energy in Buildings and Communities Programme

International Energy Agency

Experimental facilities and methods for assessing energy flexibility in buildings

Energy in Buildings and Communities Programme

Annex 67 Energy Flexible Buildings

June 2019

Editors

Catalonia Institute for Energy Research, IREC
Jaume Salom, jsalom@irec.cat
Thibault Péan, tpean@irec.cat

Authors

NTNU — Francesco Goia, francesco.goia@ntnu.no
Aalto University — Kilpeläinen Simo, simo.kilpelainen@aalto.fi
Danish Technological Institute — Søren Østergaard Jensen, sdj@teknologisk.dk
VTT — Ala Hasan, ala.hasan@vtt.fi
Polytechnique Montréal — Michaël Kummert, michael.kummert@polymtl.ca
University of Applied Sciences and Arts Northwestern Switzerland FHNW — Manuel Koch, manuel.koch@fhnw.ch; Monika Hall, monika.hall@fhnw.ch; Achim Geissler, achim.geissler@fhnw.ch

iea Energy Technology Network

Published by Danish Technological Institute, Denmark

ISBN: 978-87-93250-07-9
ISSN: 1600-3780

Participating countries in EBC:

Australia, Austria, Belgium, Canada, P.R. China, Czech Republic, Denmark, Finland, France, Germany, Greece, Ireland, Italy, Japan, Republic of Korea, the Netherlands, New Zealand, Norway, Poland, Portugal, Singapore, Spain, Sweden, Switzerland, Turkey, United Kingdom and the United States of America.

Additional copies of this report may be obtained from:
www.iea-ebc.org
essu@iea-ebc.org

Preface

The International Energy Agency

The International Energy Agency (IEA) was established in 1974 within the framework of the Organisation for Economic Co-operation and Development (OECD) to implement an international energy programme. A basic aim of the IEA is to foster international co-operation among the 28 IEA participating countries and to increase energy security through energy research, development and demonstration in the fields of technologies for energy efficiency and renewable energy sources.

The IEA Energy in Buildings and Communities Programme

The IEA co-ordinates research and development in a number of areas related to energy. The mission of the Energy in Buildings and Communities (EBC) Programme is to develop and facilitate the integration of technologies and processes for energy efficiency and conservation into healthy, low emission, and sustainable buildings and communities, through innovation and research. (Until March 2013, the IEA-EBC Programme was known as the Energy in Buildings and Community Systems Programme, ECBCS.)

The research and development strategies of the IEA-EBC Programme are derived from research drivers, national programmes within IEA countries, and the IEA Future Buildings Forum Think Tank Workshops. The research and development (R&D) strategies of IEA-EBC aim to exploit technological opportunities to save energy in the buildings sector, and to remove technical obstacles to market penetration of new energy efficient technologies. The R&D strategies apply to residential, commercial, office buildings and community systems, and will impact the building industry in five focus areas for R&D activities:

- Integrated planning and building design
- Building energy systems
- Building envelope
- Community scale methods
- Real building energy use

The Executive Committee

Overall control of the IEA-EBC Programme is maintained by an Executive Committee, which not only monitors existing projects, but also identifies new strategic areas in which collaborative efforts may be beneficial. As the Programme is based on a contract with the IEA, the projects are legally established as Annexes to the IEA-EBC Implementing Agreement. At the present time, the following projects have been initiated by the IEA-EBC Executive Committee, with completed projects identified by (*) and joint projects with the IEA Solar Heating and Cooling Technology Collaboration Programme by (☼):

Annex 1: Load Energy Determination of Buildings (*)
Annex 2: Ekistics and Advanced Community Energy Systems (*)
Annex 3: Energy Conservation in Residential Buildings (*)
Annex 4: Glasgow Commercial Building Monitoring (*)
Annex 5: Air Infiltration and Ventilation Centre
Annex 6: Energy Systems and Design of Communities (*)
Annex 7: Local Government Energy Planning (*)
Annex 8: Inhabitants Behaviour with Regard to Ventilation (*)
Annex 9: Minimum Ventilation Rates (*)
Annex 10: Building HVAC System Simulation (*)
Annex 11: Energy Auditing (*)
Annex 12: Windows and Fenestration (*)
Annex 13: Energy Management in Hospitals (*)
Annex 14: Condensation and Energy (*)

Annex 15: Energy Efficiency in Schools (*)
Annex 16: BEMS 1- User Interfaces and System Integration (*)
Annex 17: BEMS 2- Evaluation and Emulation Techniques (*)
Annex 18: Demand Controlled Ventilation Systems (*)
Annex 19: Low Slope Roof Systems (*)
Annex 20: Air Flow Patterns within Buildings (*)
Annex 21: Thermal Modelling (*)
Annex 22: Energy Efficient Communities (*)
Annex 23: Multi Zone Air Flow Modelling (COMIS) (*)
Annex 24: Heat, Air and Moisture Transfer in Envelopes (*)
Annex 25: Real time HVAC Simulation (*)
Annex 26: Energy Efficient Ventilation of Large Enclosures (*)
Annex 27: Evaluation and Demonstration of Domestic Ventilation Systems (*)
Annex 28: Low Energy Cooling Systems (*)
Annex 29: Daylight in Buildings (*)
Annex 30: Bringing Simulation to Application (*)
Annex 31: Energy-Related Environmental Impact of Buildings (*)
Annex 32: Integral Building Envelope Performance Assessment (*)
Annex 33: Advanced Local Energy Planning (*)
Annex 34: Computer-Aided Evaluation of HVAC System Performance (*)
Annex 35: Design of Energy Efficient Hybrid Ventilation (HYBVENT) (*)
Annex 36: Retrofitting of Educational Buildings (*)
Annex 37: Low Exergy Systems for Heating and Cooling of Buildings (LowEx) (*)
Annex 38: ☼ Solar Sustainable Housing (*)
Annex 39: High Performance Insulation Systems (*)
Annex 40: Building Commissioning to Improve Energy Performance (*)
Annex 41: Whole Building Heat, Air and Moisture Response (MOIST-ENG) (*)
Annex 42: The Simulation of Building-Integrated Fuel Cell and Other Cogeneration Systems (FC+COGEN-SIM) (*)
Annex 43: ☼ Testing and Validation of Building Energy Simulation Tools (*)
Annex 44: Integrating Environmentally Responsive Elements in Buildings (*)
Annex 45: Energy Efficient Electric Lighting for Buildings (*)
Annex 46: Holistic Assessment Tool-kit on Energy Efficient Retrofit Measures for Government Buildings (EnERGo) (*)
Annex 47: Cost-Effective Commissioning for Existing and Low Energy Buildings (*)
Annex 48: Heat Pumping and Reversible Air Conditioning (*)
Annex 49: Low Exergy Systems for High Performance Buildings and Communities (*)
Annex 50: Prefabricated Systems for Low Energy Renovation of Residential Buildings (*)
Annex 51: Energy Efficient Communities (*)
Annex 52: ☼ Towards Net Zero Energy Solar Buildings
Annex 53: Total Energy Use in Buildings: Analysis & Evaluation Methods (*)
Annex 54: Integration of Micro-Generation & Related Energy Technologies in Buildings
Annex 55: Reliability of Energy Efficient Building Retrofitting - Probability Assessment of Performance & Cost (RAP-RETRO) (*)
Annex 56: Cost Effective Energy & CO_2 Emissions Optimization in Building Renovation (*)
Annex 57: Evaluation of Embodied Energy & CO_2 Emissions for Building Construction (*)
Annex 58: Reliable Building Energy Performance Characterisation Based on Full Scale Dynamic Measurements (*)
Annex 59: High Temperature Cooling & Low Temperature Heating in Buildings (*)
Annex 60: New Generation Computational Tools for Building & Community Energy Systems (*)
Annex 61: Business and Technical Concepts for Deep Energy Retrofit of Public Buildings (*)
Annex 62: Ventilative Cooling (*)
Annex 63: Implementation of Energy Strategies in Communities (*)
Annex 64: LowEx Communities - Optimised Performance of Energy Supply Systems with Energy Principles (*)
Annex 65: Long-Term Performance of Super-Insulation in Building Components and Systems (*)
Annex 66: Definition and Simulation of Occupant Behaviour in Buildings
Annex 67: Energy Flexible Buildings

Annex 68: Indoor Air Quality Design and Control in Low Energy Residential Buildings
Annex 69: Strategy and Practice of Adaptive Thermal Comfort in Low Energy Buildings
Annex 70: Building Energy Epidemiology: Analysis of Real Building Energy Use at Scale Annex 71: Building Energy Performance Assessment Based on In-situ Measurements
Annex 72: Assessing Life Cycle Related Environmental Impacts Caused by Buildings
Annex 73: Towards Net Zero Energy Public Communities
Annex 74: Energy Endeavour
Annex 75: Cost-effective Strategies to Combine Energy Efficiency Measures and Renewable Energy Use in Building Renovation at District Level
Annex 76: ☼ Deep Renovation of Historic Buildings towards Lowest Possible Energy Demand and CO_2 Emissions
Annex 77: ☼ Integrated Solutions for Daylight and Electric Lighting
Annex 78: Supplementing Ventilation with Gas-phase Air Cleaning, Implementation and Energy Implications
Annex 79: Occupant-Centric Building Design and Operation
Annex 80: Resilient Cooling
Annex 81: Data-Driven Smart Buildings

Working Group - Energy Efficiency in Educational Buildings (*)
Working Group - Indicators of Energy Efficiency in Cold Climate Buildings (*)
Working Group - Annex 36 Extension: The Energy Concept Adviser (*)
Working Group - HVAC Energy Calculation Methodologies for Non-residential Buildings
Working Group - Cities and Communities
Working Group - Building Energy Codes
Working Group - International Building Materials Database

Management summary

The energy flexibility of a building is defined as the ability to manage its demand and generation according to local climate conditions, user needs, and energy network requirements. energy flexibility of buildings will thus allow for demand side management/load control and thereby demand response based on the requirements of the surrounding energy networks.

This report constitutes one of the main outputs of the IEA EBC Annex 67 which aims to increase the knowledge, identify critical aspects and possible solutions concerning the energy flexibility that buildings can provide, plus the means to exploit and control this flexibility. One of the means to increase this knowledge is testing devices and control systems, which can potentially activate energy flexibility in buildings, in controlled environments as laboratories. Experimental tests in laboratories complements research works based on simulation and field tests in buildings.

The report describes six facilities around the world (Switzerland, Canada, Norway, Denmark, Finland and Spain) specially conceived to test control strategies and the combination of components under controllable, yet realistic, conditions. Five out of the six laboratories uses the hardware-in-the-loop concept as the other one is a Living Lab being a zero energy house. Beyond the description of the architecture and main features of the laboratories, the report describes and show results of performed experiments on energy flexibility in buildings. The below table depicts which are the objectives of the experiments performed in each lab, as well of the location of the facilities.

Table 1 Objectives of experiments on energy flexibility in buildings and laboratories where they have been performed.

Lab	Location	Main objective
IREC	Tarragona, Spain	Test MPC strategies to minimize energy costs or CO_2 emissions
Aalto	Espoo, Finland	Test EMS to minimize energy costs in a NZEB
DTI	Taastrup, Denmark	Quantification of energy flexibility and validation of simulation tool
NTNU/SINTEF	Trondheim, Norway	Parameter identification of a building control oriented model
FHNW	Muttenz, Switzerland	Test EMS to increase PV self-consumption
POLYMTL	Montréal, Canada	Quantification of energy flexibility

These laboratory tests are complex and need a lot of effort and know-how to be performed. Lessons learnt after performing energy flexibility experiments are reported by researchers in charge. From this know-how, some best practices and recommendations for future testing have been summarized for the ones interested to perform experiments on energy flexibility in buildings. Quite a few common points exist as the laboratories have a common approach and the performed tests have strong similarities. Recommendations cover the different phases from the planning and

the preparation of the experiments to the tasks when experiments have finalised, as well of a set of best practices for running this kind of facilities. They were designed as flexible facilities to test new components and their integration and management involving electrical and thermal systems. Their potential comes hand in hand with a large complexity due to the hardware and software elements that need to be in place. So, practical advices when designing or maintaining this kind of test facilities should be useful for readers of the report.

Table of content

Abbreviations

Abbreviations	Meaning
AC	Alternate Current
ANN	Artificial Neural Network
BMS	Building Management System
CHP	Combined Heat and Power
COP	Coefficient Of Performance
DC	Direct Current
DER	Distributed Energy Resources
DHW	Domestic Hot Water
DLC	Direct Load Control
DR	Demand Response
EMS	Energy Management System
EN	European Normative
FCU	Fan Coil Unit
FMU	Functional Mock-up Unit
GFR	Grid Frequency Regulation
GSHP	Ground Source Heat Pump
HiL	Hardware in the Loop
HVAC	Heating, Ventilation and Air Conditioning
IEA-EBC	Energy in Buildings and Communities Programme of the International Energy Agency
MPC	Model Predictive Controller
NZEB	Net Zero Energy Buildings
nZEB	nearly Zero Energy Buildings
OEF	Onsite Energy Fraction
OEM	Onsite Energy Matching
PCM	Phase Change Material
PRBS	Pseudo Random Binary Signal
PV	Photovoltaics
RES	Renewable Energy Sources
RH	Relative Humidity
SC	Space Cooling
SEILAB	Semi-Virtual Energy Integration Laboratory
SH	Space Heating
SLP	Successive Linear Programming
SPF	Seasonal Performance Factor
VSHP	Variable Speed Heat Pump
ZEB	Zero Energy Building

1. Introduction to Annex 67

Substantial and unprecedented reductions in carbon emissions are required if the worst effects of climate change are to be avoided. A major paradigmatic shift is, therefore, needed in the way heat and electricity are generated and consumed in general, and in the case of buildings and communities in particular. The reduction in carbon emissions can be achieved by firstly: reducing the energy demand as a result of energy efficiency improvements and secondly: covering the remaining energy demand by renewable energy sources. Applying flexibility to the energy consumption is just as important as energy efficiency improvements. Energy flexibility is necessary due to the large-scale integration of central as well as decentralized energy conversion systems based on renewable primary energy resources, which is a key component of the national and international roadmaps to a transition towards sustainable energy systems where the reduction of fuel poverty and CO_2-equivalent emissions are top priorities.

In many countries, the share of renewable energy sources (RES) is increasing parallel with an extensive electrification of demands, where the replacement of traditional cars with electrical vehicles or the displacement of fossil fuel heating systems, such as gas or oil boilers, with energy efficient heat pumps, are common examples. These changes, on both the demand and supply sides, impose new challenges to the management of energy systems, such as the variability and limited control of energy supply from renewables or the increasing load variations over the day. The electrification of the energy systems also threatens to exceed already strained limits in peak demand.

A paradigm shift is, thus, required away from existing systems, where energy supply always follows demand, to a system where the demand side considers available supply. Taking this into consideration, flexible energy systems should play an important part in the holistic solution. Flexible energy systems overcome the traditional centralized production, transport and distribution-oriented approach, by integrating decentralized storage and demand response into the energy market. In this context, strategies to ensure the security and reliability of energy supply involve simultaneous coordination of distributed energy resources (DERs), energy storage and flexible schedulable loads connected to smart distribution networks (electrical as well as thermal grids).

Looking further into the future, the ambition towards net zero energy buildings (NZEB) imposes new challenges as buildings not only consume, but also generate heat and power locally. Such buildings are commonly called prosumers, which are able to share excess power and heat with other consumers in the nearby energy networks. Consequently, the energy networks must consider the demand of both heat and electricity as well as the local energy generation. If not, it may result in limitations of the amount of exported energy for building owners to avoid power quality problems; for example, Germany has already enforced restrictions on private PV generation exported to the grid. Furthermore, today the distribution grid is often sized based on

buildings that are heated by sources other than electricity. However, the transition to a renewable energy system will, in many areas, lead to an increase in electrical heating, by heat pumps for example, which will lead to an increase in the electricity demand even if the foreseen reduction in the space heating demand via energy renovation is realized. The expected penetration of electrical vehicles will increase the loads in the distribution grids, but they may also be used for load shifting by using their batteries; they could in effect become mobile storage systems. All these factors will, in most distribution grids, call for major reinforcement of the existing grids or for a more intelligent way of consuming electricity in order to avoid congestion problems. The latter approach is holistically referred to as a 'Smart Grid' (or as a Smart Energy Network, when energy carriers other than electricity are considered as well) where both demand and local production are controlled to stabilize the energy networks and thereby lead to a better exploitation of the available renewable energy sources towards a decarbonisation of the building stock. Buildings are, therefore, expected to have a pivotal role in the development of future Smart Grids/Energy networks, by providing energy flexibility services.

As buildings account for approximately 40 % of the annual energy use worldwide, they will need to play a significant role in providing a safe and efficient operation of the future energy system. They have the potential to offer significant flexibility services to the energy systems by intelligent control of their thermal and electric energy loads. More specifically, a large part of the buildings' energy demand may be shifted in time and may thus significantly contribute to increasing flexibility of the demand in the energy system. In particular, the thermal part of the energy demand, e.g. space heating/cooling, ventilation, domestic hot water, but also hot water for washing machines, dishwashers and heat to tumble dryers, can be shifted. Additionally, the demand from other devices like electrical vehicles or pool pumps, can also be controlled to provide energy flexibility.

All buildings have thermal mass embedded in their construction elements, which makes it possible to store a certain amount of heat and thereby postpone heating or cooling from periods with low RES in the networks to periods with excess RES in the networks without jeopardizing the thermal comfort. The amount of thermal storage available and how quickly it can be charged and discharged affect how this thermal storage can be used to offer flexibility. Additionally, many buildings may also contain different kinds of discrete storage (e.g. water tanks and storage heaters) that can potentially contribute to the energy flexibility of the buildings. A simple example of a discrete storage system is the domestic hot water tank, which can be pre-heated before a fall in available power. From these examples, it is evident that the type and amount of flexibility that can be offered will vary among buildings. A key challenge is, therefore, to establish a uniform framework that describes how flexibility can be offered in terms of quantity and quality.

Storage (thermal or electrical) is often necessary in order to obtain energy flexibility. However, storage has "roundtrip" conversion energy losses, which may lead to a decrease in the energy efficiency in the single building. But as energy flexibility ensures a higher utilization of the installed RES, the efficiency of the overall energy system will increase. A decrease in efficiency will mainly be seen in well-controlled buildings, however, most buildings are not well-controlled. In the latter

case, the introduction of energy flexibility may typically lead to a more optimal control of the buildings and in this way simultaneously increase the energy efficiency of the buildings.

Various investigations of buildings in the Smart Grid context have been carried out to date. However, research on how energy flexibility in buildings can actively participate the future energy system and local energy communities, and thereby facilitate large penetration of renewable energy sources and the increasing electrification of demand, is still in its early stages. The investigations have either focused on how to control a single component - often simple on/off controlled - or have focused on simulations for defining indicators for energy flexibility, rather than on how to optimize the energy flexibility of the buildings themselves.

The concept of flexible loads, demand side management and peak shaving is of course not new, as demand response already in the 1970s was utilized in some power grids. Although the concept is not new, before now there was no overview or insight into how much energy flexibility different types of building and their usage may be able to offer to the future energy systems. This was the main, although not sole, reason why IEA EBC Annex 67 Energy Flexible Buildings was initiated.

1.1. IEA EBC Annex 67

The aim of IEA EBC Annex 67 was to increase the knowledge, identify critical aspects and possible solutions concerning the energy flexibility that buildings can provide, plus the means to exploit and control this flexibility. In addition to these technical aims, Annex 67 also sought to understand all stakeholder perspectives - from users to utilities - on energy flexibility, as these are a potential barrier to success. This knowledge is crucial for ensuring that the energy flexibility of buildings is incorporated into future Smart Energy systems, and thereby facilitating the transition towards a fossil free energy system. The obtained knowledge is also important when developing business cases that will utilize building energy flexibility in future energy systems – considering that utilization of energy flexibility in buildings may reduce costly upgrades of distribution grids.

The work of IEA EBC Annex 67 was divided into three main areas:

- terminology and characterization of energy flexibility in buildings
- determination of the available energy flexibility of devices, buildings and clusters of buildings
- demonstration of and stakeholder's perspective on energy flexible buildings

1.1.1. Terminology for and characterization of Energy Flexibility in buildings

A common terminology is important in order to communicate a building's or a cluster of buildings' ability to provide energy flexible services to the grid. The available energy flexibility is often defined by a set of generally static Key Performance Indicators. However, the useful energy

flexibility will be influenced by internal factors such as the form or function of a building, and external factors, such as local climatic conditions and the composition and capacity of the local energy grids. There is, therefore, a need for a dynamic approach in order to understand the services a building can provide to a specific energy grid. A methodology for such a dynamic approach has been developed during the course of IEA EBC Annex 67.

The findings in the area of terminology and characterization of energy flexibility in buildings are reported in the deliverable “Characterization of energy flexibility in Buildings” mentioned below.

1.1.2. Determination of the available Energy Flexibility of devices, buildings and clusters of buildings

Simulation is a powerful tool when investigating the possible energy flexibility in buildings. In IEA EBC Annex 67, different simulation tools have been applied on different building types and Common Exercises have been carried out on well-defined case studies. This approach increased the common understanding of energy flexibility in buildings and was useful for the development of a common terminology.

Simulations are very effective to quickly test different control strategies, among which some may be more realistic than others. Control strategies and the combination of components were, therefore, also tested in test facilities under controllable, yet realistic, conditions. Hardware-in-the-loop concepts were utilized at several test facilities, where, for example, a heat pump and other components were tested combined with the energy demand of virtual buildings and exposed to virtual weather and grid conditions.

The results of the investigations are described in several of the below mentioned publications by IEA EBC Annex 67.

1.1.3. Demonstration of and stakeholders perspective on Energy Flexible Buildings

In order to be able to convince policy makers, energy utilities and grid operators, aggregators, the building industry and consumers about the benefits of buildings offering energy flexibility to the future energy systems, proof of concept based on demonstrations in real buildings is crucial. Example cases of obtaining energy flexibility in real buildings have, therefore, been investigated and reported in reports, articles and papers and as examples in the deliverables of IEA EBC Annex 67.

When utilizing the energy flexibility in buildings, the comfort, economy and normal operations of the buildings can be influenced. If the owner, facility manager and/or users of a building are not interested in in exploiting energy flexibility to increase building smartness, it does not matter how energy flexible the building is, as the building will not be an asset for the local energy

infrastructure. However, the involvement of utilities, regulators and other stakeholders, for example, building automation providers, can provide incentives and increase awareness of and thereby participation in providing energy flexibility. It is, therefore, very important to understand which barriers exist for the stakeholders involved in the energy flexible buildings and how they may be motivated to contribute with energy flexibility in buildings to stabilize the future energy grids. Investigating the barriers and benefits for stakeholders is, therefore, of paramount importance and work was completed in IEA EBC Annex 67 to understand these in more detail. Findings from this work are described in the report "Stakeholder perspectives on energy flexible buildings" mentioned below.

1.1.4. Deliverables from IEA EBC Annex 67

Many reports, articles and conference papers have been published by IEA EBC Annex 67 participants. These can be found on annex67.org/Publications/Deliverables.

The main publications by IEA EBC Annex 67 are, however, the following reports, which all may be found on annex67.org/Publications/Deliverables.

Principles of Energy Flexible Buildings summarizes the main findings of Annex 67 and targets all interested in what energy flexibility in buildings is, how it can be controlled, and which services it may provide.

Characterization of Energy Flexibility in Buildings presents the terminology around energy flexibility, the indicators used to evaluate the flexibility potential and how to characterize and label energy flexibility.

Stakeholder' perspectives on Energy Flexible buildings displays the view point of different types of stakeholders towards energy flexible Buildings.

Control strategies and algorithms for obtaining Energy Flexibility in buildings reviews and gives examples on control strategies for energy flexibility in buildings.

Experimental facilities and methods for assessing Energy Flexibility in buildings describes several test facilities including experiments related to energy flexibility and draws recommendations for future testing activities.

Examples of Energy Flexibility in buildings summarizes different examples on how to obtain energy flexible buildings.

Project Summary Report brief summary of the outcome of Annex 67.

2. About test facilities to assess energy flexibility in buildings

This report constitutes one of the main outputs of the IEA EBC Annex 67 which aims to increase the knowledge, identify critical aspects and possible solutions concerning the energy flexibility that buildings can provide, plus the means to exploit and control this flexibility. In the framework of IEA EBC Annex 67, the determination of the available energy flexibility of devices and buildings is done mainly by means of simulation studies. Beside works based on simulation, one of the means to increase this knowledge is testing devices and control systems in controlled environments as laboratories. Experimental tests in laboratories complements research works based on simulation and field tests in buildings. Some partners of the Annex 67 have been testing components and/or advanced control strategies experimentally with the hardware-in-the-loop (HiL) concept. Test and demonstration in real buildings is preferable when evaluation new concepts like energy flexibility in buildings, however, there are many non-controllable variables in a real building, which makes it difficult to draw reliable, significant conclusions - unless the concept is demonstrated in several buildings. Moreover, test and demonstration in real buildings is time consuming and very expensive. Simulation is on the other hand cheap and fast, so that parametric studies can easily be performed. However, since all inputs and the environment are often specified in a very simple way, this may lead to conclusions that are not likely in real life. Many components are exposed to certified tests in order to prove their performance. These tests in laboratories give insight into important parameters of the components, which are necessary input for simulations. However, the tests do not answer the question of how the component will perform in a building under realistic use, as the components are tested under standardized steady-state conditions, which often do not resemble the dynamic conditions that the components will be exposed to in real environments. Hardware-in-the-loop (HiL) test facilities, where parts of a system are physical components while others are virtual, establishes a bridge between the three approaches described above. Systems and energy flexibility strategies are usually developed through simulations, so there is a need for validation through tests under dynamic, real (or as close as possible to real) operating conditions. HiL represents, therefore, a necessary tool where researchers and industry can test, under controlled conditions, the performance of new systems before they are implemented in real buildings and/or field tests. Compared to field testing, dynamic tests in a controlled laboratory environment with a semi-virtual approach offer the flexibility of imposing well-controlled and repeatable boundary conditions on the equipment, without waiting for given conditions to occur in the real world. The same system can be tested in different environment (e.g. connected to different building types, or exposed to different climatic conditions) quickly by reconfiguring the simulation of the virtual parts. Unwanted interferences (e.g. from users) can be avoided and the accuracy of measured data is generally better in a controlled laboratory than in a field study. Of course, field tests are still necessary for a complete

performance assessment, but semi-virtual testing allows going further than conventional laboratory tests at a fraction of the cost of a pilot project.

Several partners have made their laboratory facilities available for Annex 67 as well for the scientific community and the industry. The test facilities, see Table 2, are described extensively in the internal Annex 67 report about Laboratory facilities (Péan and Salom, 2019).

Table 2: Laboratories for testing energy flexibility in buildings (Péan and Salom, 2019).

Name	Managed by	Location
SEILAB	IREC - Catalonia Institute for Energy Research	Tarragona, Spain
NZEB Emulator	Aalto University	Espoo, Finland
OPSYS test rig	Danish Technological Institute (DTI)	Taastrup, Denmark
ZEB Living Lab	NTNU / SINTEF	Trondheim, Norway
Energy Research Lab	Institute Energy in Building, FHNW	Muttenz, Switzerland
Semi-Virtual Laboratory	Polytechnique Montréal	Montréal, Canada
EnergyVille labs	EnergyVille (VITO, KU Leuven, IMEC)	Genk, Belgium
Test Lab Heat Pumps and Chillers	Fraunhofer Institute for Solar Energy Systems	Freiburg, Germany
Energy Smart Lab	IREC - Catalonia Institute for Energy Research	Barcelona, Spain

From the available facilities, six of them executing flexibility related experiments in the timeframe of Annex 67 have been selected to be part of this report. This report is structured in the form that each chapter describes each of the facilities and an energy flexibility test performed in each one. The subsection about the laboratories includes a general overview of the facility, a detailed description and some examples of previous tests related with energy flexibility. The subsection about the tests includes the purpose of the test, a brief description, the results obtained and the conclusions and lessons learnt when performing the experiments. From the lessons learnt during those experimental tests, a final chapter offers recommendations to the scientific community and industries when these types of experiments are being utilized.

3. IREC. The Semi-virtual Energy Integration Laboratory

3.1. General presentation of the lab facilities

The Semi-Virtual Energy Integration Laboratory (SEILAB) provides advanced expertise to assess the development and integration of renewable energy solutions and innovative thermal and electrical equipment that are designed to improve energy efficiency in buildings and energy systems. The laboratory is provided with cutting-edge technology comprising systems for energy generation, heat and cold storage and state-of-the-art facilities for testing HVAC equipment and the interaction of energy systems with the grid. The laboratory operation is based on a semi-virtual testing approach, which allows for real equipment to be operated as a function of the behaviour of a dynamic virtual model (hardware-in-the-loop concept). The laboratory is pioneer in addressing the smart integration of electrical and thermal components and aims to become a leading experimental facility for improving the development of Net Zero Energy Buildings and Energy Flexible buildings.

3.2. Description of the test facility

3.2.1. General principle and testing possibilities

General testing principles

The general concept of the semi-virtual testing is presented in Figure 1. A real physical device is placed in the laboratory, where it is studied under specific conditions that are simulated with a numerical model implemented in the virtual environment. The overall principles are as follows:

- Testing the performance of components or complex energy systems under well-defined building and environmental conditions.
- Development and integration of innovative sustainable, renewable building energy supply systems.
- Analysis of equipment behaviour at particular transient phases.

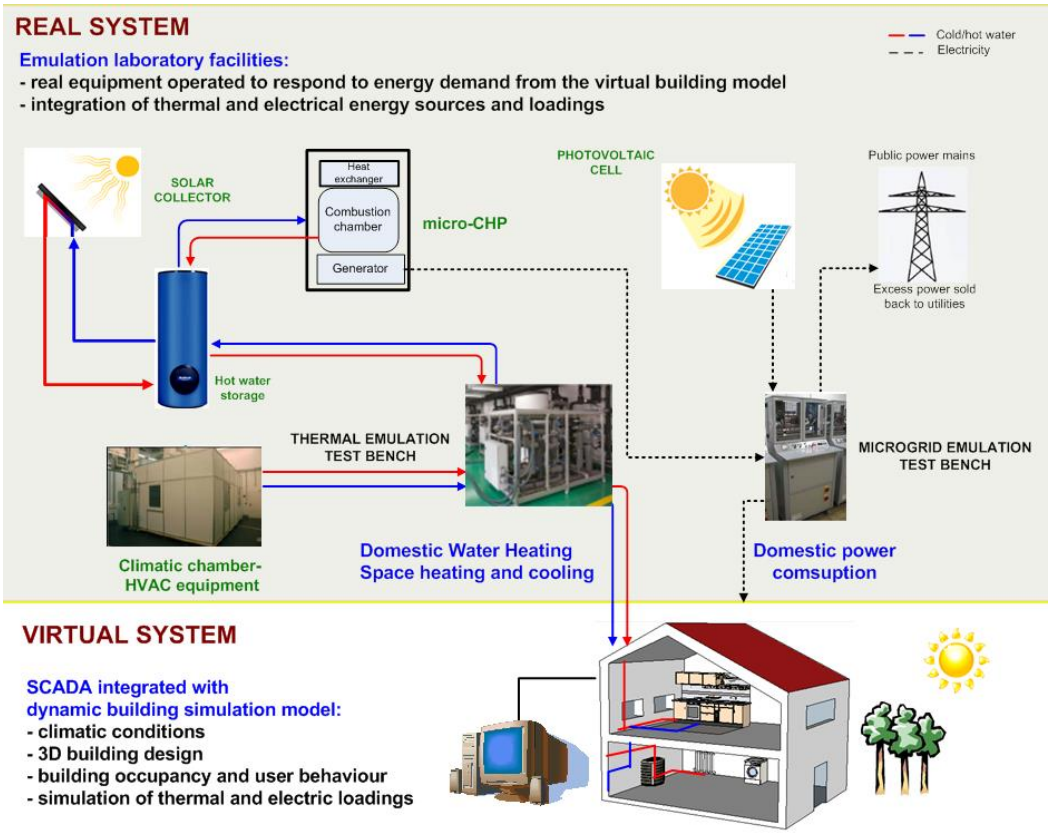

Figure 1. General concept of the semi-virtual testing.

Detailed testing principles

- Experimental testing of thermal and electrical equipment performance under realistic dynamic conditions, addressing a range of climate zones and energy demand profiles and scenarios.
- Comparison on the performance of equipment provided with particular innovative control concepts to ensure adequate system reliability in real applications.
- Assessment and improvement of innovative efficient energy technologies, such as energy storage systems, photovoltaic and thermal solar systems, nanofluids for HVAC equipment and micro-cogeneration.
- Development of novel measurement methodologies and test protocols to assess realistically the energy performance of thermal and electrical equipment beyond testing methods established in current international standards, including analysis of the Seasonal Performance Factor.
- Optimisation of operation for multiple energy sources and loads for matching energy generation and demand, including microgrid interaction.

- Development of detailed and/or simplified models for use in system simulation software and of learning-methods / predictive techniques of thermal components performance that are validated using test bench experimental data.
- Research on the integration and effects of local building components in smart energy systems to achieve Zero and Positive Energy Buildings, and optimal matching between demand and RES-based production profiles, to contribute to building stock decarbonisation.
- Research on control systems for energy flexible buildings, including renewables.

3.2.2. Equipment available and specifications

Climate chamber

The laboratory includes a walk-in climate chamber (shown in Figure 2) for testing different devices. The climate chamber generates the environmental air characteristics (temperature and humidity) according to the climate conditions defined in the test standards. The chamber is equipped with a set of 24 Pt100 temperature sensors, 2 pressure sensors, 4 humidity sensors and 10 hot wire anemometers for air velocity measurement. All sensors are regularly maintained and calibrated. The climate chamber has an inner volume of 45 m^3. Indoor environment can be controlled within the following range:

- Temperature: -30 to +60°C
- RH: 15 - 98%
- Air flow: 8000 - 10000 m^3/h
- Maximum power of condenser: 46.8 kW

Figure 2. Picture of the SEILAB climate chamber.

Hydraulic thermal test benches

The laboratory has a set of thermal test benches for emulating the heat and load source, as specified in standards EN14511, EN16147 and EN14528. The thermal test benches consist of a set of hydraulic loops comprising flow meters and motorized valves to control the flow and temperature of the fluid entering the heating/cooling unit under test. Water circulation is achieved by means of circulating pumps equipped with frequency inverters and high speed modulating control valves with magnetic actuators. The hydraulic circuits include expansion vessels and safety valves. Pipes are insulated with 30 mm synthetic rubber material. The heat transfer fluid which is generally used in the installations is decalcified and mechanically filtrated water. Temperatures in the circuit are measured with Pt100 sensors (3-wire configuration) with terminal

head form B tolerance class A (EN 60 751). Calibration of the flow meters and the temperature sensors is performed regularly. Hydraulic pressure is measured in every test bench with digital pressure meters.

Along with measurement systems, the test benches are equipped with the following control elements:

- 2 magnetic-inductive flowmeters Endress & Hauser per test bench for volume flow measurement.
- 2 precision control valves for flow and temperature control per test bench.

The available thermal test benches have the following characteristic in terms of heating performance:

- water temperature range: -7 ºC – +150 ºC
- water flow rate range: 3.5 – 9 m^3/h
- maximum heating power per unit: 30 kW
- maximum cooling power per unit: air-to-water 15 kW, water-to-water 30 kW

Temperature, flow rate and pressure measurements in the test benches fulfil requirements specified in the EN14511, EN14528 and EN16147 standards. The instrumentation in the laboratory allows a very fast control of temperatures and water flows to emulate both steady-state and transient dynamic load profiles.

PV system

Figure 3. PV equipment on the roof of SEILAB.

A PV system with a 3.5 kWp capacity is installed on the roof of the laboratory. A picture of the equipment is presented on Figure 3.

Other equipment

Several other devices are available in the lab:

- 1 heat pump air-to-water Buderus (7.4 kW heating, 8 kW cooling)
- 1 heat pump water-to-water Dynaciat (40 kW heating, 34 kW cooling)
- Water storage tanks of 1500, 1000 and 300 L.

- Micro data centre of 1.2 kW partially water cooled
- Gas boiler Saunier Duval Themafast 25-A
- 2 electrical test benches (5.5 kVA emulated power, 10 kVA maximum connected generation , 10 kVA maximum connected consumption)

3.2.3. Data acquisition and control

The tests are performed by means of a control system created in the laboratory. The software allows visualising the operation of the laboratory equipment, controlling the test performance and performing data acquisition. Communications are based on Modbus TCP and RTU industrial protocols, with the laboratory software communicating with actuators and sensors via automatic controllers and data acquisition modules through RS485 connections.

A LabVIEW interface (Figure 4) enables to communicate with the different elements being tested in the lab. This interface can be connected to transient simulation software TRNSYS, where building models can be implemented to simulate the heating or cooling loads of a building or the performance of the virtual part of the system. Other software than TRNSYS, such as Energy Plus or IDA-ICE, can be connected with the LabVIEW interface. Remote visualisation of experiments in real time is possible for external collaborators.

In addition, a weather station is placed on the roof of the laboratory and connected to the interface. It measures the outdoor air temperature, wind velocity, relative humidity and the global and diffuse radiation. In some experiments weather measured data are transferred to buildling models to compute the building performance.

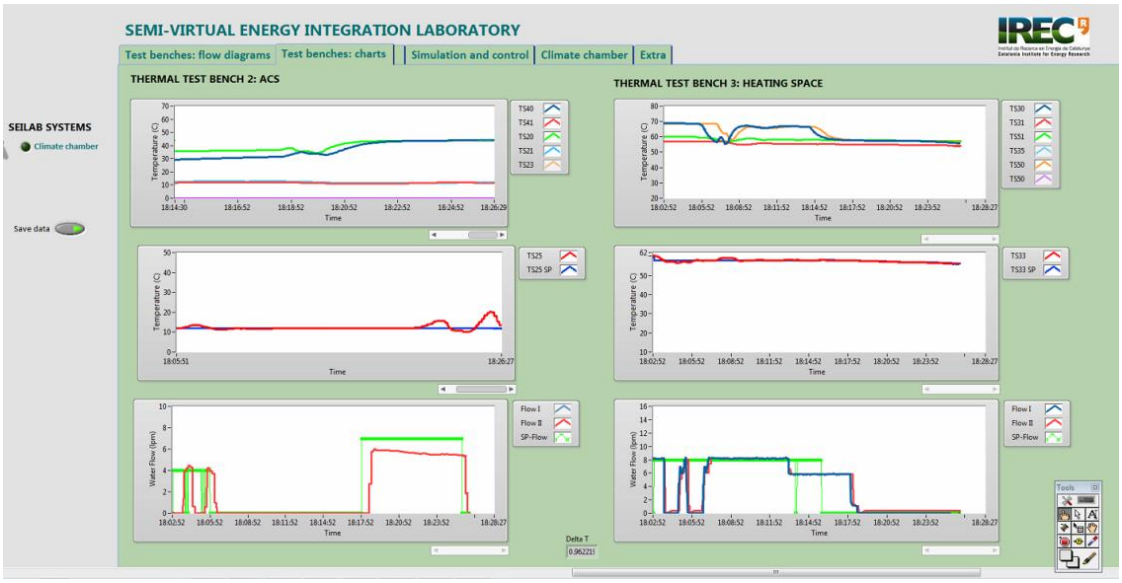

Figure 4. Screenshot of the LabVIEW interface.

3.3. Examples of previous studies

3.3.1. Experimental study of grid frequency regulation ancillary aervice of a variable speed heat pump

This study (Kim et al., 2016) describes an analysis of a variable speed heat pump (VSHP), which responds to direct load control (DLC) signals to provide grid frequency regulation (GFR) ancillary service, while ensuring the comfort of building occupants. A data-driven dynamic model of the VSHP is developed through real-time experimental studies with a time horizon ranging from seconds to hours. The model is simple, yet still sufficiently comprehensive to analyze the operational characteristics of the VSHP. The DLC scheme is then experimentally applied to the VSHP to evaluate its demand response (DR) capability. Two control methods are considered for a practical implementation of the DLC-enabled VSHP and a further improvement of the DR capability, respectively. Additionally, a small-signal analysis is carried out using the aggregated dynamic response of a number of DLC-enabled VSHPs to analyze their contribution to GFR in an isolated power grid. For experimental case studies, a laboratory-scale micro-grid is then implemented with generation and load emulators. It is showned that the DLC-enabled VSHP can effectively reduce grid frequency deviations and required reserve capacities of generators. The experimental setup used for this study is presented in Figure 5. This experimental study was performed in the framework of a collaboration with MIT (USA) and HITACHI.

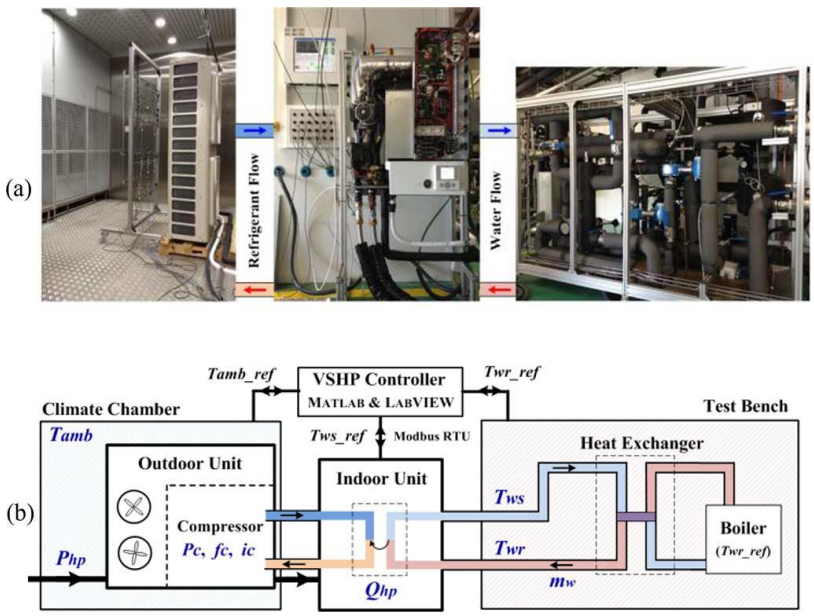

Figure 5. Experimental setup and corresponding diagram

3.3.2. *Partial load efficiency degradation of a water-to-water heat pump under fixed set-point control*

This laboratory study (Waddicor et al. 2016) evaluates the influence of fixed set-point control strategies on the partial load behaviour of a water-to-water heat pump of 40.5 kW heating capacity. Experimental results indicate that the control configuration is highly influential on the heat pump cycling response and efficiency degradation at part load. Deterioration of energy performance occurred mainly during system start-up, with additional efficiency loss caused by short cycling for supply temperature control at low loads. It was concluded that a minimum of 20 min compressor run time is necessary to reduce degradation effects, suggesting that installers and heat pump manufacturers should ensure minimum operation times to improve systems efficiency. Comparison of models and experiments indicate that it is important to adequately account for both stand-by and start-up efficiency losses for improving predictions of part load performance by steady-state heat pump models. The experimental setup and results are shown in Figure 6. This project has been developed in the framework of EU project TRIBUTE (http://www.tribute-fp7.eu/).

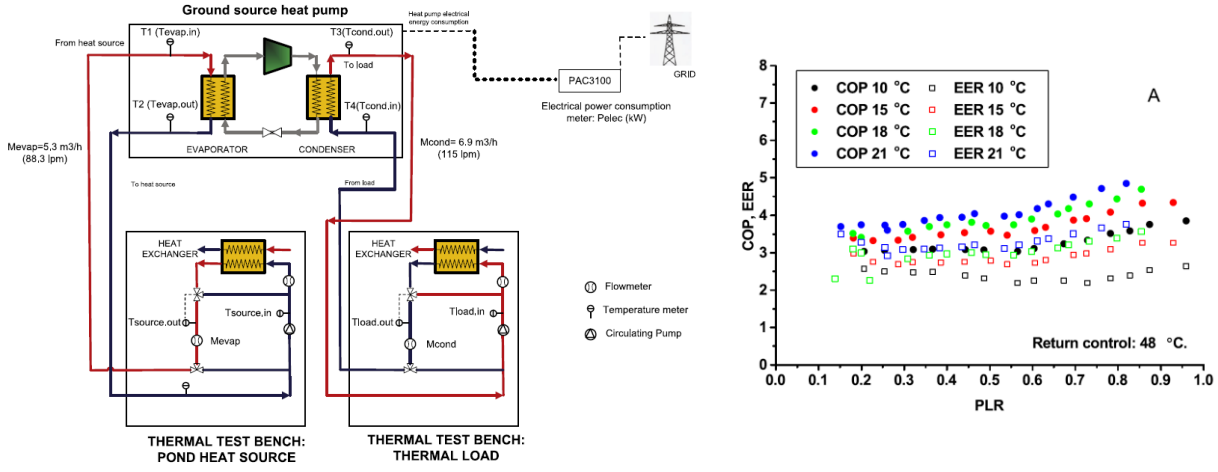

(a) (b)

Figure 6. Experimental setup (a). COP and EER as function of the part-load ratio (PLR) (b).

3.4. Experiment on energy flexibility

3.4.1. Objective

A series of dynamic experimental tests were carried out in the SEILAB facilities of IREC, which aimed at operating a real heat pump under a model predictive control framework and observe its performance in more realistic conditions than with only simulations. Prior to the latter, a first series of static tests were conducted to record the performance of the chosen heat pump (an air-to-water, inverter driven reversible system) in all its range of operating conditions, both in heating and cooling modes. These static tests precisely characterized the heat pump performance by fitting mathematical functions which were then used as input to the model predictive controller (MPC) of the dynamic tests.

The dynamic tests evaluated the response of the heat pump to different configurations of the MPC. The benefits in terms of energy flexibility for the different MPC configurations were assessed with the same heat pump operating in heating mode in winter, in cooling mode in summer, and for production of DHW in both seasons. This range of combinations has been investigated to a low extent in the literature on MPC for energy flexibility, and few studies use a real heat pump system in an experimental setup. Furthermore, implementing such advanced control strategies on a real system helped to identify the bottlenecks that could hinder the deployment of MPC, propose solutions to improve them, and emphasize some lessons learnt from the realistic experiment.

3.4.2. Brief description

For the dynamic tests, the experimental setup is presented in Figure 7. The tests consist in operating the heat pump during three consecutive days in real time and under dynamic conditions together with the virtual building model.The outdoor unit of the heat pump is placed in the climate chamber, where the air temperature and relative humidity are controlled according to a predefined climate file. The indoor unit, with its integrated tank of 200 L for DHW, is placed outside the chamber, as one can see in Figure 8. The heat pump is an inverter driven Yutaki heat pump model from Hitachi, with nominal heating power of 11 kW for a COP of 3.98, and a nominal cooling power of 7.2 kW for an EER of 3.3.

The heat pump is “connected” to a virtual building model running in the TRNSYS software in real time. The simulated building is a residential flat situated in Spain, conditioned with a fan coil unit (FCU) distribution system which is supplied with cold or hot water from the heat pump. The supply water temperature and flow from the heat pump are measured and fed as information into the building model. TRNSYS then calculates the return temperature from the FCU, which is emulated as the actual water temperature returning to the real heat pump by means of the heat exchangers of the thermal benches. For DHW production, the heat pump runs an internal water circuit which

heats up its integrated tank. The DHW extractions follow a predetermined profile according to the European standard EN12976-2 and are reproduced in an additonal thermal test bench. The hot water flow is extracted from the tank following the programmed DHW tapping profile while the water intake temperature is controlled in an external tank of 1000 L which conditions the water at the temperature of the mains according to the period of the year.

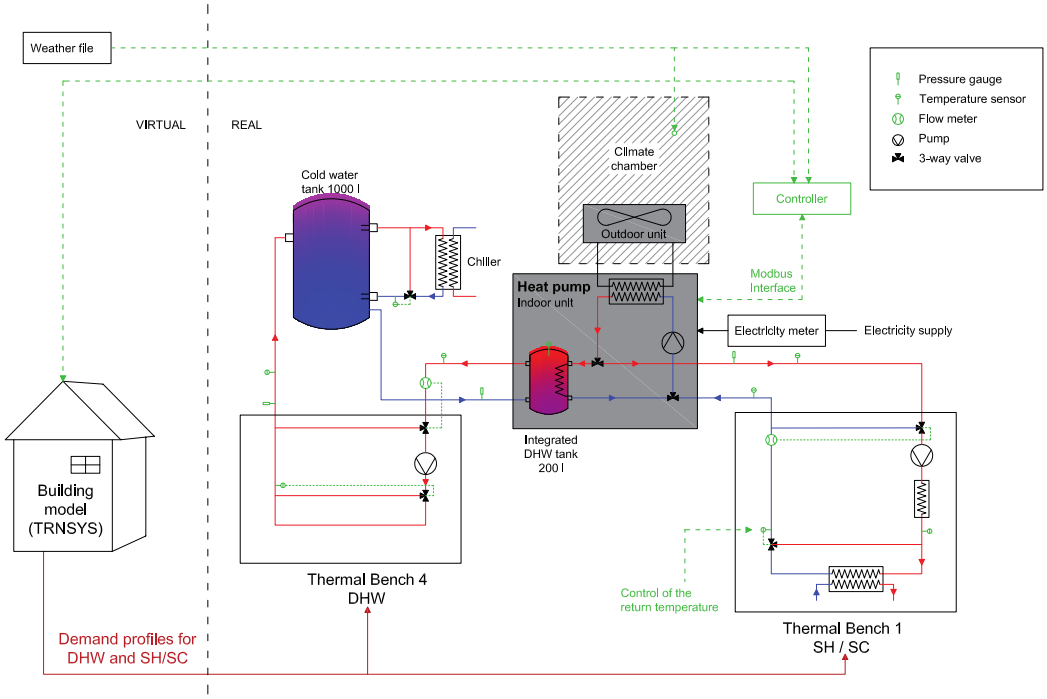

Figure 7. Scheme of the experimental setup used for dynamic tests.

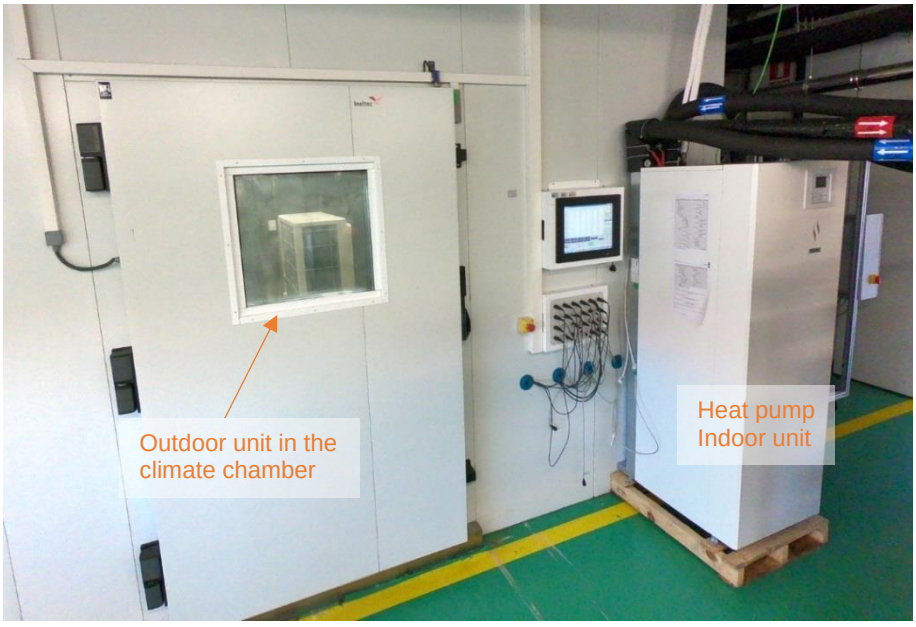

Figure 8. The tested heat pump installed in the lab, with the outdoor unit inside the climate chamber.

All the systems are managed from a central interface programmed with the software LabVIEW. This interface communicates with the building simulation tool (TRNSYS), the heat pump (through a Modbus gateway), the controller (in Matlab), and the rest of the sensors and actuators in the climate chamber and the thermal benches. The MPC controller was designed and implemented in Matlab using the program's optimization features. Different configurations of MPC for energy flexibility were used and compared. A first one called MPC ThEnerg, intends to minimize the thermal energy delivered to the building. A second one called MPC Cost, minimizes the costs of the heat pump operation by reacting to an electricity price signal. A third one called MPC CO_2, minimizes the CO_2 emissions by reacting to a CO_2 marginal emission factor signal.

3.4.3. Results

Figure 9 shows the time series of several parameters recorded during the 3 days of one of the experiments with the MPC Cost configuration in heating mode.

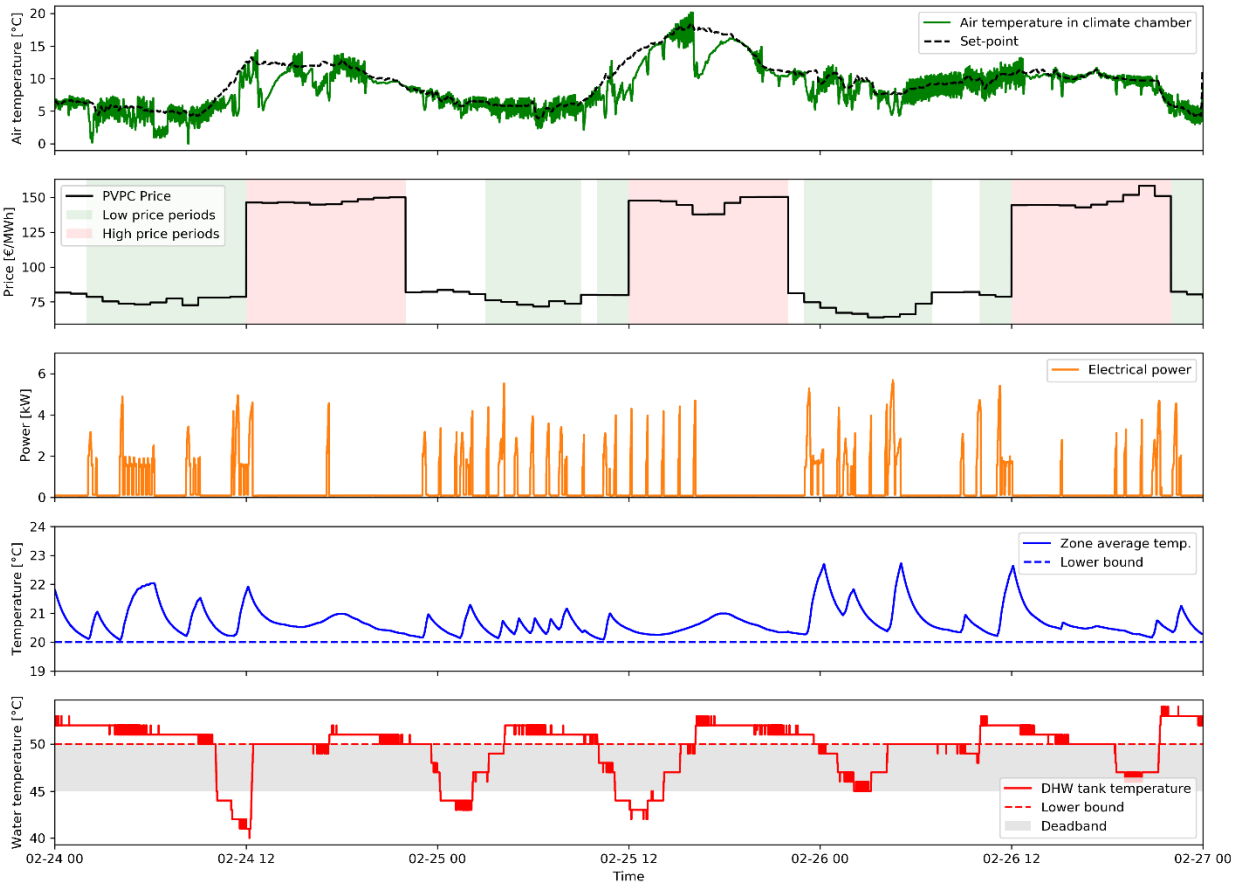

Figure 9. Time series of the 3-day experiment with MPC Cost in heating mode.

On the top graph, the outdoor temperature set-point (from a climate file) is displayed, as well as the real air temperature measured in the climate chamber. On the second graph, the input price signal is shown. Highlighted in red, the periods where the price is considered high (hence when

the MPC will tend to avoid operating the heat pump). The third graph shows the heat pump power consumption, i.e. when it was activated by the MPC. The last two graphs show the resulting temperatures in the indoor space and in the tank, with their respective constraints.

It can already be observed in this figure that the MPC Cost strategy shifted the operation of the heat pump away from the high price hours, and forced it during the low price hours. In this way, the total cost can be decreased. The principle would be similar for the MPC CO_2 configuration to reduce the emissions, except that the input signal would be the emissions factor from the grid instead of the electricity price.

The load shifting effect is further depicted in Figure 10. On the top row, the electricity consumption of the heat pump is divided between low, medium and high price hours. On the bottom row it is divided between low, medium and high emissions hours.

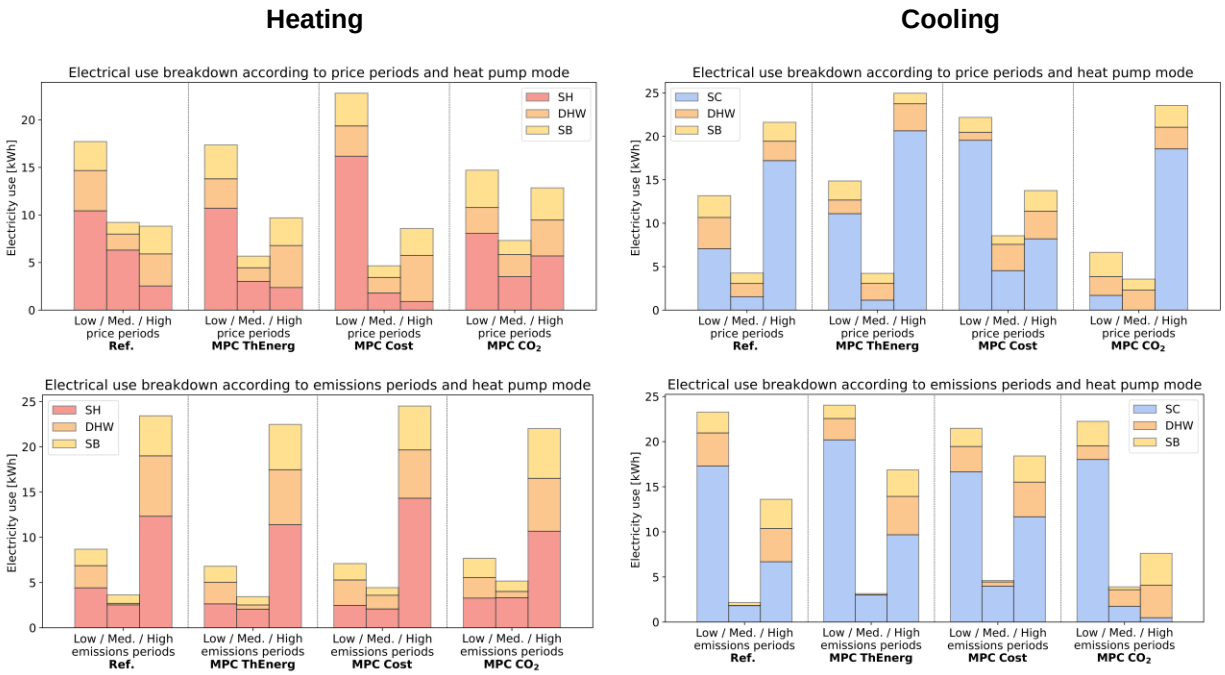

Figure 10. Breakdown of the electricity use according to the high/low penalty periods and the heat pump mode (SH/SC, DHW, SB), both in heating and cooling seasons.

It can be observed that the MPC Cost configuration is the most effective at shifting the loads towards low-penalty periods (whether price or emissions). In heating mode, the reference case already uses energy mostly in low-price periods, leaving little room for improvement. MPC Cost still manages to improve the shifting of the SH loads. Almost no SH operation occurs during high price periods in this case, and most of it is moved to low price hours. The DHW loads are actually shifted in the wrong direction, with an increase of these loads during high price hours.

In cooling mode, the reference case uses most of the energy in high price periods, therefore MPC Cost has a great potential to improve the distribution of the load. It effectively manages to do so and inverse the trend, especially for the SC load which is shifted in great part from high to low

price hours. These results reveal the good performance of MPC Cost in cooling mode. it uses effectively the available thermal storage of the building (thermal mass and water tank) to flexibly operate the loads, and thus relieves the grid during the most critical hours.

The load shifting is much less visible for the MPC CO_2 configuration, which shows difficulties in increasing the load at low emission hours. In fact, in heating mode, the operation of the system does not differ much from the reference case. The energy use at high emissions hours is only slightly reduced. In cooling mode, the SC load is almost entirely suppressed from the high emissions periods. However, it is not moved towards the low emissions hours, which results in a lower energy use, greater emissions savings, at the cost of a slight degradation of the comfort conditions.

Table 3 presents selected results of the total resulting costs and emissions. More details can be found in (Péan et al., 2019). It can be observed that thanks to the load shifting previously described, all these MPC configurations achieve their declared objective. MPC Cost decreases the heat pump operational costs compared to the reference thermostatic case, while MPC CO_2 reduces the carbon emissions. The percentages of reduction are however quite small, especially in heating mode (only -1% in costs and -3.3% in emissions), compared to what could be expected from MPC strategies (7 to 35% savings reported in the literature). It should be noted that the objectives of cost reduction and emissions reduction are rather contradictory. When one of them gets improved, the other one usually worsens. This is mainly due to the input signals used, which have an opposite behavior: the peaks of the electricity price correspond to low emissions periods, and vice-versa.

Table 3 Results summary of the MPC Cost and CO_2 configurations

Variations compared to the reference case		HEATING		COOLING	
		MPC Cost	MPC CO2	MPC Cost	MPC CO2
Cost	€	-0.04	+0.21	-0.24	-0.17
	%	**-1.03%**	+6.15%	**-6.84%**	-4.78%
Marg. Emissions	$kgCO_2$	+0.14	-0.32	+1.41	-1.51
	%	+1.41%	**-3.29%**	+15.4%	**-16.5%**

The MPC framework operates well in general and provides better comfort and higher efficiency of the system operation, which is an important validation. Some practical issues and bottlenecks however occured which prevented the MPC strategies to yield even higher savings than what could be expected. These aspects were revealed thanks to the experimental nature of this study, and the implementation of the MPC controller on a real heat pump system.

The first problem concerned the DHW tank charging. The MPC determines when it is optimal to charge the DHW tank, and then sends the corresponding command to the heat pump through a

communication gateway. However, activating this command (called “DHW Run/Stop”) does not automatically trigger the DHW tank charging, instead it only enables the “availability” of the DHW tank charging, and then the internal controller decides whether or not to start the heat pump, based on the actual temperature in the tank. On average, the charging of the DHW tank occurred 17 times over the studied periods of 3 days. A DHW command was sent on average 12 additional times but ignored by the local controller of the heat pump. This behavior affected the moment when the DHW tank was actually charged, and thus explains why the DHW load was not always shifted to the low penalty periods, as seen in Figure 10.

The second issue concerned the discrepancy between the optimal plan calculated by the MPC and its fulfilment by the real heat pump. An example is illustrated in Figure 11: the MPC decided to activate space heating during one hour, at a thermal power of around 6 kW. However, the real heat pump behaved differently than planned by the MPC. Several transitory phases took place before reaching a steady state (delay, ramping, overshoot, shutdown). During these transient phases, the thermal power was on average higher than the original plan of the MPC. Therefore the heat pump consumed more energy than planned, and this could have been the cause of why the achieved savings were not higher.

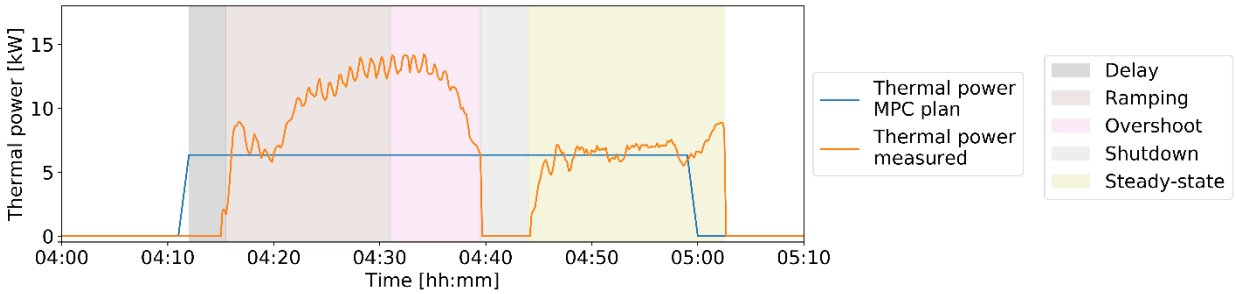

Figure 11. Discrepancy between the MPC plan and the actual heat pump operation

3.4.4. Conclusions and lessons learnt

The developed MPC framework yielded satisfactory results, achieving in general its objective of reducing the operational costs or emissions due to the heat pump use, compared to a reference thermostatic control. The obtained savings were not as high as one could expect from an MPC strategy, given the higher performance usually reported the existing literature (mainly on simulation-based studies). However the MPC strategies consistenly improved the indoor thermal comfort and the efficiency of the systems.

Implementing MPC on a real heat pump system leads to the discovery of some practical obstacles or bottlenecks. For instance, with the chosen heat pump model, it is not possible to force the charging of the DHW tank. It is only possible to activate the “availability” of this function, but then the internal control of the heat pump decides whether or not to turn the compressor on and provide heat to the tank. This can cause problems with MPC, since that type of controller intends to optimize the heating schedule, and therefore would rather force the DHW tank charging at some

periods where the internal heat pump control would not do so. Furthermore, the expected plan of the MPC is not fulfilled exactly by the real heat pump, since transient phases due to the internal control of the heat pump come into play. These discrepancies could as well affect the performance of the MPC, and could only be discovered by an experimental study such as the one presented here.

Testing energy flexibility in a laboratory setup (and it would also be true in a real building) requires complicated communication framework, since many different software and acquisition tools are needed: direct communication to operate remotely the real systems (heat pump), optimization tools (MPC in MATLAB), connection with external services (to retrieve forecasts of weather and grid parameters), real-time simulation of a building model (in TRNSYS). Achieving a fluid communication and operation between all these elements is a challenging task.

4. Aalto University. The NZEB Emulator

4.1. General presentation of the laboratory facilities

The nearly-zero energy building (nZEB) emulator is a platform for studying the performance of a building with different renewable energy production and storage equipment fitted into a fully functional system operating in Finnish climate conditions. The platform is based on a semi-virtual approach comprising of real components for energy generation, conversion and storage connected with a simulated building and a ground source heat pump borehole. This arrangement makes the system very flexible as different types and sizes of buildings may be studied by simply changing the simulation model. The system is also equipped with an energy management system (EMS) developed at VTT which can direct energy flows in an optimal way by assessing the current and future energy status as well as the availability of renewable sources (sun, wind). The nZEB emulator platform is a unique facility for assessing the real-time performance of advanced energy solutions and investigating the energy flexibility in buildings towards achieving set targets in the building and fit with the requirements of the grid.

4.2. Description of the test facility

4.2.1. General operation principle and research possibilities

General operation principles

The general operation concept of the nZEB emulator is presented in Figure 12. The platform is designed to resemble a single-family house with respect to component sizing but the operation can be scaled to match different building types. The actual building is a TRNSYS simulation running in a computer and the physical devices are operated according to electricity and heating demands given by the simulation at six minute (changeable) intervals. The physical part of the system is operated in real-time and according to real weather conditions as there is no weather chamber. The platform is equipped with an energy management system (EMS) which optimizes the energy use and flows by assessing the energy prices and weather. The general uses for the platform are as follows:

- Analysis of local energy matching in buildings.
- Performance evaluation of different control strategies for achieving optimal use of energy resources
- Gathering of high-resolution data from the various components for validating component models used in simulations and optimizations

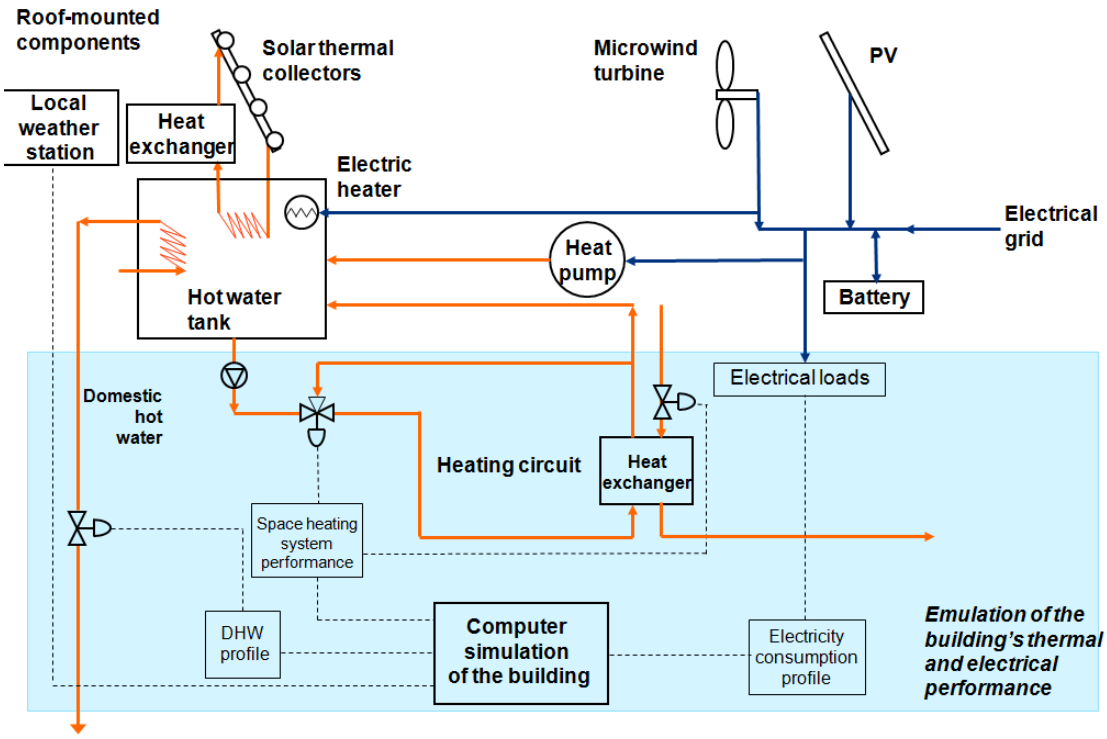

Figure 12 Operation and basic component diagram of the emulator platform.

Examples of research possibilities

- Experimental testing of novel energy solutions related to local production and storage of electricity and heat such as PV panels, solar thermal collectors, micro wind turbines, heat pumps, batteries and heat storages
- Development and testing of new control strategies for energy systems in smart buildings
- Monitoring and recording the behaviour of different components present in the system
- Using the data to calibrate the models for building simulation tools
- Optimization of energy flows in order to improve energy generation/demand matching and interactions with bidirectional future hybrid smart electricity and heating grids
- Evaluation of modelled electric/hydrogen vehicle as a part of the nZEB concept
- Evaluation of the energy flexibility performance of building's energy systems e.g. for minimizing operating energy costs, environmental impacts or responding to grid requirements.

4.2.2. Equipment and specifications

PV panels

A PV plant consisting of 18 panels in two rows is installed on the roof of the lab (Figure 13). The panels have a nominal capacity of 240 Wp each, for a total of 4.32 kWp. Both panel rows are

equipped with separate SMA Sunny Boy 2000 HF inverters. The production is monitored with one- minute resolution via a Bluetooth interface.

Figure 13 PV panels and micro wind turbine on the roof of the building where nZEB emulator is located.

Micro wind turbine

In addition to PV panels, a Finnwind Tuule E200 micro wind turbine with a rated capacity of 4 kW has been installed on the roof of the laboratory (Figure 13). The turbine is located at the top of a 9-meter high steel mast, accounting for a 25-meter total distance from the ground level. The turbine automatically rotates towards the wind direction and is equipped with storm protection, which turns it away from the wind if the gusts become too strong. The wind plant is equipped with an SMA Windy Boy 3600 TL inverter which, like its PV counterparts, is monitored with a one-minute resolution via Bluetooth.

Island electricity network

The PV panels and the wind turbine are connected to an island electricity network via an SMA Sunny Island 6.0H inverter. The island network is equipped with a 48 V, 200 Ah battery (four 12 V 200Ah lead acid batteries in series). It also contains ten 600 W electric heaters which emulate the electricity loads of a house according to the simulation's load profiles. The battery state-of-charge is monitored by the inverter and communicated to a computer via an Ethernet cable.

Solar thermal collectors

For heat production, two sets of four solar thermal collectors have been installed on the roof of the laboratory (Figure 14). One of the sets consists of Oilon Solarpro flat-plate collectors whereas the other one contains AMK-Solac OWR 12 evacuated tube collectors. Each set has a capacity

of around 4 kW at typical Finnish summer conditions and is equipped with a Sonnenkraft SKSC3+ controller/pumping station, which controls the brine flow rate in the circuit.

Figure 14 Flat-plate solar collectors on the roof of the building where nZEB laboatory is located.

Ground source heat pump (GSHP)

The other method for heat production in the platform is an Oilon Geopro GT 5 ground source heat pump with a nominal capacity of 5 kW. There is no real ground borehole so a hydraulic circuit including a 500 L buffer tank filled with brine is used as a heat source for the GSHP. The brine flow rate and return temperature are emulated according to the borehole output results from the TRNSYS simulation. The buffer tank is heated up by the rejected heat from the system that would normally be used for the space heating of the building.

Hot water storage

The emulator platform is equipped with three Akvaterm Akva Solar hot water storage tanks (Figure 15). Two of the tanks have a capacity of 500 L while the third is slightly smaller with 300 L. Each tank is equipped with three heating coils (solar thermal, DHW pre-heating, DHW heating). There is a plate with a small opening in the middle of the tank for separating the top and bottom parts from each other. The temperature stratification is monitored by five thermocouples placed inside the tank at different elevations. One of the 500 L tanks is equipped with a 6 kW electric heater. The 300 L tank is prepared for the future implementation of phase-change materials as a heat storage. The storage tanks have flexible connections so it is possible to have them in series or parallel configuration, or a combination of the two.

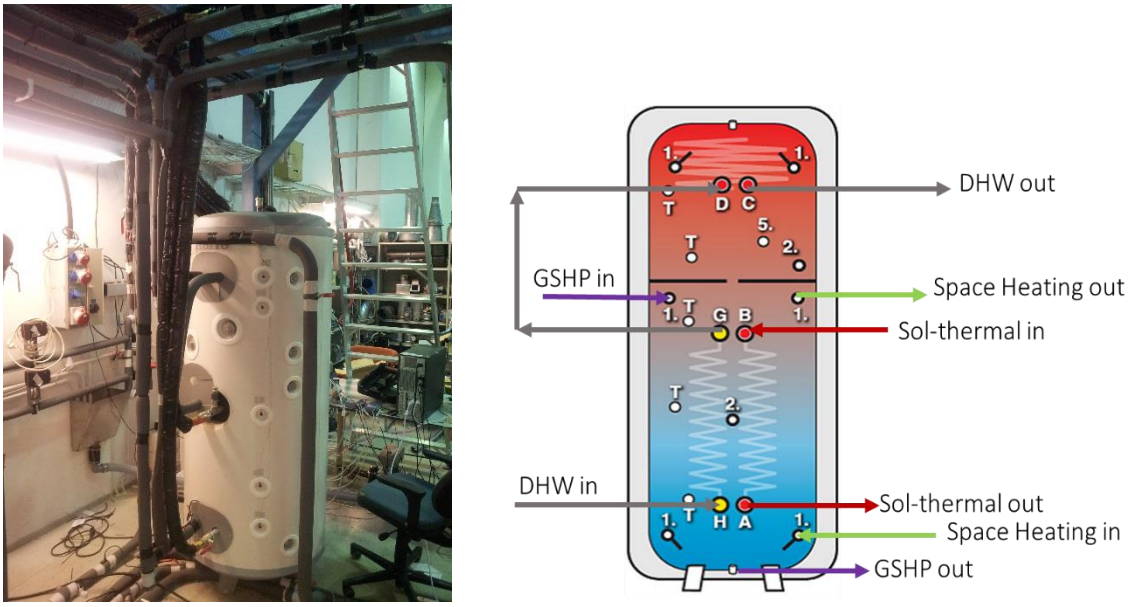

Figure 15 One of the hot water tanks (left); Schematic of the storage tank connections (right).

Other equipment

- Vaisala AWS330 weather station for measuring temperature, humidity, wind speed/direction and solar irradiance
- Water-to-air heat exchanger on the roof for emulating export of excess solar thermal heat into district heating network

4.2.3. Data acquisition and control

The majority of the components in the emulator platform are controlled by a LabVIEW-based software developed at Aalto University (Figure 16). This software is also used for data acquisition from the roughly 100 thermocouples, resistance temperature detectors (RTDs) and flow sensors the system is equipped with. The sensor data is collected mainly via National Instruments DAQ modules connected to the computer through USB ports.

The production facilities (PV, wind turbine, solar thermal collectors) are operated by their own factory-supplied controllers and their data is acquired via dedicated software, written into CSV files and then read by the LabVIEW main program.

The rest of the system is controlled with PID and on/off controllers implemented into the LabVIEW program. For supplying control voltage (0-10V) to the various actuators, pumps etc., analog voltage output modules connected to the computer's USB ports are used.

Besides acting as the data acquisition and control hub of the system, the LabVIEW program also acts as an user interface for operating the system, and communicates with the simulation software (TRNSYS) containing the building and the GSHP borehole as well as with the energy

management system which gives decisions on how to direct the different energy flows in the system. The communication between LabVIEW and the other software is done via text files.

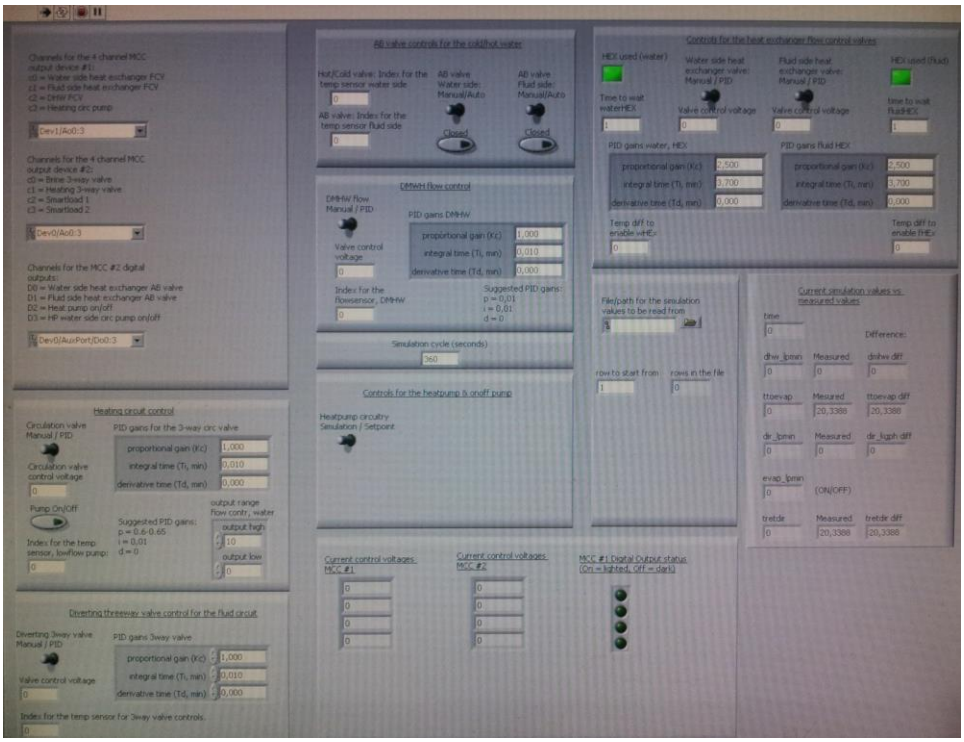

Figure 16 Screenshot of the LabVIEW interface.

The heat and electricity demands of the building under investigation are calculated at fixed time intervals (currently six minutes) by the TRNSYS simulation program and then supplied to the physical part of the system via LabVIEW. While the simulation calculates the heating demands and the space heating water return conditions, it uses typical profiles for the household electricity consumption and domestic hot water DHW, along with the prevalent weather conditions. In addition to providing energy demands, TRNSYS also simulates the GSHP borehole and gives LabVIEW the temperature of the brine returning from the ground to the heat pump.

The energy management system (EMS) is a Matlab-based program which optimizes the energy flows in the system based on a successive linear programming (SLP) approach. While nonlinear methods are generally preferable, this approach works well here since the problem set is mostly linear and the real-time operation of the system calls for a fast algorithm. With the help of real-time and forecast energy pricing and weather data, EMS can instruct the system on how to deal with locally produced and imported energy i.e. to cover the demand, convert or store the energy in the same or another form (e.g. electricity to heat), or to export/import to/from the connected networks. The EMS is connected to the online Nordpool spot electricity pricing database as well as to the online weather forecast from the Finnish Metrological Institute. In its current iteration, EMS manages the temperature set points for the GSHP, electric heater and excess solar heat export. It also decides when and how much electricity is imported, exported or stored in the batteries.

4.3. Examples of previous studies

The first task of the emulator platform is to provide experimental data for a joint Aalto/VTT Academy of Finland project dealing with nearly-zero energy buildings and supply/demand matching. In this project, the emulated building is a 150 m^2 well-insulated Finnish single-family house with four occupants. The emulator is operated for two full calendar years with the first one having finished in spring 2016 and the second one to finish in late 2017.

In the first year, the system was run with its original components and settings, and the results were analysed both to study the operation and performance of the different components, and to come up with ideas of improvement for the second year of operation. In general, the system performed reasonably well. There were a couple of issues with the most notable one being the poor performance of the batteries in the PV/wind system. To give an example of the data analysis, Figure 17 shows the monthly onsite energy fraction (OEF) and onsite energy matching (OEM) indices for electricity during a six-month period from September 2015 to February 2016. The OEF (demand cover factor) is the portion of the total electricity consumption covered by local production whereas the OEM (supply cover factor) is the portion of self-consumption from the total local electricity generation. As one can see from the figure, OEF is high during autumn when there is still PV generation whereas OEM is better in winter when the constant electricity demand due to heating is high.

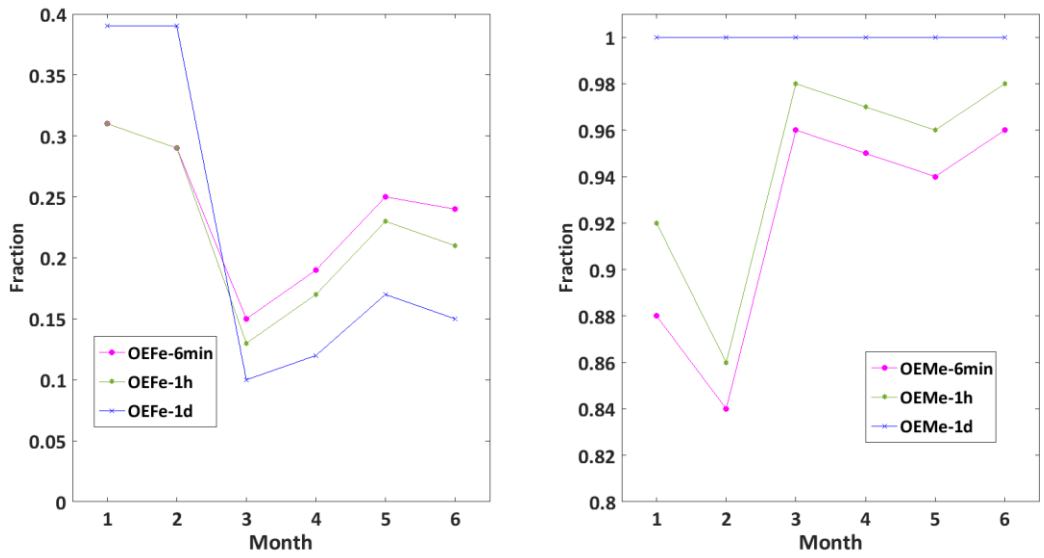

Figure 17 Monthly average matching indices OEFe and OEMe at different time averaging intervals.

After year one was passed, some modifications and additions were made for the second year during several weeks maintenance break. The most notable changes were the additions of the intelligent EMS software as a master controller of the system (done in early 2017), and a heat exchanger on the roof for emulating heat export from the solar thermal system to the district

heating grid. The batteries of the PV and wind plants were replaced as the original ones had reached the end of their lifetime. On the simulation side, TRNSYS was set to use real-time weather data from the weather station instead of a weather profile from the past.

4.4. Experiment on energy flexibility

4.4.1. Objective

The objective of the study was to test the capabilities of the successive linear programming – based energy management system EMS when linked to a real system, the nearly zero-energy building emulator. In particular, the interest was in finding out how well the EMS is able to control the system according to anticipated changes in both weather and electricity pricing, and by doing so minimize the energy costs of the studied building.

4.4.2. Brief description

For this study, a representative week from April 2015 (6^{th} - 13^{th}) was chosen as a basis since it had variation in both weather conditions and electricity pricing and the actual measurement was conducted during the last week of June in 2018. To run the system based on historical data, energy-producing components (PV panels, solar thermal collectors, wind turbine) were disconnected as their operation reflects the real-time weather conditions. PV and wind turbine production were simulated with TRNSYS according to the weather profile of the studied week whereas the solar thermal system was omitted altogether. Also, the building energy demands were calculated based on the historical weather data instead of present-day weather. Otherwise, the emulator system operation was the same as depicted in section 4.2.

The energy management system, which normally gets real-time weather and electricity pricing data from the Internet, was given the actual electricity prices from the studied week and an artificial weather forecast. The latter was generated from the actual weather by adding random noise (multiplicative for wind speed and solar radiation; additive for temperature, humidity and wind direction) and smoothing the final result with 24-sample LOESS regression. By doing so, EMS could be operated with similar knowledge as it would have in real-time operation mode.

The potential flexibility sources investigated in this study were the electric battery and the hot water storage tank. Load shifting of appliances was not included in the control scheme of the EMS.

4.4.3. Results

The electricity and heating demands for the studied building are shown in Figure 18 and Figure 19, respectively. The electricity demand was divided into three parts: base demand, heat pump and electric heater. The base demand comprises appliances, lighting and ventilation fans, and it was calculated based on a standard occupancy profile of the building. Heat pump and electric heater demands were obtained from measurements.

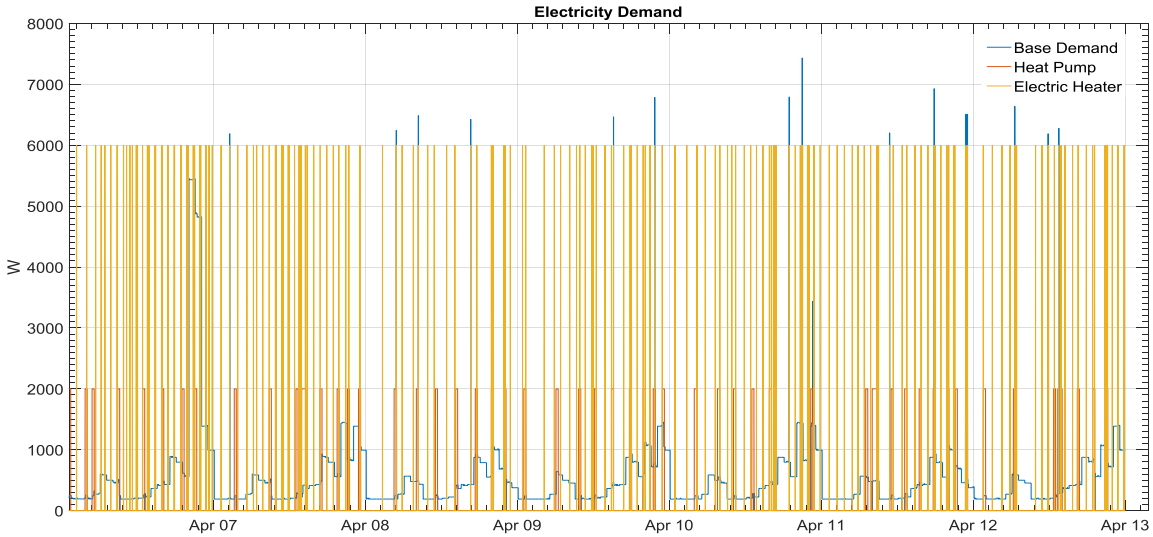

Figure 18 Electricity demand during the studied week.

Heating demand was divided into two parts: DHW and space heating. The DHW use profile was calculated based on building occupancy and weather whereas the space heating demand was obtained from simulation of the studied building with the actual weather conditions during the studied week.

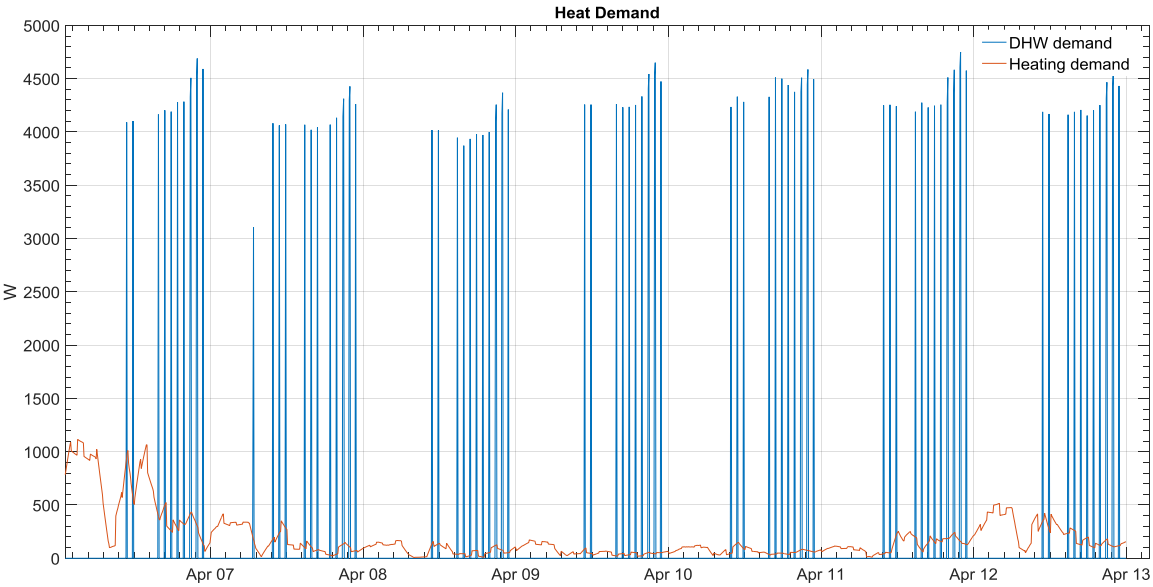

Figure 19 Heat demand during the studied week.

The real electricity import prices during the studied week are shown in Figure 20. The total import prices include energy price, transfer fee and tax. The export price is not shown but it was assumed to be equal to the energy price portion of the total import price. While there were no large changes in the import price throughout the week, it nevertheless fluctuated for most of the time, thus giving opportunities for the EMS to make different decisions.

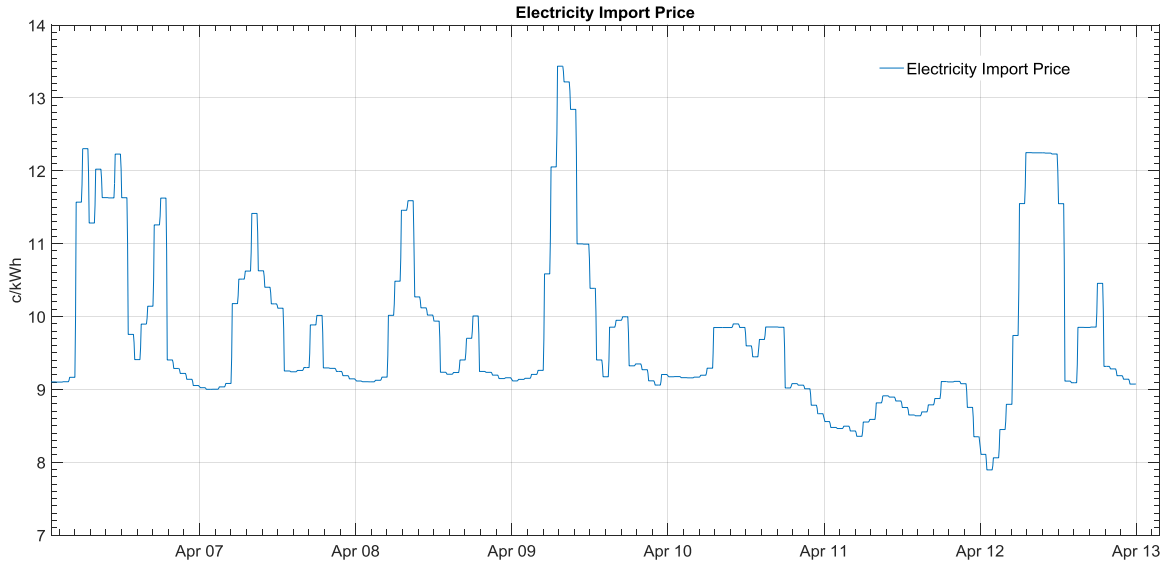

Figure 20 Electricity import price during the studied week.

In Figure 21, the calculated renewable production for the studied week is shown. Since both PV and wind turbine systems feed electricity into the same local grid, the generation was summed up to make the figure clearer. As shown in the figure, the beginning of the week had very little overall production, in the middle there were days with plenty of wind and sun, and at the end of the week renewable generation came mostly from the PV system.

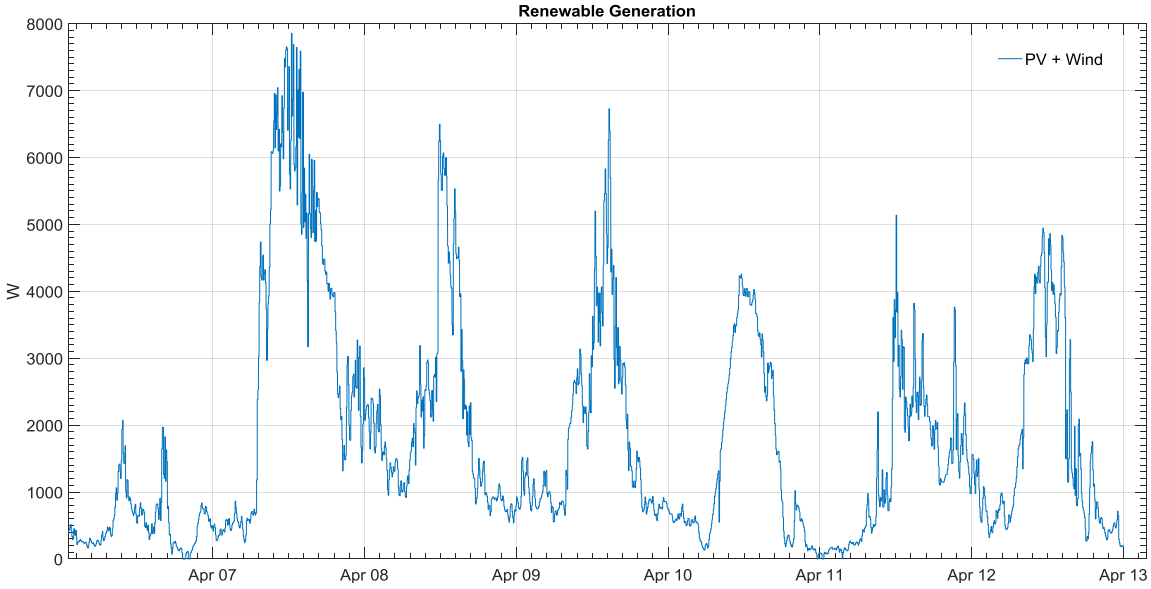

Figure 21 Renewable generation during the studied week.

The energy storages of the system (virtual battery, real hot water tank) were also monitored. Their states throughout the week can be seen in Figure 22 and Figure 23, respectively. The battery was operated from 38 to 96 % of its nominal capacity. It started out empty and, due to the first days having very little renewable production, was not really used until the third day of the study period. Throughout the rest of the week, the EMS managed the charge/discharge cycles.

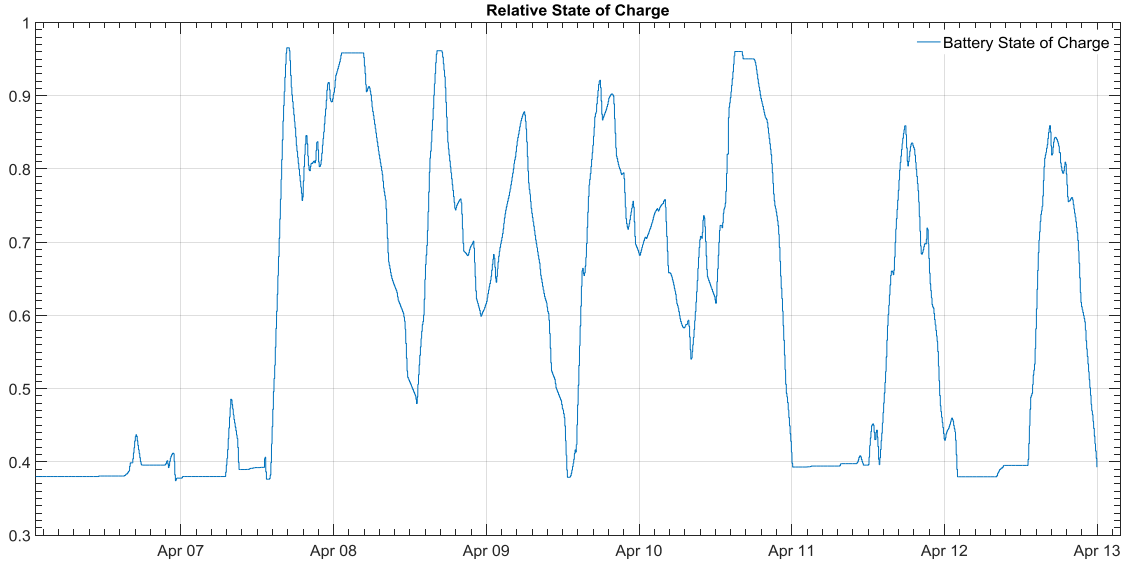

Figure 22 Relative state-of-charge of the electrical battery.

The hot water tank was monitored with thermocouples at five different heights (Figure 23). The upper part of the tank, responsible for DHW heating, was kept at 60 °C or higher at all time due to Finnish legionella regulation. The lower part, used by space heating, was however allowed to cool down according to decisions made by the EMS.

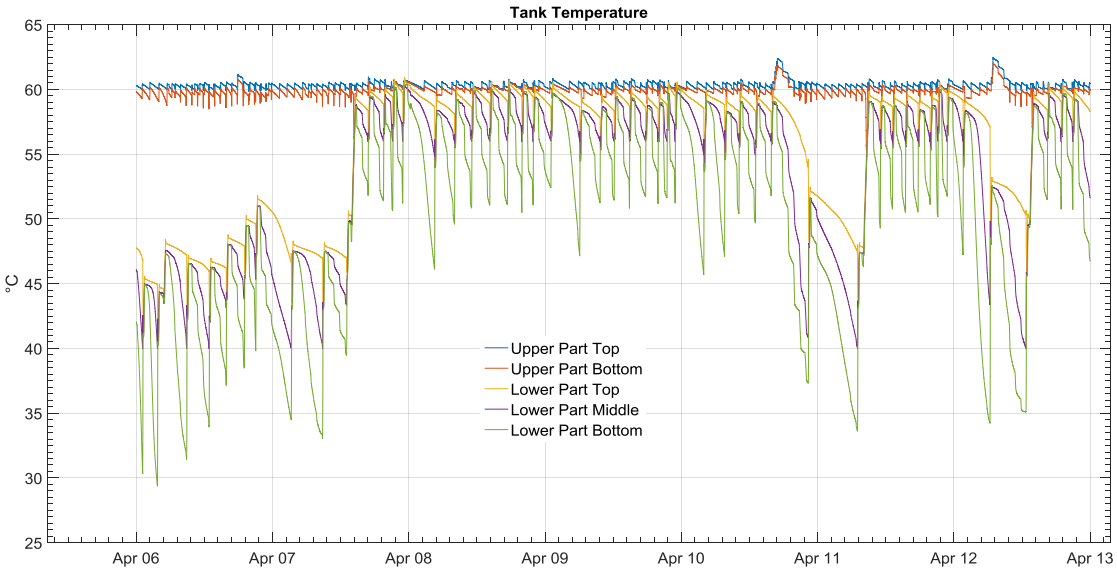

Figure 23 Hot water storage tank temperatures.

The electricity interactions of the system, both with the national grid and the equipped battery, can be visualized in Figure 24. Negative numbers in the figure represent electricity deficit, or import from the grid/discharging of the battery, and positive numbers are surplus, or export to the grid/battery charging.

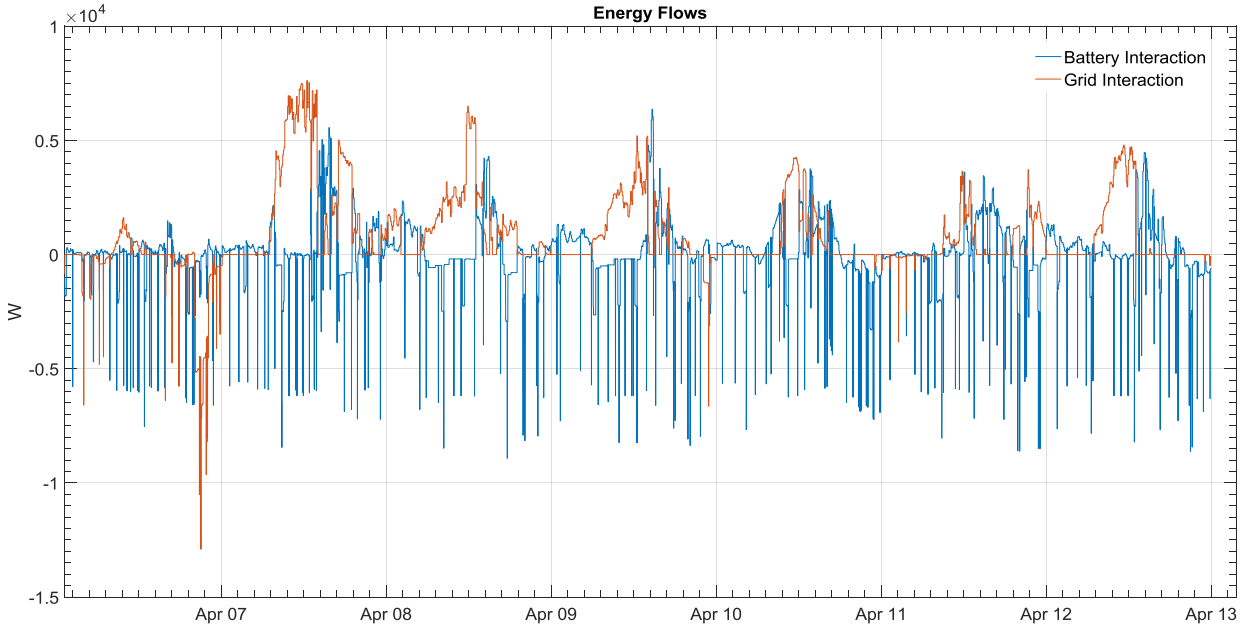

Figure 24 Battery and grid interaction during the studied week.

4.4.4. Conclusions and lessons learnt

By comparing the battery state-of-charge with the electricity price, it can be seen that the EMS was improving the overall electricity use of the emulated building. It anticipated upcoming increases in electricity price by charging the battery. Furthermore, it was able to optimize the self-consumption of the local electricity production by firstly using local generation to cover the demand in the mornings when electricity was generally more expensive and then charging the battery with cheap imports during afternoons.

The hot water storage tank was also utilized by the EMS to optimize the energy flexibility use of the building during the studied week. The bottom part of the tank was allowed to cool down during periods when local electricity generation was low and space heating demand high. In the middle of the week, there were a couple of warm and sunny days during which the EMS charged the tank to a higher temperature so that the extra heat could be used later on. It is worth noting that the GSHP used in the emulator platform had a maximum condenser side temperature of 60 °C, heavily limiting the charging possibilities of the tank. The tank was also equipped with an electric heater but converting electricity into heat at a COP of one is typically not worthy for storage purposes. Nonetheless, there were two occasions when local electricity demand was very low, battery full and electricity price low all at the same time. During these two periods, the EMS used

the heater to raise temperature of the top part in the tank by a few degrees to anticipate upcoming DHW use.

Overall, the EMS performed according to design in this study and gave added flexibility to the energy use of the building. The largest contributor to flexibility was the electric battery. The potential of the hot water storage tank could not be utilized to its fullest due to the GSHP only being able to provide a maximum temperature of 60 °C, which was coincidentally also the minimum temperature required for the DHW heating. Load shifting of appliances was not considered in this study as a source of flexibility as its contribution to the overall energy use was estimated to be very minor compared to that of the battery and the storage tank. However, it would have most likely had a substantial effect if the study focused on peak load shaving instead.

A model predictive controller (MPC) was developed in the project as part of the EMS using optimization methods to make optimal decisions at each time step to minimize the operating energy cost considering the weather forecast and the energy price in the next time-steps. The MPC uses successive linear programming (SLP) to solve the handled optimization problem (Kilpeläinen et al., 2019) (Ruusu et al., 2019). The MPC can control the operation of the GSHP and the electric heater installed in the hot water tank, as well as charging/discharging the battery and interactions with electricity and the heat networks.

We can indicate the following points that need to be considered for integrating the MPC in the real facility operation:

- The MPC was first run under a simulation environment to test the speed and robustness of the results of the optimization before installing it to the real facility.
- It is important to select a fast enough optimization algorithm that should be suitable to work within the selected time step in the real facility.
- To use a fast method, this may need to apply simplifications on the handled optimization problem (e.g. converting a nonlinear problem into a linear problem). However, this may lead to non-optimal results, especially when the problem is non-convex.
- To evaluate the accuracy of the implemented algorithm, the results were compared with those from a time consuming but more accurate algorithm that was making exhaustive search for finding the optimal solutions at each time step.

5. Danish Technological Institute. The OPSYS test rig

5.1. General presentation of the laboratory facilities

The OPSYS test rig emulates a house with an underfloor heating system to which a ground source heat pump can be connected. Figure 25 shows a principle sketch of the system. The system has two main elements denominated the hot side and the cold side as seen from the point of view of the heat pump (cold side = evaporator side, hot side = condenser side).

The hot side emulates the underfloor heating system (can also emulate a radiator system) with the possibility of using a buffer tank. The underfloor heating system is emulated via a series of parallel-connected heat exchanges resembling each room in the house. Hot water draw off may also be emulated, but this is currently not part of the test setup.

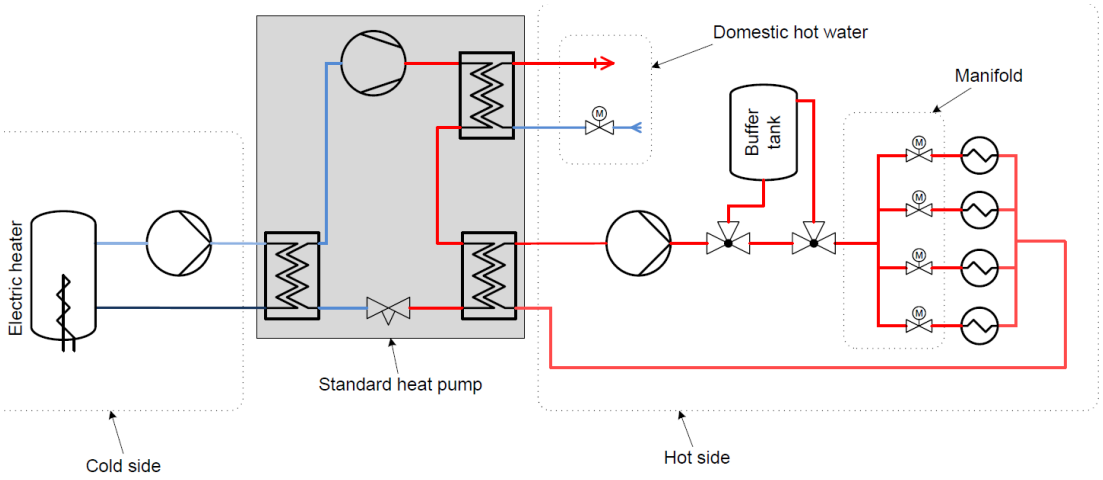

Figure 25 Principle sketch of the OPSYS experimental setup.

The heat consumption is programmable in order to simulate different sized rooms of a house with different load conditions. The controller of the experimental setup is running a simulation program, which calculates the heat demand of the rooms and provides an emulated room temperature as well as an emulated return temperature of the water from each “room” as input to the control of the manifold. On the one hand, this makes it possible to emulate the today typical control of an underfloor heating system in an ordinary home. On the other hand, other more advanced control strategies may also be tested. The sizes and functions of the “rooms” can easily be changed in the simulation program by changing the load pattern and the heat loss of the “rooms”.

The cold side of the experimental setup (see Figure 25) emulates a heat source, e.g. the ground. This is an electric heater, which is controlled in order to obtain a brine temperature defined by the

simulation program. With this method, seasonal variations of the ground temperature and different lengths of tubes in the earth can be emulated as well.

5.2. Description of the test facility

5.2.1. General principle and testing possibilities

General testing principles

The general concept of the semi-virtual test rig is presented in Figure 26. An actual device (heat pump or control of the thermostats in the heating system) is placed in the test rig, where it is studied under specific conditions which are simulated and implemented in the virtual environment. The overall principles are as follows:

- Test of the components under defined building and environmental conditions.
- Development and integration of innovative control of heating systems.
- Analysis of equipment behaviour at specific transitory phases for performance improvement.

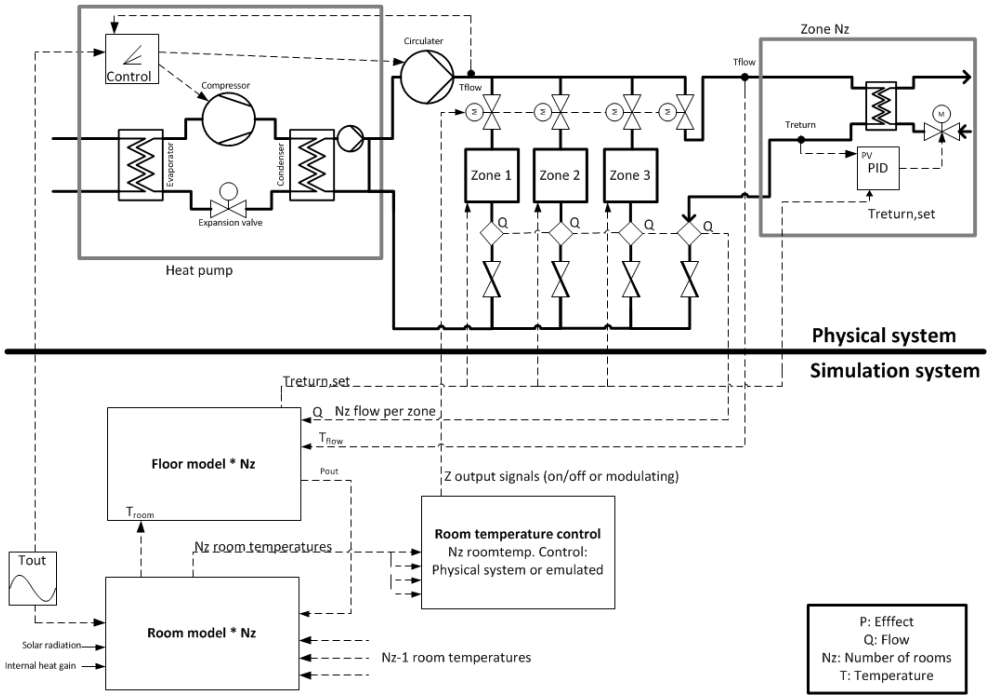

Figure 26 General concept of the semi-virtual OPSYS test rig.

Detailed testing principles

- Experimental testing of the control of the forward temperature of a heat pump.
- Experimental testing of the control of the water flow through a heat pump and through the different circuits of a heat emitting system.
- Demonstration of optimal combined control of a heat pump and the heat emitting system in a house.
- Demonstration of advanced control of a heat pump and the heat emitting system in a house with the purpose of optimizing the efficiency of the complete system and/or providing energy flexibility to the surrounding grid.

5.2.2. Available equipment and specifications

Heat emitting system

The heat emitting system consists of four heat exchangers, which emulate the heat demand of the house (see Figure 28 and 29). If necessary, more heat exchangers may be added to the test rig.

The virtual heat load on each heat exchanger is simulated by a house model, which is developed in Dymola (Modelica) and embedded in the control system of the test rig as an FMU (Functional Mock-up Unit). The physical heat loads on the heat exchangers are created by the central cooling system at Danish Technological Institute, Energy and Climate Division. The flow rate of the cooling water in each heat exchanger is determined by the return temperature of the warm water leaving the underfloor heating, which is simulated by the house model.

The hot water flows in the heat exchangers are controlled by traditional actuators for underfloor heating systems. The actuators consist of valves controlled by a wax motor (see Figure 27). When heating the wax with an electric current, the valves open. The valves close again when the current is turned off. The valves may either be on/off controlled or be kept partly open by pulsing the current through the wax motors. The position of the actuators is determined by the simulated room temperature and the implemented control algorithms of the actuators. The heat exchangers are Reci PHE-TYPE: LP80Tx40 with a capacity of 8 kW. The actuators are from Uponor. The running time from fully closed to fully open and vice versa is 300 seconds.

The test rig is developed in a Danish project with the aim of increasing the Seasonal Performance Factor of heat pumps by optimization of the forward temperature from the heat pump and the flow rate through the heat pump (Jensen et al, 2018). However, as the control of the system is on the computer connected to the test rig, many different control options may be tested. One option is to control the heat pump according to the need of the surrounding power grid in the terms of providing energy flexibility. Traditionally, energy flexibility of heat pumps has been tested by switching the heat pump on and off. However, increased energy flexibility may be achieved by

pre-heating the building within the comfort limits of the room temperature before the heat pump is switched off due to a period with limited power in the grid. This requires a more advanced control including forecast of the future power level in the grid and the heat demand of the house. As the control of the test rig is implemented on the controlling computer, highly advanced control scenarios may be tested in the test rig and subsequently transferred to commercial control devices.

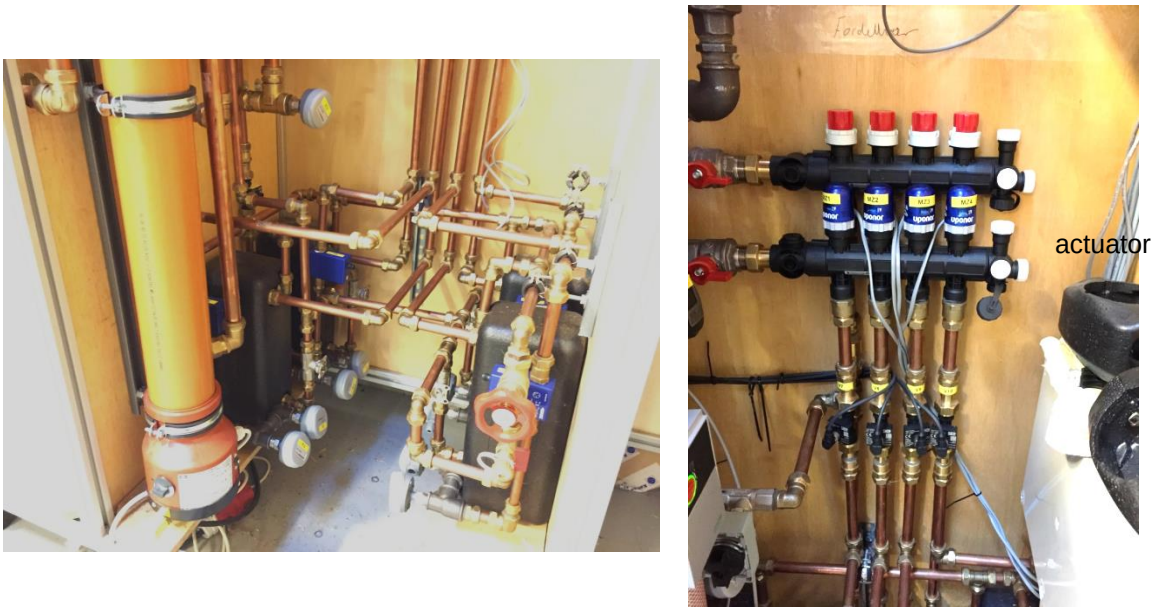

Figure 27 The heat exchangers emulating the heat emitters in a heating system (left). The actuators of the heating system (right).

Brine circuit

The brine circuit consists of a heating element in series with a 300 L insulated buffer tank. The heating element is controlled in order to provide the heat pump with the desired brine temperature. The simulation program controls the brine temperature so that it matches the time of the year run by the simulation program.

The buffer tank smoothens out any temperature variations of the brine temperature created by the control of the heating element, which has a capacity of 7 kW.

Originally, the test rig is designed for testing ground source heat pumps, which has been the most commonly used type of heat pump in Denmark. If an air-to-water heat pump needs to be tested in the test rig, the outdoor unit of the heat pump should to be located in one of the climate chambers at the Energy and Climate Division, DTI.

Heat pump

The first heat pump installed in the OPSYS test rig was a ground source heat pump from Bosch: Bosch Compress 7000 LWM 3-12 kW (Bosch, 2017). The heat production can be varied continuously between 3 kW and 12 kW. Below 3 kW on/off control is necessary.

The heat pump may be controlled by five inputs and five outputs in the control of the test rig. The simplest way to control the forward temperature of the heat pump is to manipulate the ambient temperature, which the heat pump "senses". For the above-mentioned heat pump from Bosch, the ambient sensor was replaced with a controllable voltage signal, which - when knowing the heating curve of the heat pump - may be adjusted so that the heat pump delivers the desired forward temperature.

5.2.3. Data acquisition and control

The test rig is controlled by a Python script running on a PC and a BMS system on the test rig. Figure 28 shows the connections between:

- the computer running the Dymola house model (as a FMU), the interface to the Trend BMS (CTS 963 software) and the control of a separate datalogger (Agilent DAQ)
- the Trend controllers (BMS) via the sip
- the datalogger (Agilent)

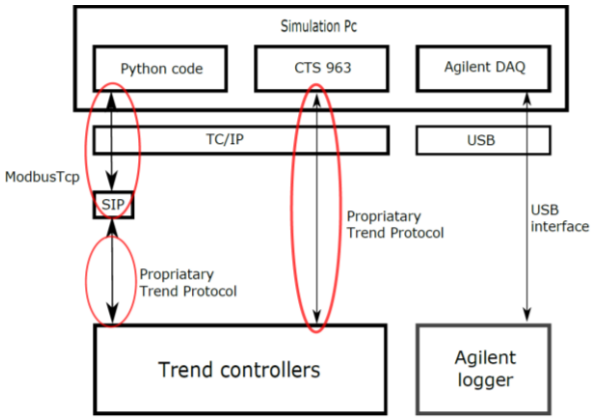

Figure 28 The connections between the test rig, the simulatior and the datalogger.

The BMS system of the test rig is composed of modules from Trend: one IQ4E and four 8UIO modules. The BMS is developed and interfaced by the Trend 963 software. Trend 963 is a Windows based software package, which provides a management interface between the user and the Trend IQ building control system.

The Trend BMS modules communicate with the components of the test rig via a sip ModBus/vIQ module. The sip is an interface between the BMS and the components of the test rig using the serial ModBus protocol.

The heart of the virtual part of the test rig is the FMU, which runs a simulation of the heat demand of a typical Danish house. Three typical Danish houses with a floor area of 150 m^2 from three different time periods have been developed (Jensen et al., 2018):

- a house from the 1970's
- a house built according to the Danish Building Regulation 2010
- a house built according to the Danish Building Regulation 2015

The house models contain typical free gains from occupants, appliances and solar radiation. The house models use typical Danish weather conditions and an annual profile for the temperature of the brine to a ground source heat pump.

The parameters and values of the house models may be changed to reflect other building types and weather conditions.

The house models simulate the heat demand of the rooms of the house and transfer the room temperatures and the return temperatures of the underfloor heating system of the rooms to the control script, which also runs on the computer.

Figure 29 shows a screenshot of the interface of the BMS with the four heat emitting systems. The test rig can either be controlled by the Python control script which runs on the computer,or manually to perform step response tests for example.

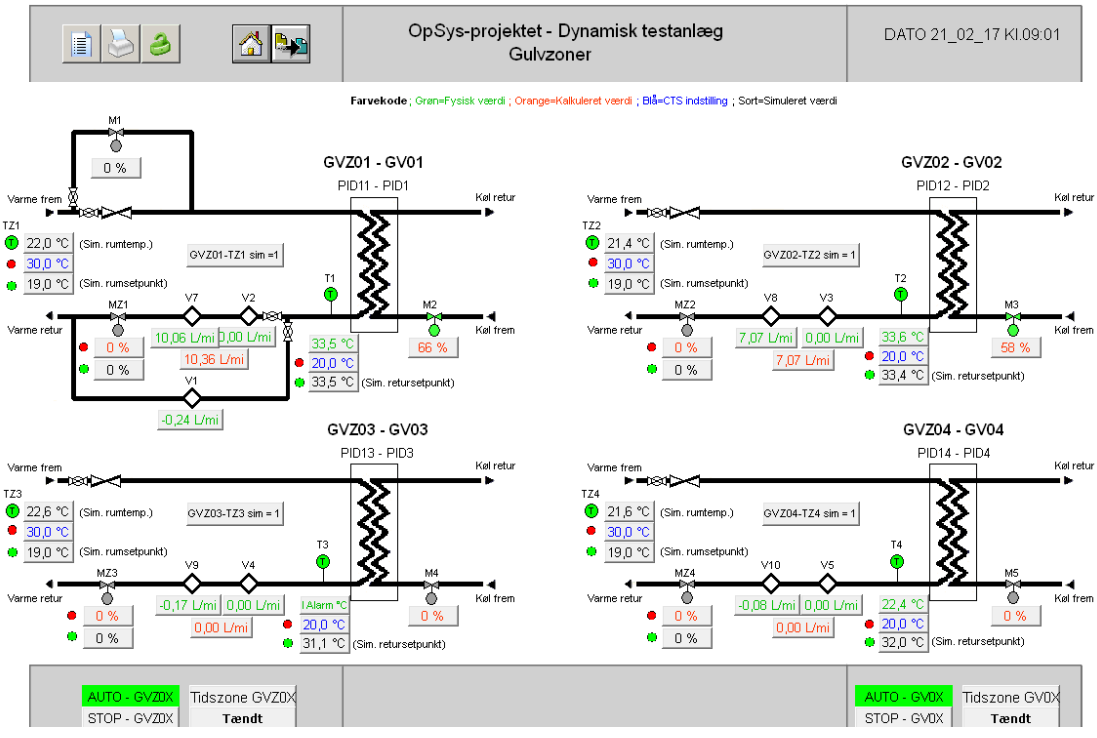

Figure 29 Screenshot of the OPSYS BMS interface showing the heat emitting system.

The test rig is equipped with several physical and simulated virtual sensors measuring/calculating temperature, flow, energy, and actuator positions -please see (Jensen et al., 2018) for a description of the sensors configuration-. The measurements are collected by the BMS, the

datalogger and the house model, and subsequently transferred to a database on the computer which runs the test rig.

Special purpose Python scripts have been developed for extraction and alignment in time of the measured data from the database.

5.3. Example of previous studies

5.3.1. Underfloor heating and heat pump optimization

The OPSYS test rig has been developed as a central part of the Danish research project: Underfloor heating and heat pump optimization (Jensen et al, 2018).

The purpose of the project was to minimize the gap between the accredited efficiency of domestic heat pumps and the actual efficiency when being installed in a house. Unfortunately, measurements on existing heat pump installations (Poulsen et al, 2017) have shown Seasonal Performance Factors (SPF mean annual efficiency) well below expectations as the heat pumps and the heat emitting systems are rarely properly adjusted at the installation of the heat pumps. Moreover, the operating parameters are not continuously adjusted according to the actual operating conditions. As an example, the supply temperature is often set too high in order to guarantee sufficient space heating. A supply temperature higher than needed results in a lower SPF. Typically, an increase of 1°C in the temperature difference between the cold side and the hot side of a heat pump leads to a decrease of 2-3% in the COP (instant efficiency of the heat pump).

Therefore, the aim of the OPSYS project was to develop and test optimized control strategies for making heat pump installations more efficient. To facilitate this, two tools have been developed: the OPSYS test rig and the OPSYS annual simulation tool.

The OPSYS test rig and the annual simulation tool were tested in terms of simulating traditional on/off control of the heating system. The two tools gave realistic and comparable results. Then, the two tools were tested with a more advanced control for obtaining energy flexibility to deliver services to the electrical grid as described in the following section. For this case as well, the two tools gave realistic and comparable results showing that they are capable of investigating more advanced controls.

Two more advanced controllers: a Model Predictive Controller (MPC) and an Artificial Neural Network (ANN) controller were investigated using the annual simulation tool. Savings of the electricity demand to the heat pump of up to 13 % were found for the investigated periods. These savings were obtained even when the overall COP of the system was as high as 3.9 with the traditional PI controller. Thus, the hypothesis of savings up to 25 % for a heat pump installation

with traditional control and a SPF of around 3 (which is typical for Danish heat pump installations) seems realistic.

MPC and ANN controllers require more computational resources than traditional PI controllers, but certainly not prohibitively so. It is estimated that the supervisory controller, in either nonlinear MPC or ANN configuration, can easily be implemented and executed on e.g. a cheap Raspberry Pi with 0.5 GB RAM or similar industry-standard hardware. Furthermore, the supervisory control configuration makes it reasonably easy to interface with the heat pump and the underfloor heating subsystems.

The above results are very encouraging and lead to the conclusion, that MPCs and ANNs are promising candidates for optimized control of heat pump installations, where the performances of both the heat pump and the heat emitting system are optimized together. Therefore, the problems with poorly performing heat pump installations documented in (Poulsen et al, 2017) may most likely be solved by switching from traditional PI control of the heat emitting system to advanced combined control.

5.4. Experiment on energy flexibility

5.4.1. Objective

A first study with a simple control to obtain energy flexibility with the purpose of supporting grid operation has been conducted both in the OPSYS test rig and with the OPSYS simulation tool. The aim of the study was to determine if the OPSYS test rig and the developed simulation tool are also suitable for research and development in the field of advanced controllers for obtaining energy flexibility from the combined system of a heat pump and a heat emitting system.

The results of the simulations and the test in the OPSYS test rig have been documented in (Jensen et al., 2018). A brief summary of the results are described in this section.

5.4.2. Brief description

The focus of the study was a Danish single-family house from the 1970's with a set point indoor temperature of 22 °C during the day and the night setback at 19 °C as shown in Figure 30 (blue line). The aim of the tests was to study the obtainable energy flexibility if the set point for the room air temperature was decreased at the beginning of the cooking peak (red line after 17:00). The "cooking peak" (green box) is when people return home from work and start cooking and use other electrical appliances. This is the highest peak in the Danish power grid. To increase the obtainable energy flexibility, excess heating of the house before the cooking peak was also carried out by increasing the room set point temperature (red line before 17:00). Different scenarios were investigated with the OPSYS simulation tool, where different decreases and increases of the set

point (1 K and 2 K) were investigated together with a variation of the length of the increase of the set point (one or two hours) before the cooking peak.

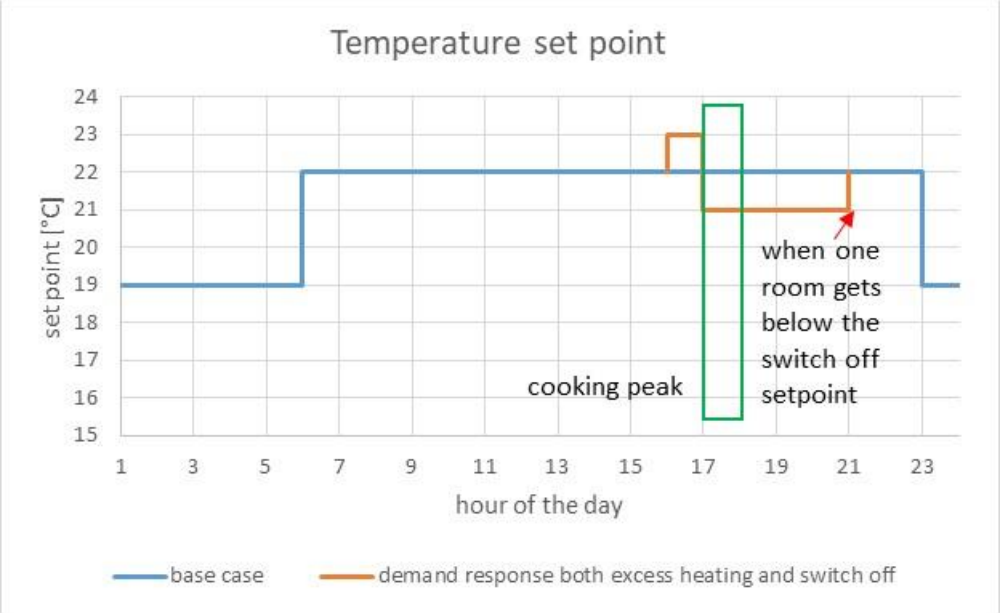

Figure 30 Variation of the room set point temperature during the study.

5.4.1. Results

The main analysis was carried out with the fast simulation tool as the OPSYS test rig runs at real time, which makes it less suitable for carrying out large series of parametric studies.

One specific scenario was also carried out in the OPSYS test rig: the increase of the set point with 1 K one hour before the start of the cooking peak and a decrease of 1 K (2 K compared to the increased set point) at the start of the cooking peak. This scenario is illustrated by the red line in Figure 30. A comparison between the simulation and the measurements showed remarkably good compliance, as seen in Figure 31 comparing the room temperatures and the duration of the possible set back for one day. The test rig and the simulation tool gives almost identical results and equal duration of the possible set back from the start of the cooking peak (black curve in Figure 31).

The simulation tool includes a rather simple model of a heat pump in order to make the simulations fast. The hydronic of the simulation tool is also fairly simple. In comparison the test rig includes a real heat pump and real hydronic with all the complexity this involves. In spite of this, the two tools give rather identical room air temperatures and similar integrated power demands of the heat pumps, although the actual patterns of the power uptake of the heat pumps are somewhat different due to the simple model of the heat pump in the simulation tool. The set point responds as desired: it increases and decreases when asked to. More importantly, it is able to respond to the actual state of the house, i.e. return the set point back to the base case when, in this case, one of the room needs heating. Based on this and the previously mentioned tests with MPC and

ANN, it is assessed that the OPSYS tools will be valuable when developing more advanced control for obtaining energy flexibility. Especially, where the control set up is developed using the simulation tool while the chosen concept is tested as hardware in the loop in the test rig in order to determine if the developed control strategies will perform as expected in a more realistic environment.

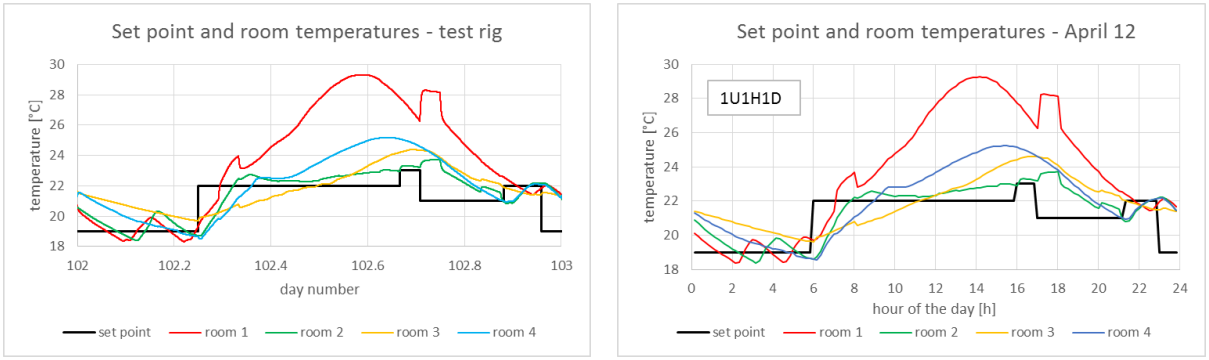

Figure 31 Room temperatures and set point from the test rig (left) and simulation tool (right). The more squared appearance of the set point curve from the test rig is due to measurements taken every 15 seconds while the time step of the simulation was 10 minutes.

Several combinations of set point increase before the cooking peak (xU), time of the start of the increase of the set point (xH), and decrease of the set point at the start of the cooking peak (xD) were studied. The labelling of the different tests was xUxHxD – i.e. the test configuration presented in Figure 31 was 1U1H1D.

Figure 32 shows a day were the only set point change was a decrease of either 1 or 2 K at the start of the cooking peak. For this day, the increased setback of 1 K (from 22 to 21 °C) leads to an increase of the possible duration of the setback from 1 hour and 40 minutes to 3 hours and 10 minutes (almost a doubling of the possible duration time).

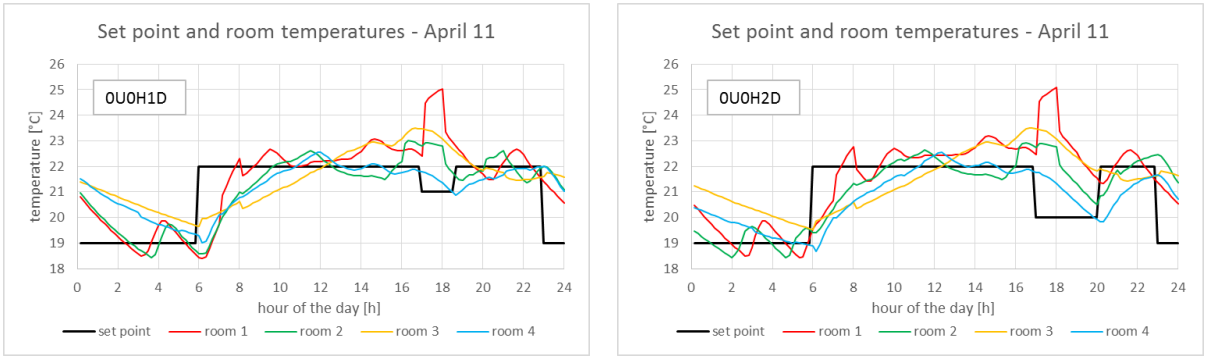

Figure 32 Comparison of the possible duration of the setback period with a set point decrease of 1 K (left) and 2 K (right) on April 11th.

However, the possible duration of the setback varies over the year due to the ambient temperature and the solar radiation. The high temperature in room 1 shown in Figure 31 was due to clear sky

conditions, which resulted in much solar radiation coming into room 1. Figure 32 shows the next day with cloudy conditions. Here, the room temperatures are lower, which leads to a shorter duration of the possible setback. As the possible duration and thereby the possible amount of energy, which can be shifted away from the cooking peak, vary over the year, there is a need for some kind of indicators which allows for a comparison of different control strategies. (Jensen et al, 2018) investigate three possible indicators: mean monthly duration of the setback (Figure 33), shiftable power, and shiftable energy (Figure 34).

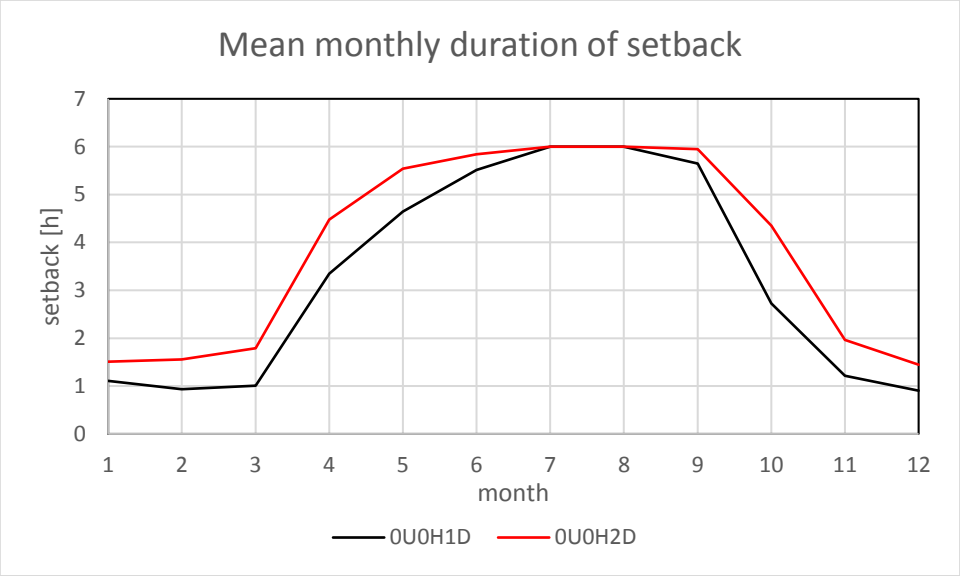

Figure 33 Comparison of possible mean monthly duration of the setback period with a set point decrease of 1 K (0U0H1D) and 2 K (0U0H2D).

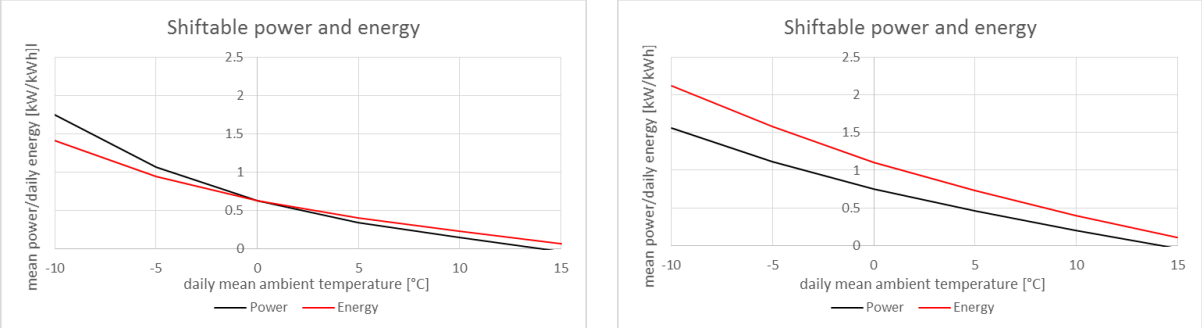

Figure 34 Comparison of (trend lines for) the possible amount of daily shiftable energy and the mean shiftable power at a set point decrease of 1 K (0U0H1D - left) and 2 K (0U0H2D - right) for the considered 150 m^2 house.

The values in Figure 33 and Figure 34 are only probable values and not necessarily obtainable as e.g. the influence of solar radiation is significant. However, it gives an idea of the magnitude of energy flexibility which a house may offer to the grid.

Furthermore, it is not known when energy is available for being shifted during the possible setback as seen in Figure 35. On April 10th, shiftable energy is first available from 8 pm while the next day with cloudy conditions, shiftable energy is available from 6 pm. This means that during these days, no energy can be shifted during the actual cooking peak. The reason for this is the large amount of heat from cooking and using other appliances to the main room 1 during the cooking peak. Thus, it could be argued that this specific house already delivers energy flexibility to the grid without advanced control as no power to the heat pump is needed during the cooking peak. However, this is only true for the type of days shown in Figure 35. During colder periods, it is possible to shift energy during the cooking peak if the heat pump is sufficiently powerful to restore the room temperatures to normal shortly after the cooking peak.

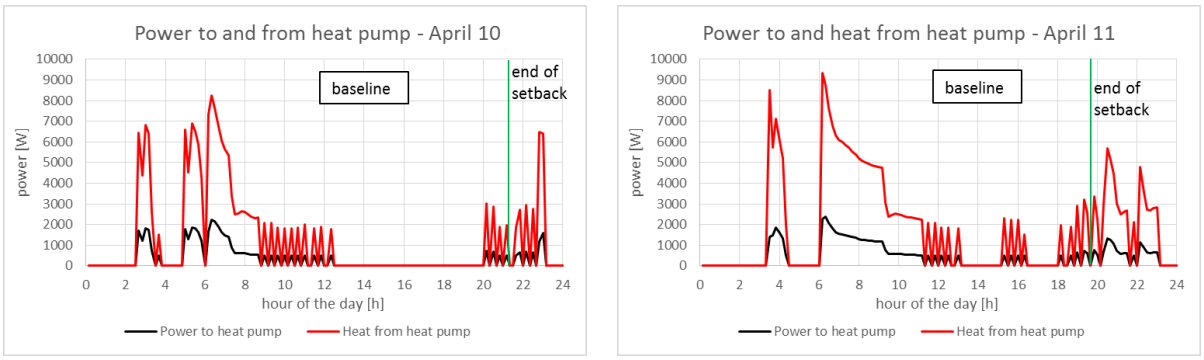

Figure 35 Power demand and heat production without control for gaining energy flexibility.

Similar to Figure 32, parametric studies with excess heating prior to the cooking peak have also been carried out, where the set point was increased by 1 or 2 K one or two hours before the cooking peak. The results for this specific house show that if the set point is decreased 2 K at the start of the cooking peak, the duration of the setback and the possible amount of shiftable energy do not increase significantly when excess heating is introduced prior to the cooking peak. However, if the decrease of the set point at the start of the cooking peak is only 1 K (e.g. due to comfort reasons) excess heating prior to the setback would increase the duration of the setback significantly.

After a setback of the set point, there will typically be a rebound effect where more heat is needed to restore the room air temperatures to the normal level. In the investigated cases, the annual energy demand to the heat pump varies less than 1 %. The reason for this is the night setback. If the end of the setback is close to or beyond the start of the night setback, the necessary rebound energy will be small or non-existent as the heat pump will be switched off at the start of the night setback. The night setback temperature in this case is lower than the set point temperature for obtaining energy flexibility.

5.4.2. Conclusions and lessons learnt

Based on the above described study, it is assessed that the two OPSYS tools are suitable for investigating and developing more advanced controls for obtaining energy flexibility from houses with heat pumps.

However, it is very important that the two tools are calibrated together to ensure similar results. This is not an easy task and it should be carried out very carefully. The main problem is that the simulation tool is very simplified in order to be fast, while the test rig carries all the complexity of real life and even more, as the heat load and heat uptake has to be emulated.

As the brine side is emulated with a heating element and the heating load is emulated via heat exchangers connected to a cooling system, there is a risk of fluctuating temperatures. The main concerns during the design of the test rig were the four heat exchangers emulating the heating loads of the house. Would it be possible to obtain stable conditions for these when using PID control? It turned out that these four heat exchangers perform exactly as supposed. However, it was the brine side of the heat pump that gave problems with too fluctuating temperature. A 300 L buffer tank between the heating element and the heat pump improved the situation, but not enough. A careful tuning of the PI control of the heating element based on the brine temperature on each side of the buffer tank, resulted in sufficiently low fluctuations of the brine temperature.

Sensors and meters at the test rig need to be calibrated before a test in order to make sure that what is measured is correct. As an example, two flow sensors were used in each circuit of the four heat exchangers emulating the heat load: one for low flow and one for large flow. The two sensors range are overlapping (the high end of the low flow sensor is overlapping the low end for the high flow sensor), so a routine for obtaining mean values of the two measurements in this range, was needed.

Two sensor sets were used on the test rig: one set for controlling the test rig (used by BMS) and one set for partly obtaining values that were not measured by the first sensor set and partly as sensors in parallel with the first sensor set. The latter in order to be able to control important BMS measurements being used for controlling the test rig. The second sensor set proved to be very valuable when calibrating the test rig.

Test on the test rig runs in real-time as it is a hardware in the loop setup. This means that one has to be very careful when defining and setting up a test. It is also important to follow the tests very closely in order to quickly correct any problems so that valuable time is not lost due to an otherwise necessary restart of a test. If e.g. a problem occurs at the end of a two-week test, it is important that the problem is dealt with immediately in order to prevent that the test needs to be re-run.

6. NTNU/SINTEF. The ZEB Living Laboratory

6.1. General presentation of the laboratory facilities

The ZEB Living Laboratory test facility is a single family house with a gross volume of approximately 500 m^3 and a heated surface (floor area) of approximately 100 m^2. The building was realized with state-of-the-art technologies for energy conservation measurements and renewable energy source exploitation. It was designed to carry out experimental investigations at different levels, ranging from envelope to building equipment components, from ventilation strategies to action research on lifestyles and technologies, where interactions between users and low (zero) energy buildings are studied. The building is equipped with multiple energy systems and monitoring technologies and it is controlled by an on-purpose developed system which allows different types of experimental campaigns, including testing energy flexibility in buildings.

The ZEB Living Laboratory is run and managed jointly by the Norwegian University of science and Technology (NTNU), and SINTEF Building and Infrastructure. It is part of the ZEB Laboratories system, which also includes the ZEB Test cell Laboratory, and the ZEB Advanced Materials and Component Laboratories.

The ZEB Laboratories system is involved in numerous projects with different partners:

- Direct contracts for equipment testing, development of technical solutions, improvement of systems, etc.
- Partnership for national / international R&D projects
- Shared developments for new products

6.2. Description of the test facility

6.2.1. Architecture and building equipment

Architecture and building technology

The Living Lab (Figure 36) is organized in two main zones: a living area facing south and a working/sleeping area towards the north. The entrance is located in the southwest corner, and through a anteroom comprising a wardrobe, the user gets access to the living room. The kitchen is located at the opposite end of the living room. An automated double skin (ventilated) window is installed in the living room, covering the largest part of the south facade. At the centre of the north

zone, there is a shared studio area equipped with a long writing desk and with an automated window.

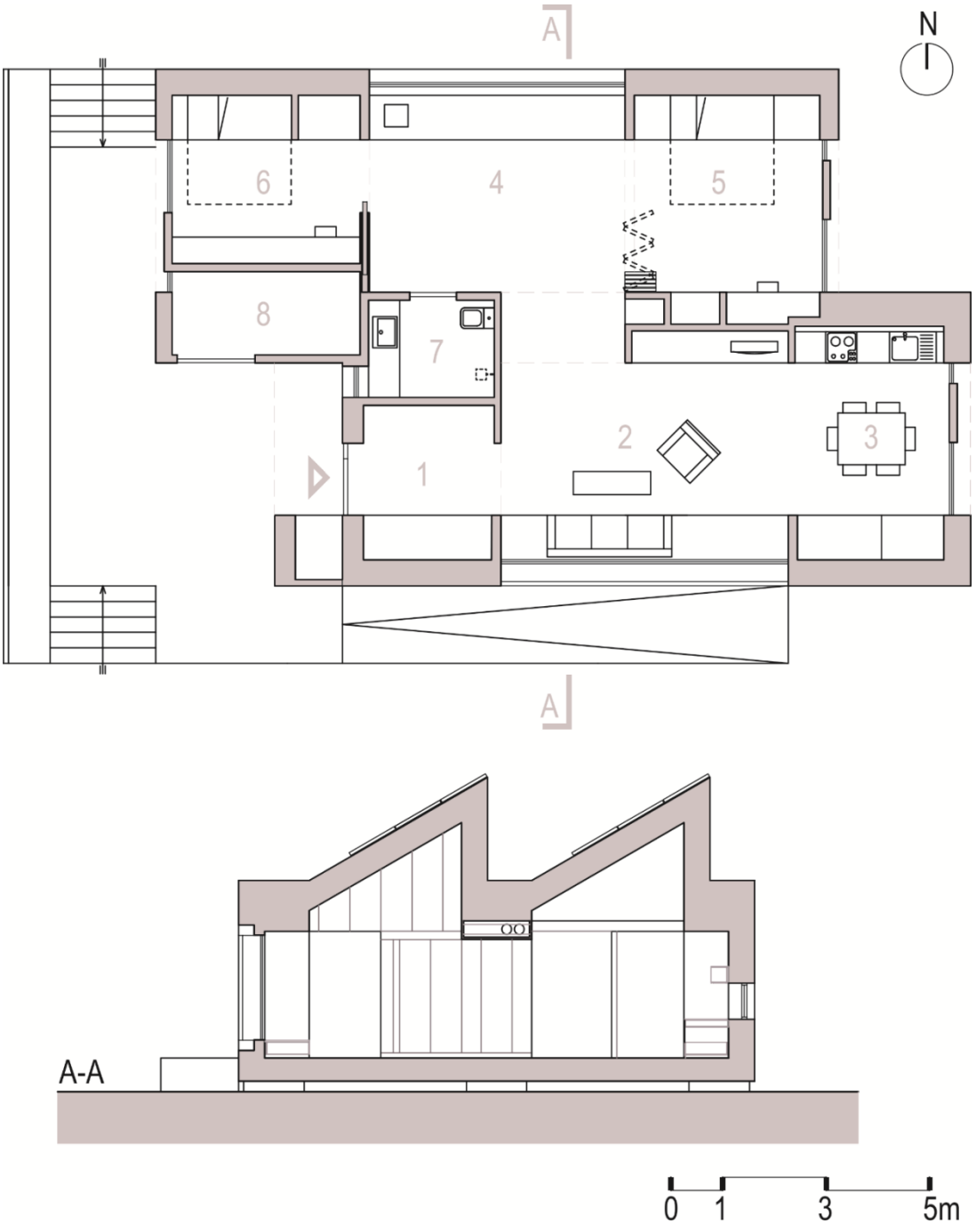

Figure 36 Plan and vertical section of the Living Laboratory (1: entrance; 2: living room; 3: kitchen; 4: studio room; 5,6: bedroom; 7: bathroom; 8: technical room). Original Figure in (Goia et al., 2015).

Two bedrooms (one facing east and one facing west) are located at the two sides of the studio room. The technical room (accessible from outside the building), bathroom (accessible from the studio room) and the kitchen are placed all along the central spine of the building in order to

optimize the distribution of the technical equipment. A small mezzanine is placed above the west bedroom. It is equipped as sleeping area for guests or as play area for children.

The building construction has been optimized through a set of preliminary simulations, resulting in a highly insulated envelope with a window-to-wall ratio of around 20%. Walls, floors and roofs are made out of a conventional wooden-frame structure with a double layer of rock wool insulation for a total thickness of 40, 40, and 45 cm respectively. The U-value of the elements is 0.11, 0.10 and 0.11 W/m^{2}K, respectively. All the windows are characterized by low U-value (Ranging from 0.65 W/m^{2}K for the south window, up to 1.00 W/m^{2}K for the roof windows).

Building equipment

The Living Lab is designed to minimize energy demand for its operation and to harvest solar energy to such an extent that converted solar energy (both through passive measures and active technologies) is larger, on a yearly basis, than the building energy demand. By making available more energy from renewable sources than that necessary to operate the building along its entire life, emissions embodied in the constructions are therefore compensated. The energy flow within the building plant, including on-site renewable energy supply, is schematically illustrated in Figure 37.

The thermal energy necessary to cover heating, ventilation and domestic hot water (DHW) demands is primarily planned to be obtained by a ground source heat pump (GSHP in Figure 37), which is connected to a surface collector field (total length of the approximately 150 m) located in the backyard on the north of the Living Laboratory. The heat pump has a nominal output of 3.2 kW (under standard test conditions B0W35) and a nominal COP of 3.7. In case of thermal output at a higher temperature level (55 °C), the nominal COP is 3.0 (B0W55) and the nominal thermal power is 2.6 kW. The heat pump has a very simple control logic, which turns on the scroll compressor to full power when a heating (thermal output at 35 °C) or DHW (thermal output at 55 °C) load is received by the controller, and turns it off when the load signal is over. Control of the signals for heating or DHW load is achieved through the building-level control system, integrated in the building monitoring and control system.

The plant-side of the heat pump is connected to an integrated tank (IWT in Figure 37) that combines a buffer tank (BT) for the heating circuit (160 L) and a DHW tank of 240 L (DHTW). The lower buffer tank is equipped with two coils: one connected to the thermal panel circuit, and the other connected to the DHW circuit for preheating of the sanitary water. After flowing in the coil of the lower tank, the DHW is stored in the upper tank. This upper tank has also one heating coil connected to the heat pump condenser. The heat pump and space-distribution circuits have a direct connection to the buffer tank. Two auxiliary electric coils (3 kW and 9 kW) are installed in the integrated water tank, one for each of the two vessels.

For research purpose, two different terminal units for the heating system are available in the building and planned to be operated independently: a floor heating system and a 2 kW high-temperature (55 °C) radiator. Underfloor heating panels are located under the entrance, the living

room, the kitchen, the studio room, the bedrooms, and the bathroom. As the building is highly-insulated, the space heating distribution can be simplified. For that purpose, a single radiator is installed in the living room, approximately at the centre of the building. It is also possible to use a combination of these two systems (e.g. the radiator can be used in combination with the floor heating in the bathroom).

Heating through the air ventilation system (ventilative heating) can also be used to cover heating demand in combination with fresh air supply. In this case, underfloor heating in the bathroom is expected to operate in combination with the overheated fresh air supply.

The building is equipped with a balanced mechanical ventilation with nominal air flow of 120 m^3/h, and possibility to regulate the airflow up to 360 m^3/h. Air diffusers are evenly distributed in the building (living room, studio room and two bedrooms), while extraction takes place in the kitchen (to a small extent) and in the bathroom (to a larger extent). Air supply and exhaust are managed by a compact air handling unit that integrates a heat recovery system with rotatory wheel. The nominal heat recovery efficiency of this system is 85% (with a flow rate of 250 m^3/h). The unit is equipped with an electric coil (1.2 kW) capable of heating the supply air up to 40 °C (for ventilative heating purpose). A water coil (2 kW) is also available for post-heating of supply air and it is connected to the buffer tank. The unit can only control the temperature but not the relative humidity.

The air handling unit has an integrated controller that manages the equipment independently by the centralized control/monitoring system. The unit is however connected to the (upper) building level control system, which can therefore manage the ventilation unit through its embedded controller. Hybrid ventilation strategies (combination of mechanical and natural ventilation) can also be activated thanks to the possibility offered by some of the windows in the building, which are equipped with electric driver to allow automated opening.

The artificial lighting of the Living Laboratory is based on an extensive use of LED strips and LED luminaires. Conventional LED strips (12 V DC) with nominal power input of 4.8 W/m, 9.6 W/m and 14.4 W/m are installed according to locations and the required luminous flux.

Floor lamps and a pendant lamp above the dining table complete the lighting configuration. All the luminaires are controlled by the building level control system and can be dimmed from 0 to 100% of the power through both physical (pulse switches) and virtual (on touch screen) interfaces. The central building control system records the status of the physical and virtual signals and consequently acts on 24 fast-response solid state relays to manage the LED stripes and lamps. The total installed power (including outdoor lighting) of the lighting appliances is 1.2 kW (DC side). The AC to DC conversion is assured by a transformer with an efficiency of 87%.

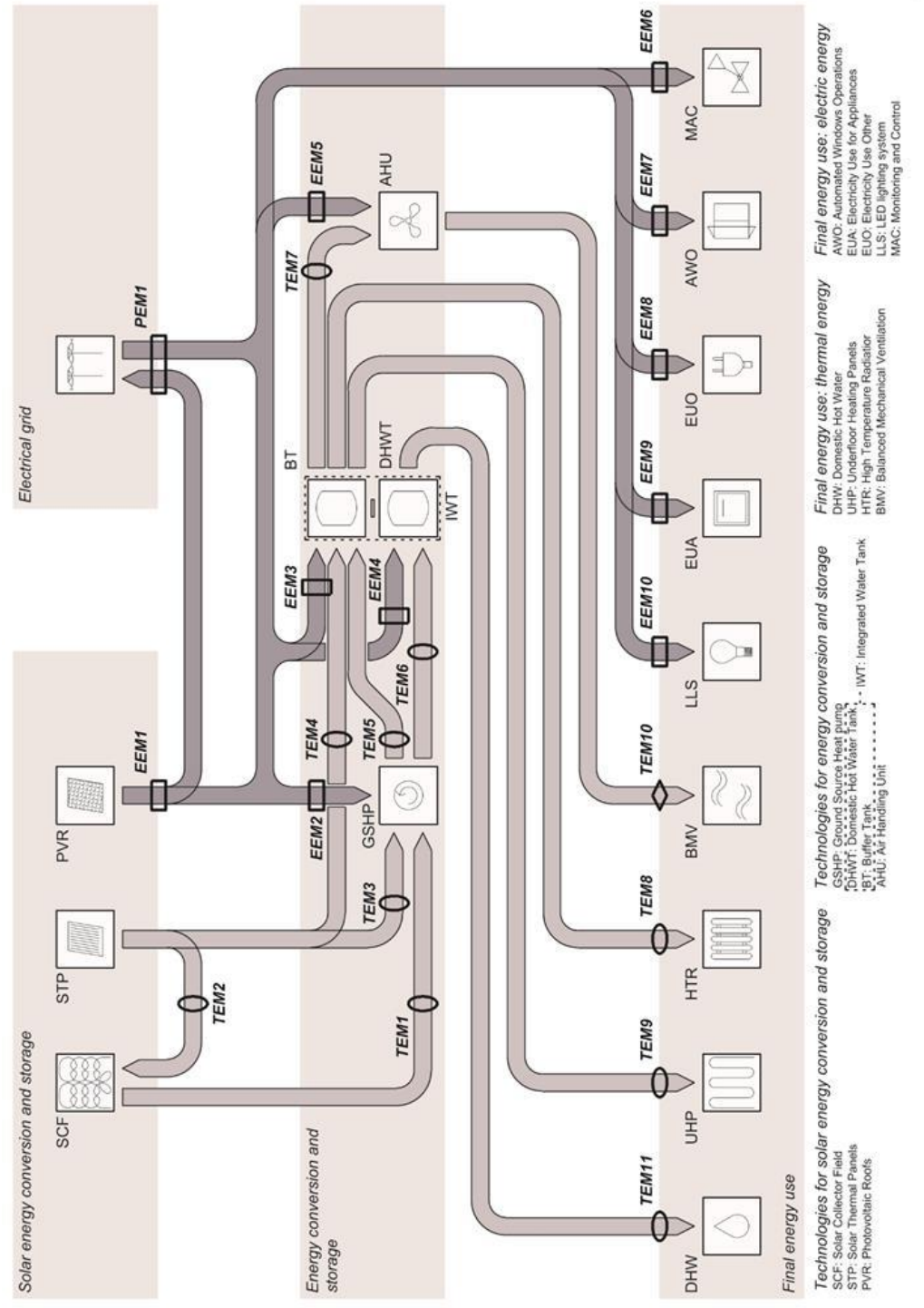

Figure 37 Thermal and electrical energy/power flow in the Living Laboratory; technologies and devices for energy conversion and storage and associated monitoring system. Original figure in (Goia et al., 2015).

Technologies for onsite renewable energy harvesting

Two façade-integrated solar thermal panels are installed on the south-facing façade of the building. They cover a total area of little more than 4 m^2, have optical efficiency of 0.82, and are connected to the buffer tank and to the GSUH-SCF circuit. A series of dedicated valves can change the direction of the flow of the heat carrier fluids in these circuits and different paths are therefore possible.

A total of 48 photovoltaic (PV) modules are installed on the two roof slopes of the building, 24 modules for each slope. Each PV module has a nominal power (values at STC) of 260 W, and the efficiency is just below 16%. The total installed power (DC) is thus approximately 12.5 kWp for both the roofs. Each PV roof is connected to a power inverter with a nominal AC rated power output of 4.6 kW (single-phase, 230 V line), with an efficiency of 96.5% (European weighted efficiency). An electric battery is not installed at the moment, but it is planned to add a battery with a capacity of around 20 kWh.

6.2.2. Monitoring and control systems

The monitoring system in the Living Laboratory has been developed in order to cover the following purposes:

- to monitor the most relevant environmental quantities, both indoor and outdoor
- to record users patterns and occupants' habits
- to measure energy use for heating, ventilation, DHW, artificial lighting, appliances and other uses
- to quantify solar energy exploitation and energy from the grid
- to assess efficiency in conversion and storage of energy for different uses, as well as energy flexibility

Starting from these aims, the requirements for the selection of the components of the monitoring system were set considering that:

- A compromise between accuracy, number and type of the sensors should be found – i.e. reaching the same measurement accuracy as in a laboratory test facility was out of the scope
- Sensors should be integrated in the building as they would be in a real house, and they should be chosen among those that can be installed in a conventional application
- For research reasons, more sensors can be installed than in a conventional building, the number and location of the sensors should be as close as possible to that which would occur in a real, occupied building
- The measurement system should be very flexible and allow easy upgrade

- The characteristics of the sensors should be so that measurements and data analysis can be performed according to the relevant technical standards for energy and comfort assessment (e.g. EN 15251, IEC 62053).

Sensors and transducers

The building is equipped with a weather station that integrates measurements of outdoor air temperature (Pt 100; accuracy: ±0.3 °C), relative humidity (thin film capacitive sensor; accuracy: ±3%), barometric pressure (piezoresistive sensor, accuracy: ±50 Pa), wind velocity (ultrasonic sensor, two axes; accuracy speed: ±3%; accuracy direction: ±2 deg), global solar irradiance on the horizontal plane (thermopile; accuracy: II class pyranometer). The weather station is installed above the roof of the building. A luxmeter is installed on the roof to record global (direct, diffuse, reflected) illuminance In the horizontal plane (thermopile; accuracy: ±5%). Global solar irradiance is measured in two other locations: on the roof slope plan and on the south façade, both by means of thermopiles (accuracy: II class pyranometer).

Outdoor air temperature is also recorded by means of two additional sensors located on the south- and north-exposed façade (Pt 100; accuracy: ±0.1 °C). Both sensors are suitably protected from the influence of direct solar irradiation.

Indoor air temperature values are measured in every room of the Living Laboratory, at the height of 1.6 m from the floor. In the living room and in the studio room temperature stratification is also measured at 5 levels (0.1, 0.8, 1.6, 2.4, 3.2 m from the floor) by means of a wall mounted sensors with PT100 probe (accuracy: ±0.3 °C). Relative humidity is recorded by a wall mounted capacitive probe (accuracy: ±3%) integrated in a multi-sensor element, in all the rooms of the building. The relative humidity sensor comes in combination with a temperature sensor (Si band-gap; accuracy: ±0.8 °C) which is used as temperature signal for the controller.

Air temperature and relative humidity values are also measured near each diffuser of the ventilation plant (i.e. living room, kitchen, studio room and two bedrooms) though duct sensors that integrate a band-gap temperature sensing elements (accuracy: ±0.8 °C) and a capacitance probe for relative humidity measurement (accuracy: ±3%).

CO_2 concentration values are recorded by means of a non-dispersive infrared sensor (accuracy: ±70 ppm + 5%). One sensor is located in each room close to the correspondent temperature sensor.

A combined ceiling mounted sensor measures in each room diffuse illuminance level and people presence. The sensor contains a probe for light intensity (digital sensor for illuminance; accuracy: ±5%) and a sensing element for motion detection (infrared sensor). Users' behaviour is also monitored by recording position (open/closed) of all the windows (both automated windows and manually-operated windows) by means of a simple magnetic contact sensor, as well as artificial light use down to every single LED luminaire.

Thermal energy demand for heating purpose is measured for two independent terminal configurations (high temperature radiator, TEM8 in Figure 37, and low temperature underfloor heating panel, TEM9 in Figure 37). For both circuits, a thermal energy meter is used in combination with Pt 500 temperature probes and ultrasonic flow meters, resulting in an accuracy of 2%. Monitoring of energy demand when underfloor heating panels are in use is split in three different zones: living room, kitchen and studio; bedrooms; and bathroom. Energy demand for DHW (TEM11 in Figure 37) and waterborne energy demand for ventilation (when the water coil is activated, TEM7 Figure 37) are also monitored by means of similar configuration. Sensors used to monitor thermal energy use are different from those used to control the plant.

Airborne thermal energy demand for ventilation (TEM10 Figure 37) is calculated from measurement of air speed, temperature and relative humidity in the ventilation ducts. For this purpose, two sensors that integrates a Pt 100 probe (accuracy: ±0.3 °C) and a capacitive probe (accuracy: ±3%) are installed One is in the supply main duct and one in the extract main duct. Air speed is measured by means of one hot-wire sensor (range: 0.1…30 m/s; accuracy: 10%) in each of the two main ducts.

Electric energy use for heating ventilation and DHW is monitored by means of several electric energy meter located on the (single-phase) lines that powers different building equipment components. All have a resolution of 1 Wh and an accuracy of 2%.

Electrical energy use in the building that is not related to heating, ventilation and DHW, can be grouped in five categories: energy use for lighting (EEM10 in Figure 37), for appliances (EEM9), general electricity for other uses (EEM8), energy use for use and control of automated windows and shading systems (EEM7), and energy use for monitoring and control of the building (EEM6).

The electric energy monitoring system measures 25 power lines independently (single-phase energy meter with 1 Wh resolution and 2% accuracy), and allows a high level of detail to be able to discriminate electrical energy use of a single appliance (i.e. fridge; hob; oven; extraction hood; dishwasher; washing machine; tumble dryer), groups of sockets (i.e. sockets in living room and entrance; sockets in kitchen; sockets in studio room; sockets in bedrooms and sockets in bathroom), line to power shading devices, or line to power automated windows and their controllers. The power line for lighting is independently monitored and, as previously mentioned, through data post-processing based on control signals counters, it is possible to assess lighting energy use down to luminaire level.

Energy for auxiliaries is also monitored so that components are coherently grouped. Several power lines related to electric coils or to the heat pump, as well as auxiliary lines for power in the technical room and for the data acquisition system are monitored too.

Power converted by means of PV roofs is monitored both by two energy meters (EEM1; resolution: 1 Wh; accuracy: 2%.), one for each PV roof, and by means of data retrieved from the inverters. Among others, data retrieved from power inverter includes: operating hours; DC current

input and voltage; DC power input; AC voltage and current output; AC active, reactive and apparent power.

Three-phase electrical energy/power supply from the grid is monitored by a power meter (63rd harmonic, 128 samples per cycle), which records, for each phase, current (accuracy: ±0.5%), voltage (accuracy: ±0.2%), power factor (accuracy: ±0.002), active power (accuracy: ±0.2%), frequency (accuracy: ±0.01 Hz), active and reactive energy (accuracy: IEC 62053-23 Class 2 and IEC 62053-23 Class 0.5, respectively). The meter is designated with the code PEM1 in Figure 37.

Thermal energy/power output from the solar thermal panels is calculated from measurement of heat carrier fluid (water-glycol) flow rate with electromagnetic flow meter (accuracy: ±5%) and temperature (of flow and return) with Pt 100 probes (accuracy: ± 0.3 °C). Due to flexible use of solar thermal converted energy, this thermal output can be diverted to the surface collector field (TEM2 in Figure 37) for ground regeneration, or to the heat pump (TEM3), or to the buffer tank (TEM4).

Similarly to the solar thermal panel circuit, thermal energy/power extracted from the surface collector field (TEM1 in Figure 37) is calculated from monitoring of flow rate and temperature of flow and return. Flow rate is measured by means of an electromagnetic flow meter (accuracy: ±5%) and temperatures with Pt 100 probes (accuracy: ± 0.3 °C).

Additional temperature and humidity measurements are also performed in several other locations of the plant for different purposes (e.g. control, energy conservation equation, in-depth analysis of components). In general, temperature measurements in water or water-glycol heat carrier fluids are carried out by means of Pt 100 class I probes, while J/T type thermocouples (accuracy: ± 0.5 °C) are used to perform additional temperature measurements in air or on surfaces. Relative humidity measurements are done through capacitive sensors with accuracy ± 3%.

Data acquisition and control system

Acquisition of signals from sensors and transducers is carried out by a National Instrument system based on the CompactRIO platform. This is a modular structure, where controllers, expansion chassis, input/output modules can be freely combined in order to suit the requirement of the measurement layout. One of the main advantages of this system is that future expansion and modifications of the measurement system can easily be realized.

The chosen starting configuration for the Living Laboratory includes one controller and two expansion chassis. A total of 19 different input/output signal modules are installed, ranging from current to voltage signals, from resistance to digital signals. Modbus communication protocol is widely used to connect transducers and components with serial communication features.

Signals sourcing for building equipment control are generated by data acquisition hardware. Most common control signals are voltage/current signals, digital signals (24 V logic), and Modbus serial communication.

The integrated data acquisition and control system is managed by a National Instrument LabVIEW-based interface. This is a graphical programming environment specifically developed for experimental tests and automation. Interfaces will be developed to allow users controlling (some) of the features of the building. One of the main advantages of this system is that the degree of control that is handed out to the users can be relatively easily changed from one experiment to the other. Dedicated user interface will be developed for each experiment in order to allow occupants to control only some of the features of the building. A more comprehensive user interface handling the whole building components is developed and is used by researchers to control the building when unoccupied.

It is worth mentioning that, due to its configuration and particular features, such as centralized management of the entire building equipment, including control of power lines, actuators, artificial lighting, windows and shading system, the building can be completely operated without users living in it. Schedules can be used so that ideal occupancy can be also experimented. People heat load can be replicated through the use of thermal mannequins with heat emission controlled through the building management system.

6.3. Examples of previous studies

6.3.1. Daylighting availability in a living laboratory single family house and implication on electric lighting energy demand

The aim of this study (Lobaccaro et al. 2017) was to analyse the correlation between natural light availability and use of artificial light in a residential building located in the Nordic climate. Experimental data and numerical simulations were used to compare the use of artificial light (and the correlated electric energy demand) against the daylighting availability, in Living Laboratory, considering the six groups of residents involved in the previously described experiment. During the building occupation by the 6 different groups of people, electrical energy use for artificial lighting was continuously recorded, together with outdoor environment conditions (irradiance and illuminance on the horizontal plan). Through advanced daylighting simulations carried out with DIVA-for-Rhino, the availability of daylight (illuminance level) during the periods of occupancy has been reconstructed, using as input data the recorded outdoor environmental variables. The results, based on the analysis of the outcomes of five groups, show that the coefficient of correlation between daylight availability and energy saving (measured thorough the artificial light energy demand) is low. It appears that the use of artificial lighting is little dependent on the availability of natural light, even if the users had the possibility to dim each individual light source, in the range 0..100 %, according to their preferences.

6.3.2. Measurement of the indoor thermal environment in the Living Lab during winter time: case of floor heating and a single heat emitter

The objective of the measurements (Georges et al., 2017) was to investigate the indoor thermal environment of the building during the space-heating season. The level of insulation of the Living Lab building envelope makes it possible to simplify the space-heating distribution by reducing the number of heat emitters. To assess the performance of simplified space heating, experiments were performed using floor heating (that can provide a uniform temperature distribution inside the building) and compared to the space heating using a single heat emitter, here taken as an electric radiator. The performance of both space heating emission strategies is compared in terms of thermal zoning (i.e. temperature difference between rooms) and temperature stratification (within the room equipped with a heat emitter). To assess thermal zoning, experiments were performed with closed and open internal doors as well as with and without intermittent temperature set-point (meaning a night temperature setback). The building was unoccupied during experiments but thermal dummies (with a realistic schedule) were placed in the building to mimic internal gains from activities. These experiments were a good preliminary background as they provided knowledge of the expected thermal stratification and thermal zoning (see Figure 38). In addition, experiments using intermittent heating already gave some insight into the characteristic time constant of the building. Regarding thermal zoning, it is worth mentioning that its effect is sometimes required by occupants. In the case of bedrooms, occupants may want warm bedrooms but it is proved that many Norwegian would like cold bedrooms during winter time.

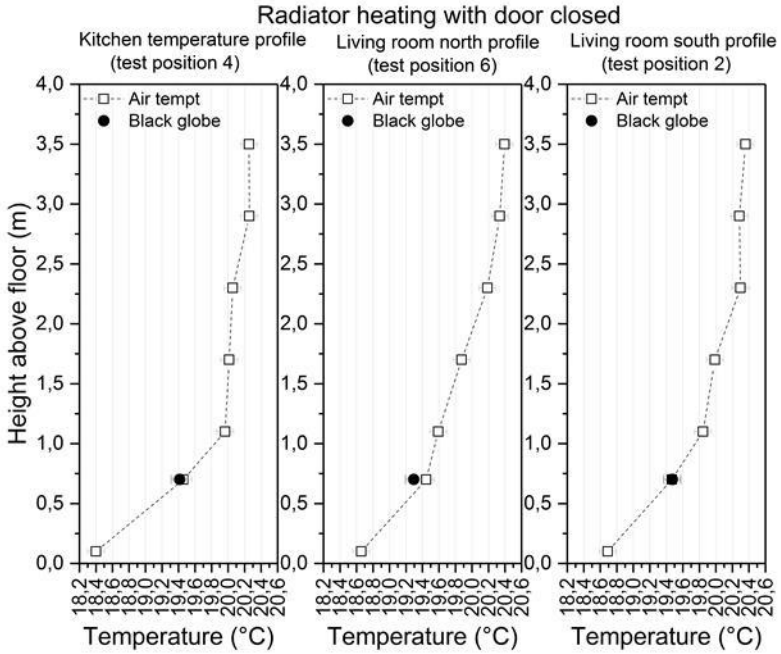

Figure 38 Temperature stratifiation in the living room North and South as well as the kitchen for the space heating using a single radiator, closed internal doors, constant temperature set-point and unheated bedrooms.

Some main conclusions resulting from these experiments, and useful to gain background understanding of the thermodynamic behaviour of the Living Laboratories can be given:

- With internal doors open, the temperature inside the Living Lab was (quasi-)uniform, even using a single heat source (i.e. the radiator). The mean radiant temperature was also very similar to the air temperature in each room. This temperature uniformity between rooms has been amplified in the ZEB Living Lab by the size of the sliding doors between the bedrooms and the studio. They are indeed very wide (more than 2 m wide).
- Closing internal doors, it was possible to create a temperature zoning between the living areas of the ZEB Living Lab and its bedrooms. A temperature difference of 4 – 5 °C has been measured.
- Nevertheless, the main merit of these experiments was to clearly show the slower thermal dynamics of super-insulated buildings. With closed internal doors, it took several days (2 to 4 days) to decrease the bedroom temperature from 21 to 16°C. This conclusion has nothing to do with the space-heating simplification concept. It is rather defined by the physics of super-insulated building envelopes with one-zone mechanical ventilation with heat recovery. This slower dynamic has indeed been found for both floor heating and the simplified distribution using one radiator.
- Applying an intermittent heating in living areas (meaning switch-off of the heating system in the living room during night-time) did not improve thermal zoning. It did not significantly accelerate the temperature decrease in bedrooms.
- The temperature stratification has been measured in living areas. This stratification was limited. It was an expected result for floor heating but it had to be proved for the radiator case. No local discomfort due to stratification was reported according to the limits of ISO 7730.

6.4. Experiment on energy flexibility

The first experiment dedicated to the topic “Energy Flexibility” carried out in the ZEB Living Laboratory was a cooperation between Neogrid Technologies ApS, Aalborg University, NTNU, and SINTEF, and its results were presented in March 2018 at the Cold Climate HVAC conference (Vogler-Finck et al. 2018). Moreover, the dataset from the experiment has been published online on the open-data platform Zenodo (Vogler-Finck et al. 2017). This experiment has also been used for the calibration of a building envelope model of the LivingLab in the dynamic building performance simulation software IDA ICE (Clauß et al. 2018).

6.4.1. Objective

The aim of the experiment carried out in the ZEB Living Laboratory was to identify a control-oriented model for a super-insulated single-family house (the ZEB Living Laboratory), as well as

to test the experimental procedure for the identification and calibration of models in small buildings characterised by a high energy performance. The scope of such models is to provide a robust numerical tool that can be used in connection with advanced controls of buildings, such as model predictive control (MPC). Model predictive control is a control technique well established in different engineering fields, which has gained attention in the HVAC sector because of its potential to increase energy efficiency and reducing environmental impact of building operation. MPC is also considered a promising technique to optimally utilise the flexibility of the building heat demand in order to achieve a defined objective, such as for example minimizing the peak load of a cluster of buildings, or the greenhouse gas emissions from the power consumed.

A key aspect in the implementation of MPC is the identification of a dynamical model of the thermophysical behaviour of a building and its heating system to be controlled. Here, suitable models must have a low computational cost in order to be usable in optimisation and must be identifiable with a reasonable amount of data. Hence, linear models are typically preferred. A large variety of models can be used, from so-called 'black-box' models (built solely using data and statistical considerations) to so-called 'grey-box' models (built with a simplified physical description with parameters calibrated using statistical methods), with variable levels of complexity. In principle, the aim is to find a model that is the simplest possible, while representing the dynamics well-enough and requiring a reasonably short data collection period. Currently, there is no universal and standardised method to build such a dynamical model for any given building, which makes the work challenging. Moreover, the slow dynamics of the building, and need to collect data with a variety of boundary conditions adds a further layer of complexity, especially when aiming at modelling occupied buildings.

In the case of the Living Laboratory, the thermal environment is also complex, due to the possibility of zoning (through operation of doors), ventilative heating and cooling, and significant stratification within the building. The study therefore benefited from the previous work on the characterisation of the indoor environment described earlier in the section presenting Study 4 in the Living Laboratory. Through the identification of the model's variables, the study also allowed the thermal capacity of the building structure and furniture to be assessed as built. The knowledge of such a feature of the building can be used, in an energy flexibility perspective, to exploit heat storage in the passive components of the building and to combine this with different operational strategies.

6.4.2. Brief description

The tests carried out in the Living Lab were organized in three successive experiments, without the presence of users in the buildings. The goal of the experiments was to heat up the building through a known (i.e. monitored) and simple heat source, and to characterize its performance by following the evolution of the indoor air temperature. While conventional buildings need multiple heat sources, distributed in the different areas, because of the compactness and layout of the ZEB Living Laboratory, just one heat emitter (a couple of electric radiators with a combined rated

power of 1.8 kW located side by side) was used in the experiments. The nominal power of the heat source was sized using a detailed dynamic simulation of the building, here using IDA ICE (Clauß et al. 2018). The use of a single source for heating in the building is in line with the aim of a simplification of the heat distribution in zero emission buildings, as well as a functional feature in relation to the testing of experimental method – to use limited heat sources decreases complexity and costs of the experiments. The mechanical ventilation system (balanced mechanical ventilation, regulated to a constant airflow rate of 130 m^3/h estimated by a previous experiment) of the building was kept in operation during the experiments, with different supply air set-point values (initially 30 °C to use ventilative heating in a first experiment, and then 18 °C to represent typical conditions), and the supplied heat monitored.

During the experiments, the following physical quantities were continuously recorded: power to the heat emitter, indoor air temperature (measured in different areas of the building with both the building's initial sensors and extra Pt 100 sensors with higher precision), operative temperature (through globe thermometers equipped with Pt 100 sensors, which can provide a better insight into thermal comfort than air temperature), global solar irradiance on the horizontal plane, outdoor air temperature, as well as any heat gain from appliances and lighting installed in the building (and in use), and the heat rate supplied through the ventilation system (computed indirectly though supply/exhaust air temperature values and the estimated air flow rate). This data is presented in Figure 39, and is freely available, together with more details on the measurement instrumentation, for further reuse in benchmarking studies (Vogler-Finck et al., 2017) or additional analyses.

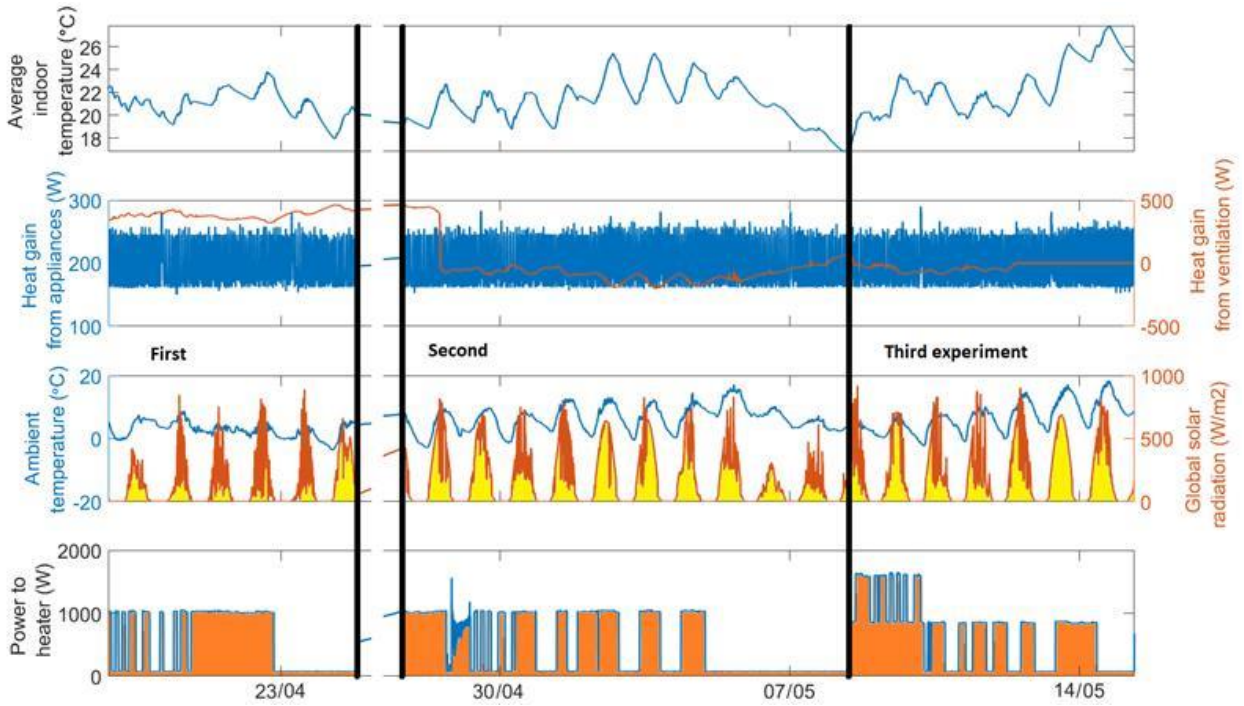

Figure 39 Evolution of indoor temperature during the experiments, together with inputs and boundary conditions.

Three different configurations were tested in the experiments, with differing opening of the internal doors, and ventilation supply air temperature, and are resumed in the table below. The doors between the bedrooms and the living room in the northern area of the building were kept opened in the first and the last test, while closed in the second. The door to the bathroom was always closed. This procedure aimed at assessing the role of the thermal zoning with internal doors open and closed, and especially in the case a single heat emitter. Closed door may lead to a non-uniform heat distribution, and therefore to different temperature values in the different areas of the building, thus impairing the capability of a simple single-zone model of replicating the thermophysical behaviour of the building. However, it should be mentioned that the ventilation plan was kept working for the entire duration of the tests in order to measure a situation that is representative of the normal operation of the building, and this might contribute to a more even distribution of the heat within the building than in the case of the ventilation plant being turned off. Detailed settings are found in Table 4.

The electric radiator, which represented the largest source of heating during the experiments, had thermostat disabled (to always operate when powered) and was operated according to a series of successions of pseudo random binary sequences (PRBS). These are specific precomputed sequences of heat release designed to excite the building over a large range of frequencies, and lead to obtaining a rich dataset for model identification, although it is not compatible with comfortable occupation of the building — unless specific precautions are taken — and should therefore be used only with unoccupied buildings (as was the case for this experimental activity).

Table 4 Different conditions for the three tests during the experiments.

Parameter	Test 1	Test 2	Test 3
Duration	6 days	11 days	7 days
Doors (bedrooms)	open	closed	open
Supply air setpoint	30 °C	18 °C	18 °C (off in the last 3 days)

6.4.3. Results

<u>On the temperature data collection and values</u>

Data on the indoor air temperature, measured in different areas of the building and at different heights, show that significant disparities of the air temperature occur within the building (difference between coldest and warmest simultaneous measurement was up to 10 °C). This behaviour is due to the superposition of two effects: firstly, the vertical stratification within each of the rooms, enhanced by the high ceiling of the building (in some case up to 4 meters); secondly, the horizontal inhomogeneity due to zoning, which becomes particularly evident in the case of closed doors. As far as stratification is concerned, it was possible to see that air temperature values measured at several heights showed differences as high as 4 °C in the main zone (living rooms and kitchen), between floor and ceiling levels. In particular, these variations can be explained

considering the higher solar gains in the main (southern) zone compared to the other zones of the building, and that the redistribution of the solar gain within the building was slowed down due to the closed doors between the rooms.

This inhomogeneous behaviour shows the limits of the typical single zone approach used in flexibility studies (including the modelling of this study) when it comes to describing the comfort throughout a whole building. This is why when it comes to the establishment of experimental procedure, it should be noted that it is important to have a comprehensive measurement of air temperature values all around the building – and therefore has an impact on the cost of the instrumentation necessary to carry out the test. Further investigations are however needed to precisely assess how the use of a very limited number of sensors (rather than the comprehensive set of sensors used) affects the quality of the final model itself.

On the tested first order model

The parameters of the first order dynamic model were identified using CTSM and the MATLAB System Identification toolbox (with the 'idgrey' function and a stochastic modelling approach): (Ci, UAia, Aw) corresponding to aggregated thermal capacity (kWh/K), aggregated heat loss (kW/K), and equivalent solar gain (m^2), respectively. The identification is based on the measured volume-averaged air temperature in the building. Optimisation of the parameters in the model identification procedure was made using initial values and bounds given in Table 5. The resulting parameters (and their uncertainties) are plotted in Figure 41 below.

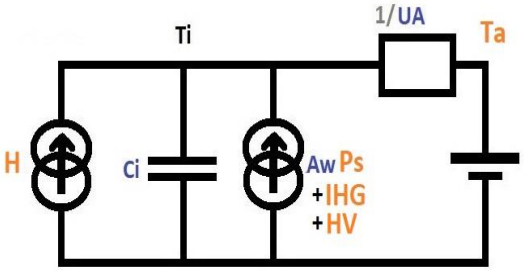

Figure 40 Structure of the first-order grey-box model used fort he Living Lab model identificaiton.

Table 5 Parameter initial values and bounds used in the model identification procedure (model calibration)

Parameter	Initial value	Lower bound	Upper bound
UAia (kW/K)	0.1	0	5
Ci (kWh/K)	4	0	100
Aw (m^2)	2 (3 in third experiment with CTSM to ensure convergence)	0	30

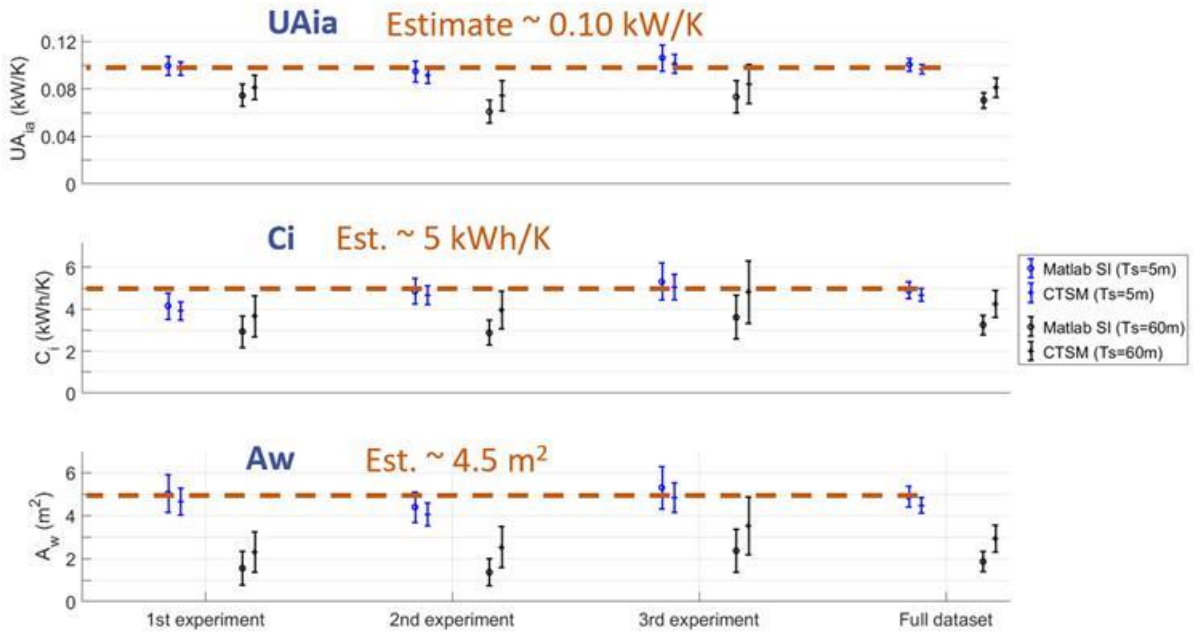

Figure 41 Estimated numerical values of the model parameters, identified by CTSM and Matlab on data with sample time 5 minutes and 1 hour.

In relation to the definition of good experimental procedure, the influence of the different sample times for the data (values of 5, 15, 30 and 60 minutes), as well as the minimum duration of the test, were considered to be an important aspect to assess, and indeed yielded different parameter values which reflect a different model behaviour.

The change in the configuration of internal doors to bedrooms resulted in small reductions of the numerical values of the global heat loss ($UAia$) and effective window area (AW) parameter. The value identified for the global heat loss was in line with the expected value from previous modelling of the ZEB Living Laboratory in the simulation software environment IDA-ICE (0.07 kWh/K — estimated by a product of average U value by envelope area). On the other hand, the heat capacity observed was an order of magnitude above the total indoor air heat capacity (0.12 kWh/K). This confirms that the heating variation activated not only the thermal capacity of the air, but also some of the thermal mass of the building envelope and furniture. Lastly, the equivalent solar gain was an order of magnitude below the glazed area (36 m^2), which is not easy to interpret as it is a simple proportional gain to the global horizontal solar radiation (while windows face specific vertical directions).

As expected, considering the whole experimentation period (rather than a sub-period) significantly reduces the uncertainty of the parameters. As they converge to a similar value, it seems that a change in the position of the doors and in the ventilation setting have a minor effect on the parameters themselves. In a similar way, the uncertainty of the estimated parameters decreases with shorter sample times. The results provide an estimation for the long-time constant of the

building (estimated by the ratio $Ci/UAia$) in the range of two days. This value is consistent with data available in the literature for well-insulated lightweight wooden structure.

Changes in the sample time of the dataset affected the value of the identified parameters according to the following characteristics. The value of the global heat loss ($UAia$) and effective window area (AW) parameters decreases as the sample time increases. This is probably due to the tendency to convert some of the solar gains in form of reduced heat losses, since both phenomena have a similar effect on the indoor air temperature. Moreover, it was observed that there is a difference between the parameters identified by Matlab's System Identification toolbox and CTSM, for all the parameters for sample times of 15, 30 and 60 minutes, in all three experiments, with Matlab generally yielding lower numerical values.

Through the tests, it has been confirmed that one week (equal to several long time constants) is a long enough period to identify a simple first order model of the building's thermal dynamics.

On the prediction capability of the identified model

The prediction capability of the models identified for the different sample times was evaluated by predicting the evolution of the indoor temperature over each of the three tests experiments. For all the cases the prediction was performed starting from the initial temperature, and assuming perfect knowledge of the disturbances and inputs.

The simple first order model trained on one week of data was capable of predicting the main slow thermal dynamics of this lightweight building over several days. It could be observed that short sample times of 5 and 15 minutes provide better overall prediction capability compared to long sample times (Figure 42).

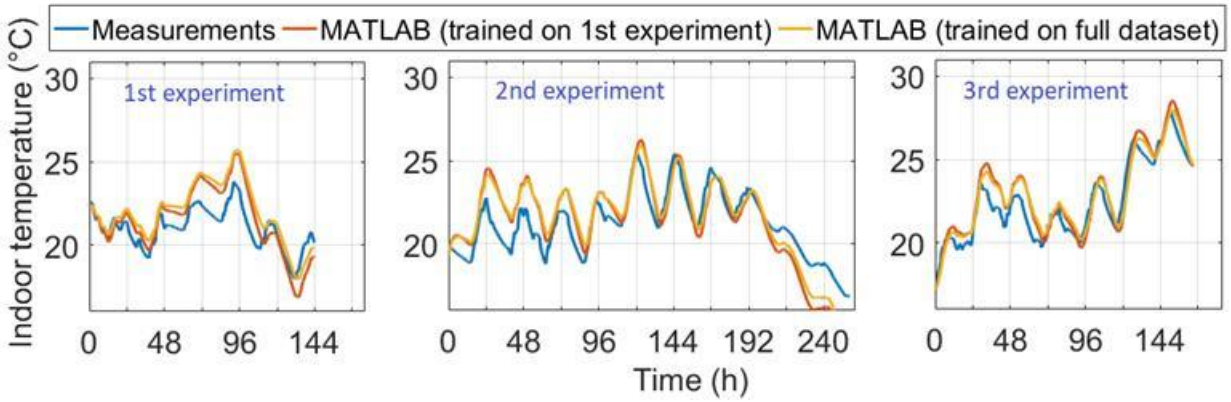

Figure 42 Prediction capability of the first order model identified on data with 15 minutes sample time (prediction are made over each whole experiment period, starting from the initial state and assuming perfect prediction of the boundary conditions) (figure adapted from (Vogler-Finck et al., 2018)).

6.4.4. Conclusions and lessons learnt

This experimental activities carried out in the Living Laboratory demonstrated that first order models can be suitable to replicate the thermophysical behaviour of a highly-insulated single family house, and that the tested experimental procedure can lead to suitable data for model identification and validation, as well as calibration of simulation models (as done by Clauß et al.(2018) in a separate work on the building)

In particular, the heating procedure was operated according to a predetermined rich excitation sequence (PRBS) executed through a single electrical heat emitter. The experiment showed that large disparities of air temperature may occur in the building, due to the combination of zoning (using doors) and air stratification. While stratification can be particularly linked to the features of the building (very high ceiling) and the heat emitter, zoning seems to be an aspect to pay care about while planning (and executing) the tests. Nonetheless, the proposed model was able to replicate the average thermophysical behaviour of the building (after appropriate training) even if different temperature values were recorded in the building. This is because the single air temperature for the model was computed as a volume-averaged temperature value, and thus by considering the different weights of the different temperature values in the building.

The investigated model was a first order model, with 3 parameters to be identified: a lumped heat loss to ambient, a heat capacity and an equivalent solar gain. Experience showed that a diffuse radiation sensor (or any setup allowing to make a split between direct and diffuse radiation) would have allowed a better modelling, by accounting for projections of the solar radiation on vertical surfaces, thereby giving a solar gain parameter which would be easier to interpret physically than a gain to the global horizontal radiation.

Two software packages were used to identify the parameters (CTSM and the MATLAB System Identification toolbox). In fact, the two software packages provided different values (and uncertainties) of the model parameters, despite identical initial values and bounds in the optimisation. However, none of the software packages was found to attain a significantly higher performance than the other.

The sampling time was also a topic investigated in this activity. It was found that an increase in the sample time of the measurements leads to a decrease in the values of the parameters in all the 3 models, and to a corresponding increase of the uncertainty of the parameters,

Operative temperature measurements were collected (and part of the open dataset), but have not been extensively used in the work. In future works, it is however recommended to evaluate the influence of using operative temperature rather than air temperature, since it represents the comfort better and would therefore be more fitting to deployment of flexibility under comfort constraints.

The prediction capability of the first order model identified in MATLAB was analysed, revealing better short-term performances for measurement sample times within 5–15 minutes. This sample

rate is therefore recommended for future tests, consistently with prior works of Annex 58 (which were not specifically targeting ZEBs).

In any case, the identified model represents well the main thermal dynamics of the building-averaged temperature, which is still relatively slow even in this lightweight building case. The experiments were carried out with the use of a fast-acting light-weight heat emitter, and results in terms of building thermal dynamic might differ when a heating system integrated in the building structure is considered. Conclusions on such a system with higher inertia (e.g. floor heating) would require a new series of experiments.

7. FHNW. The Energy Research Lab

7.1. General presentation of the laboratory facilities

The Energy Research Lab (ERL) is designed to test components for heat and power supply systems in buildings. The testing may focus on the individual performance of a component or its role within an entire system. Evaluated components include heat pumps, ice storage, solar-thermal collectors, energy management systems, photovoltaics and batteries. The ERL is run by the University of Applied Sciences and Arts of Northwestern Switzerland FHNW Institute of Energy in Building and is located in Muttenz near Basel.

7.2. Description of the test facility

The laboratory is shown in Figure 43. Its functional core is a two-stage system, capable of supplying multiple test components with temperature-controlled fluids. The first stage consists of two 1600 L tanks (1) with hot and cold water, which are connected by one heat pump, heating and cooling the respective tanks. An energy dissipater prevents overheating on the hot side. Supplied by the first stage, the second stage consists of three pairs of smaller hot- and cold-side tanks (2). Two of these pairs contain water. The third pair contains a water-glycol mixture. The purpose of the smaller tanks is to provide quick buffer capacity for generating the desired load profiles for test components. Furthermore, the temperature difference between these pairs is smaller than the temperature difference between the big tanks, allowing for easier and more accurate temperature control. This system is used to emulate sources and sinks, such as geothermal heat exchangers, solar-thermal collectors or space heating (SH). The output values for the emulated components are generated through simulations. The physical outputs are then fed to real test components, such as heat pumps (3) or DHW storage (4), also shown in Figure 44. The system can supply a maximum mass flow rate of 6000 L/h and a maximum thermal power of 16 kW at a temperature range from -10 °C to +90 °C.

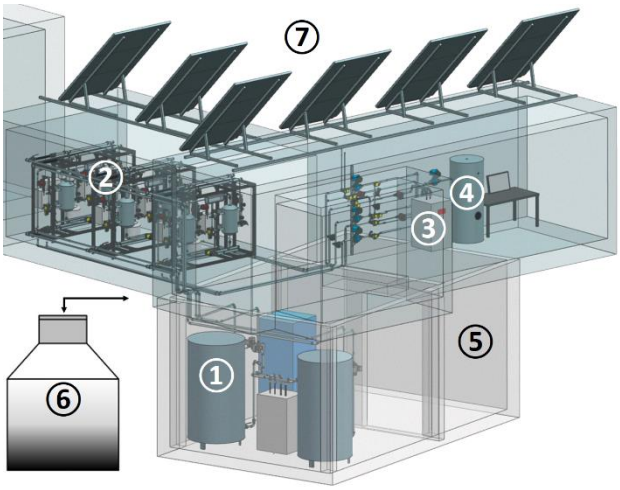

Figure 43 (1) Core stage 1; (2) Core stage 2; (3) Heat pump; (4) DHW storage; (5) Climate chamber; (6) Ice storage; (7) PV modules

A climate chamber (5) is available to condition air for testing air source heat pumps. It can supply up to 3500 m^3/h of air with a temperature range from -20 ºC to +40 °C and a humidity range from

15% to 98%. The laboratory is also equipped with a 10 m^3 ice storage (6). Its state is recorded by 41 sensors in and around the storage. While a real PV system (7) is installed, its dependence on the weather makes it unsuitable for reproducible, standardized tests. Therefore, a PV emulator with a maximum power output of 10 kW has been added to the electric setup. On the demand side, an electric load emulator with a maximum power draw of 7.2 kW and thermal energy recovery has been installed to stand in for household appliances, lighting, etc. The roof mountings can also be used for real solar-thermal collectors.

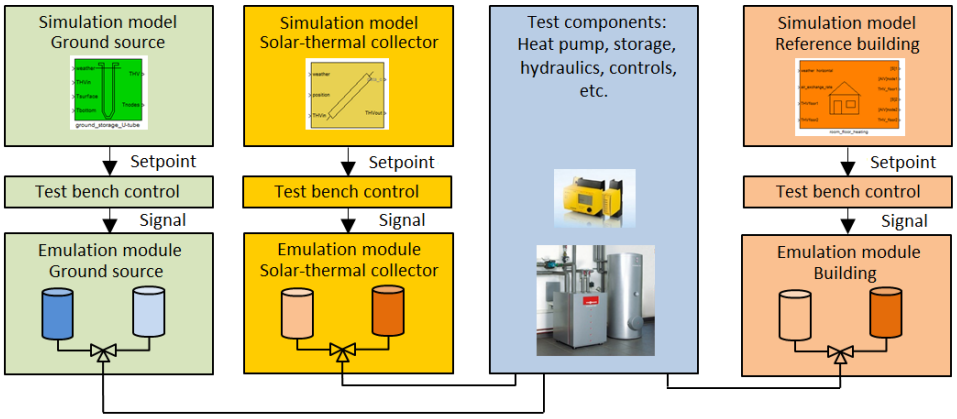

Figure 44 Second stage of the core with emulation models and real test components.

7.3. Examples of previous studies

In the past, the laboratory was mostly used to characterize individual components for numerical simulation studies. Two examples are given below. Recently, the focus has shifted from component to system analysis. Initial results thereof are described in chapter 7.4.

The charging and discharging of an ice storage tank were characterized to simulate a building heating system, combining it with solar-thermal collectors and a heat pump. Since the thermal properties of ice differ from water, these processes are more complex than for a sensible heat storage. The study yielded several conclusions regarding the described type of system: an underground ice storage should not be insulated, since heat gains from the surrounding soil in winter outweigh both heat losses to the soil in summer and heat gains from the solar-thermal collectors in the winter. A sensitivity analysis of the melting point shows no benefits for alternative storage fluids, since the increased heat gains from the soil with a lower melting point and the increased source temperature for the heat pump with a higher melting point counteract each other (Dott et al., 2016).

In another study, the influence of condensation enthalpy of humid air on the heat exchanger of an air-source heat pump was measured and resulted in 5 - 10% higher thermal output power at the same operating point, compared to dry air. Physical bottom-up modelling of this process is challenging and often neglected in numerical heat pump models. Integration of the measured

data into simulations however, revealed a relevant influence on the seasonal performance of the evaluated system (Dott et al., 2018).

7.4. Experiment on energy flexibility

7.4.1. Objective

In buildings with PV installations, it is often desired to maximize self-consumption of the generated power for several reasons. On the building side, this reduces the amount of electric energy which has to be purchased from the grid. On the grid side, power peaks during sunny weather are reduced, especially if the total PV capacity connected to the grid is high. In this study, the ability of an energy management system (EMS) to maximize self-consumption by aligning DHW generation with surplus PV generation is tested. Beyond that, the study doubles as an evaluation of short-term hardware-in-the-loop testing for controller prototypes.

7.4.2. Brief description

The EMS schedules the DHW charging cycles for time slots with expected electricity surplus, based on the recorded PV generation and electricity consumption of the three preceding days. In case of sufficient surplus, the DHW storage is charged before it reaches its standard lower temperature limit of 40 C and is heated beyond its standard upper temperature limit of 50 C. However, DHW charging is never delayed when the lower temperature limit is crossed. The set room temperature is constant.

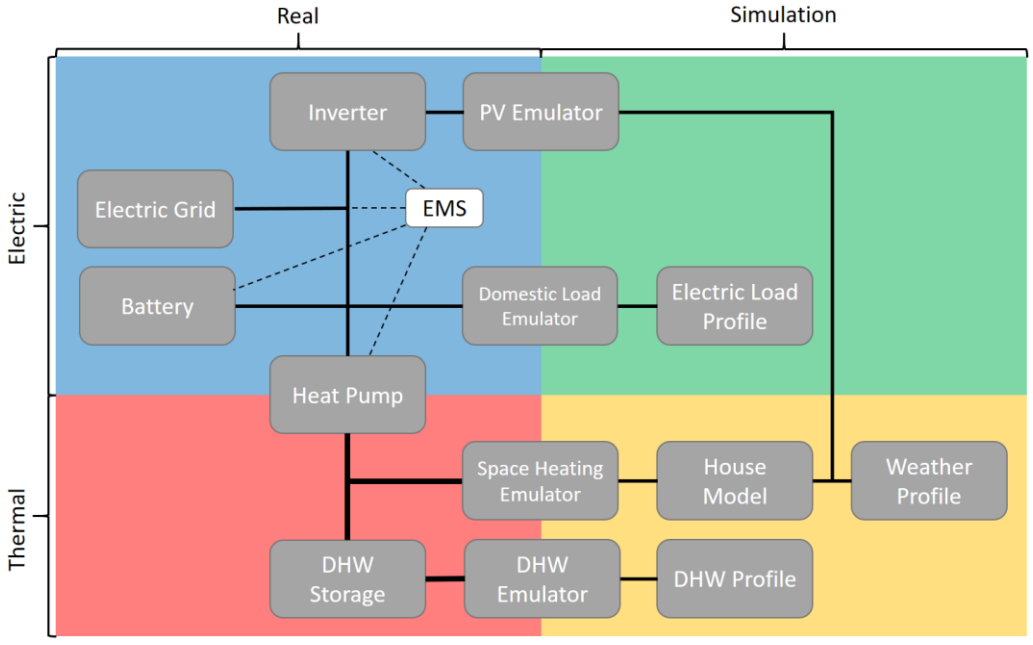

Figure 45: Test setup.

Figure 45 shows the test setup. The inverter, electric grid, battery, heat pump and DHW storage are real. The weather, domestic electric load, DHW consumption and the building are simulated. Simulation and real components are connected through emulators for the PV system, domestic electric load, space heating and DHW consumption. The EMS takes measurements from the inverter, battery, heat pump and grid connection and can control the battery and heat pump.

The boundary conditions are shown in Figure 46 and outlined in Table 6, along with the building model, controller settings and real hardware components. The building model is based on the low energy single-family house standard “KFW-40” by the German Reconstruction Credit Institute and implemented with the Carnot Blockset Toolbox, Version 6.2. It features an underfloor heating system, active window shading with external venetian type blinds and a ventilation system with heat recovery. Space heat and DHW are provided by an air source heat pump. The weather corresponds to a temperate spring day with clouds in the morning and sunshine in the afternoon. The basic profile is taken from a weather data set for Strasbourg, FR. To simplify the test, freezing at the external heat exchanger was avoided by elevating low ambient temperatures to a minimum of 7 °C. A strongly uneven irradiance is generated by setting direct irradiance during the first half of the day to zero. The DHW profile corresponds to the “Medium” profile from the European tapping cycles according to EN 13203. The electric load is based on a sample day with a total draw of 6.6 kWh, generated with the LoadProfileGenerator from the TU Chemnitz (Pflugradt, 2015).

The DHW storage is initialized by flushing it with cold water, then charging it to 45 °C. Since the EMS has no recorded data at the beginning of a test, it is fed three days of simulation-generated PV and electricity consumption data. Two four-day tests with repeating boundary conditions are conducted: one with the EMS activated and one without. The first day is required for the system to settle, leaving three days for evaluation. All data is sampled with a one-second resolution.

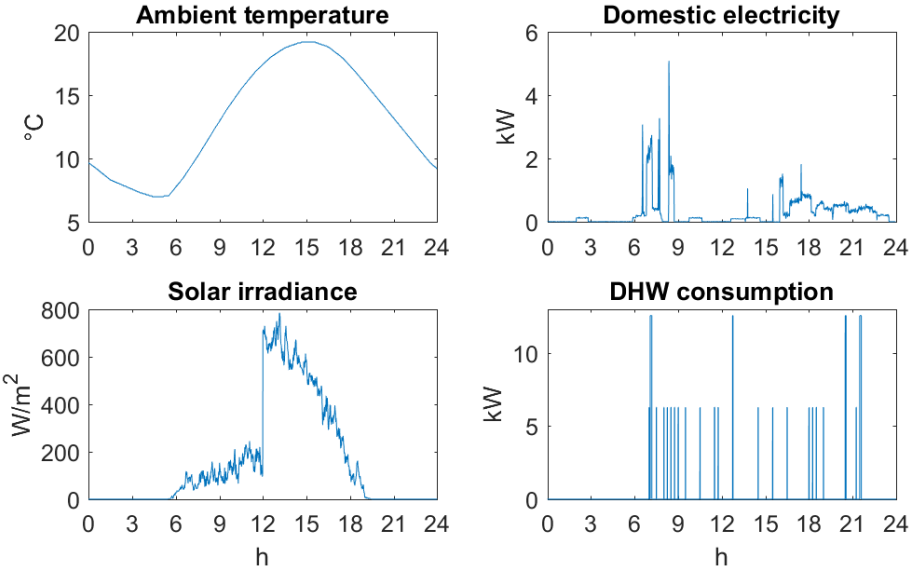

Figure 46: Boundary conditions for all days.

Table 6: Building model data, controller settings, boundary conditions and hardware components.

	Specification	Value	Unit
Building	Inhabitable area	160	m^2
	UA value to ambient	106.7	W/K
	UA value to ground	14	W/K
	Air exchange rate	0.4	1/h
	Ventilation heat recovery	80	%
	Photovoltaic capacity	5	kW_p
Controller (EMS)	Space heat	21	°C
	DHW, standard	40 - 50	°C
	DHW, overload	40 - 54	°C
Weather	Mean temperature	13.1	°C
	Total horizontal irradiance	3.7	kWh/m^2d
DHW	Daily energy	5.8	kWh/d
Domestic electricity	Daily energy	6.6	kWh/d
Air/water heat pump	Thermal power (A-7/W35)	5.53	kW
DHW storage	Volume	390	L
Inverter	Max. power	5	kW
Battery	Available Capacity	5.9	kWh

7.4.3. Results

While the tests took four days, the system requires approximately one day to settle. Therefore, only days 2-4 were used for the analysis. Table 7 compares the efficiency key performance indicators (KPI) with and without the EMS, averaged over days 2-4. The EMS increases self-generation (fraction PV generation consumed on-site and PV generation) and self-consumption (fraction of PV generation consumed on-site and consumption), while lowering grid feed-in and grid draw (Finck et al., 2018). Differences between evaluation days are small.

Table 7: Efficiency KPI for days 2-4, mean and standard deviation (±).

	Self-generation	Self-consumption	Grid feed-in	Grid draw	Grid balance
Unit	%	%	kWh/d	kWh/d	kWh/d
Without EMS	52.0 ± 0.6	46.9 ± 2.3	9.60 ± 0.42	6.43 ± 0.26	3.17 ± 0.68
With EMS	66.9 ± 0.5	61.3 ± 0.1	6.99 ± 0.02	4.72 ± 0.14	2.27 ± 0.16

Figure 47 shows the virtual electricity surplus of the system disregarding electric power required by the heat pump to supply DHW ($P_{el,surplus} = P_{PV} - P_{el,domestic} - P_{battery} - P_{el,HP,DHW}$), the electric power required by the heat pump to supply DHW ($P_{el,HP,DHW}$) and the DHW storage temperature (T_{DHW}) for the last test day with and without the EMS. The DHW storage temperature is measured with an immersion sensor slightly above the center of the tank. The shaded areas in the lower plots show the standard temperature band for the DHW storage. Without the EMS, the control system keeps the DHW temperature in this band while not using the photovoltaic surplus during the afternoon hours. With the EMS, charging of the DHW storage is moved to hours with photovoltaic surplus, overloading the DHW storage by 4 K. The temperature dips at the start of the DHW charging cycles are the result of turbulences stirring up the stratified layers of water. Figure 48 shows the temporal probability distribution of power exchange with the grid for days 2-4 with and without the EMS. With the EMS, a clear shift towards lower powers can be seen.

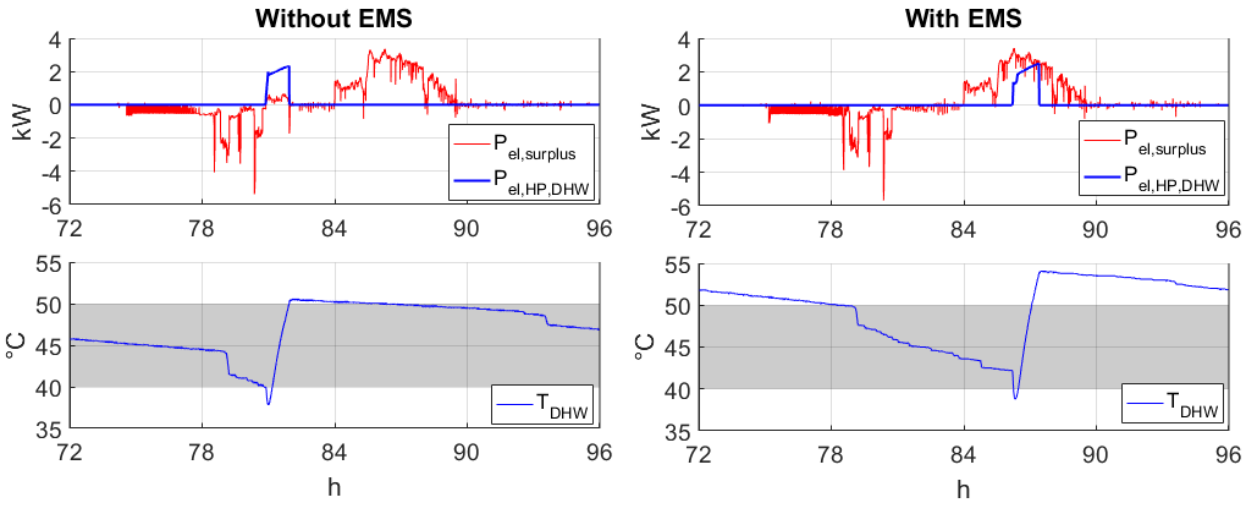

Figure 47: PV surplus power without DHW charging (red), DHW charging power (blue) and DHW storage temperature (bottom) on the fourth day with and without the EMS.

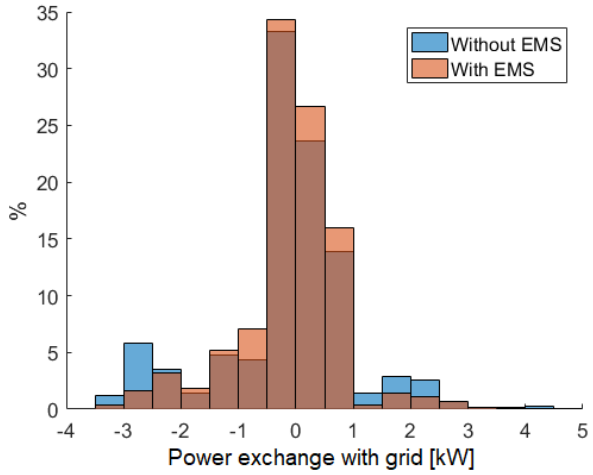

Figure 48: Temporal probability distribution of power exchange with grid for test days 2-4 with (red) and without (blue) EMS. Draw positive, feed-in negative. Pale brown marks overlapping parts of bars.

7.4.4. Conclusions and lessons learnt

The objective of the EMS is to increase self-consumption by aligning DHW charging with surplus PV generation. It performs well and consistently in this regard, for the given setup and boundary conditions. The four day test is sufficient to gain significant insights into the functionality of the system. How these findings translate to changing parameters remains to be evaluated. While the boundary conditions in this study are favorable to the EMS, its impact would likely be larger, if the building did not have a battery or if thermal overloading of the underfloor heating system were used. Developing the test setup and finding the boundary conditions for the study was an iterative process. The emulation system is complex and technical failures occured in various components. However, the vast majority of failures were in communication crossfire between components as well as logging overflows. In order to eliminate weak links and improve the reliability of the system, it was helpful to acquire a large amount of raw data from all components and visualize it. This allowed to recognize and locate malfunctions efficiently. Where possible, surveillance of the system was implemented in real-time. While the test duration was four days, many malfunctions were recognizable after a few hours. Without real-time surveillance, multiple days would have been wasted in these cases.

Another challenge was the initialization of the building model and the DHW storage. The building model has two thermal states. One for the underfloor heating system and one for the building mass. To minimize settling time, these temperatures should be initialized close to their equilibrium for the initial ambient temperature. This required several iterations of trial-and-error. Conditioning the DHW storage requires a process able to generate a certain mean temperature with a stratification close to equilibrium. This was done by flushing the storage with cold water, then heating it to the desired temperature. Regarding the boundary conditions, the initial approach was to create a challenging situation for the EMS to handle. However, in combination with the short test duration, it was then difficult to distinguish the impact of the EMS from random variations. Hence, more favorable conditions were selected. Two aspects thereof shall be highlighted here. The weather profile with solar irradiance concentrated on hours with low DHW consumption (early afternoon) creates a clear desired reaction for the EMS, which is to schedule DHW charging for these hours. Furthermore, DHW profiles with large concentrated drawings deplete the DHW storage quickly and force a charging cycle, restricting any dynamic scheduling by the EMS. Therefore, a fairly distributed DHW profile was selected, instead. Numerical simulations of the system with the various boundary conditions were helpful in the selection process.

In summary, four core points are recommended for hardware-in-the-loop testing: (1) First run the desired tests entirely as virtual, in order to have as much pre-testing information as possible. (2) Implement real-time surveillance to catch malfunctions as earliest as possible and react (3) Start with simple and clear boundary conditions in order to separate desired effects from random variations. More challenging boundary conditions can be used later. (4) Initialize models and components close to an equilibrium point to minimize settling time. This helps keeping the test duration at a minimum.

8. Polytechnique Montréal. The Semi-virtual Laboratory

8.1. General presentation of the laboratory facilities

The Semi-Virtual Laboratory at Polytechnique Montréal allows to test hydronic (water-side) heating and cooling equipment in highly dynamic conditions. Active (e.g. heat pumps) and passive (e.g. storage tanks) equipment can be tested thanks to auxiliary loops capable of producing and rejecting up to 100 kW of heat simultaneously. A key feature of the Semi-Virtual Lab is to perform Hardware-In-the-Loop testing, where HVAC equipment is tested in realistic operating conditions provided by a full system dynamic simulation with the TRNSYS program. The 2-way data exchange between LabVIEW and TRNSYS is performed at every time step through shared variables, allowing direct feedback from the experimental performance on the simulation results and vice-versa.

The objective of the Semi-Virtual Lab is to develop and validate detailed dynamic models of HVAC equipment including detailed controls, and to test new prototypes or existing equipment in realistic dynamic conditions to improve their design and standard testing methods.

Figure 49 General pictures of the Semi-virtual Laboratory at Polytechnique Montréal.

8.2. Description of the test facility

The concept of semi-virtual testing for a water-to-water heat pump is represented in Figure 50.

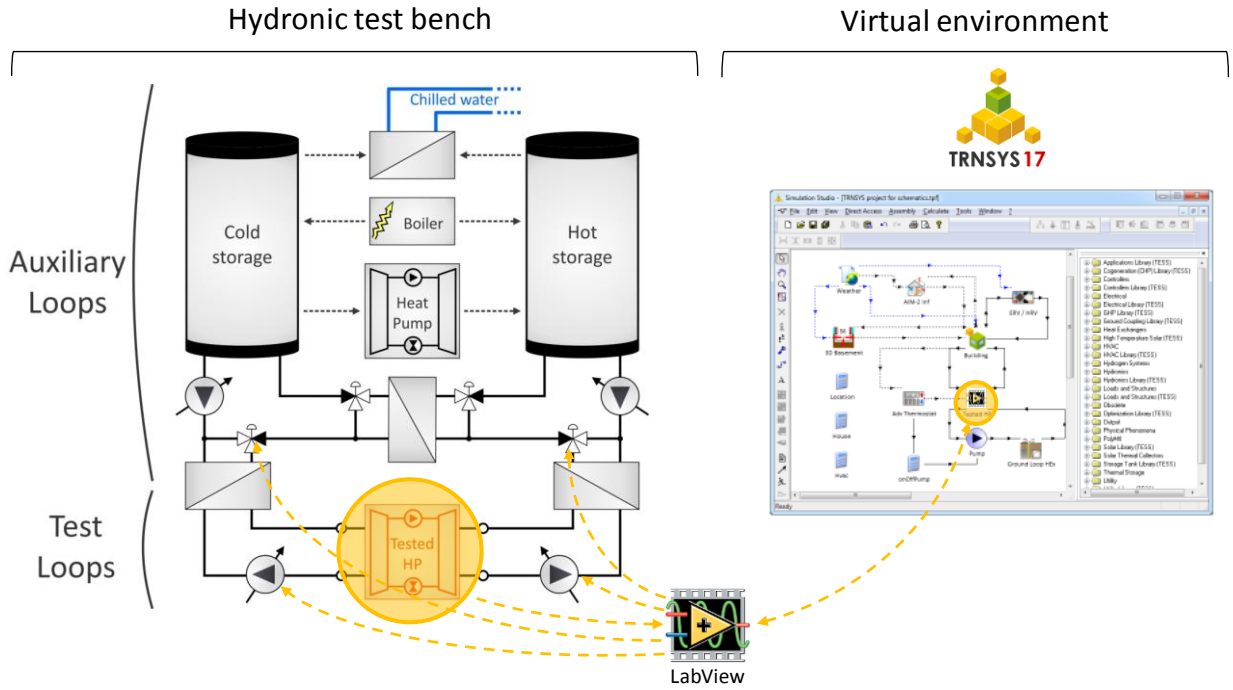

Figure 50: Semi-virtual testing at Polytechnique Montréal.

TRNSYS simulations predict system performance, calculating the flow rates and temperatures of the fluid streams entering HVAC equipment under test, which are used as actuator control signals in the Laboratory. The equipment's response to these operating conditions is sensed in the laboratory and imposed back on the building simulation.

Dynamic operating conditions are imposed on the tested equipment (e.g. a heat pump, as in the figure) based on a full system simulation. Measured outlet conditions (in this case temperature and flow rate on the source and load sides) at a given time step are sent to the simulation, which then calculates the inlet conditions for the next time step.

Testing possibilities

The flexibility of the Semi-Virtual Laboratory allows to perform different types of experimental tests:

- Standard tests imposing predefined (possibly highly dynamic) inlet conditions on HVAC equipment to assess its performance and to develop or validate numerical simulation models.
- Semi-Virtual tests where HVAC equipment is integrated within a full system simulation, therefore testing the equipment as if it was in a real system. This allows assessing the

equipment performance in these conditions and developing or validating models adapted to them.

- Semi-virtual tests also allow testing the response of the equipment's embedded controls to realistic operating conditions, therefore allowing to understand and model these controls realistically. This is especially important for recently introduced variable capacity devices (e.g. variable speed heat pumps, and Variable Refrigerant Flow devices) which often include proprietary and undocumented control strategies for which developing accurate models is a challenging task.
- Detailed testing and performance assessment for prototypes, in order to develop them and improve their performance for realistic operating conditions in addition to predefined standard tests.
- Assessment of the difference between the seasonal or yearly performance extrapolated from standard steady-state tests and the seasonal or yearly performance obtained from models validated in highly dynamic, realistic operating conditions. These studies can also inform standard certification bodies and help them develop new, more accurate standards methods of testing.

8.2.1. Equipment specifications

The 4 hydronic loops of the laboratory are shown in Figure 51. Two auxiliary loops (blue and red) can produce water at temperatures between -10 °C (with glycol solution) and +85 °C. Although the two loops are both connected to the heat production and heat rejection devices, for the sake of this explanation the blue loop will be considered as the cold loop and the red loop will be considered as the warm loop. These auxiliary loops are hydraulically isolated from the test loops (yellow and green) by plate heat exchangers equipped with 3-way valves. These heat exchangers and their control valves are used to impose the desired inlet conditions (optionally calculated from the full system TRNSYS simulation) on the tested equipment.

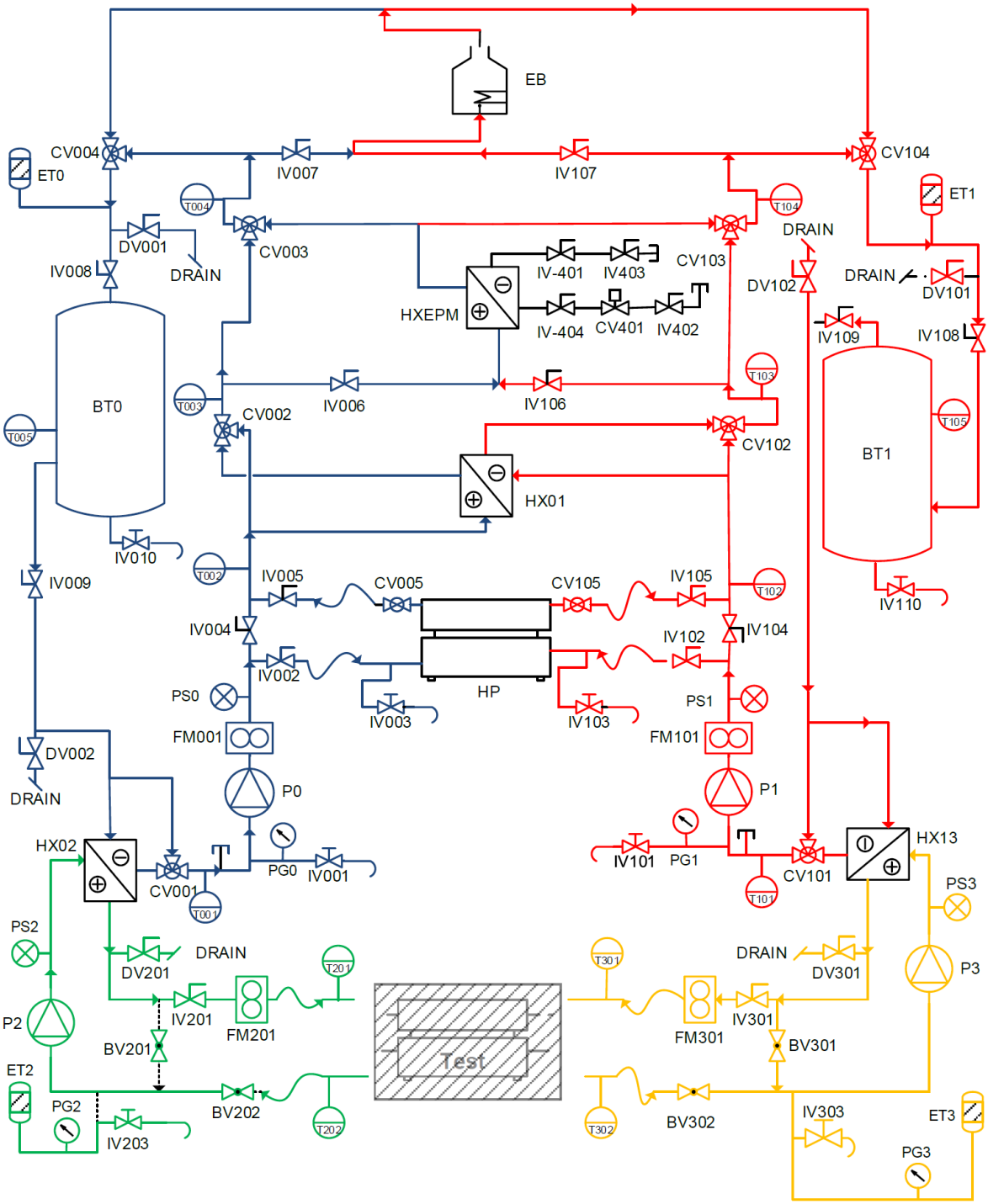

Figure 51: Hydronic loops of the Semi-Virtual Laboratory.

The hydronic loops piping has a diameter of 2.5” (62.5 mm) to allow relatively large flow rates, and adapters (with specific flowmeters) are available to reduce the test loops to a diameter better suited to smaller equipment (e.g. residential heat pumps). Operating temperature limits are between -10 C and +85 C depending on the fluid (up to 30% glycol) and the equipment used.

The nomenclature in Figure 51 uses the first digit to represent the hydronic loop: “0” and “1” to denote the auxiliary loops, “2” and “3” to denote the testing loops. CV001 for example would be the first control valve (“01”) in the “cold” auxiliary loop (“0”).

The main components are described below:

- CVnnn: 3-way valves, centrally controlled. CV103 is a special constant-pressure control valve located in the university chilled water network, allowing to obtain a constant flow rate independently of the chilled water loop operation.
- EB: electric boiler (54 kW thermal, compatible with up to 30 % glycol).
- HxEPM: heat exchanger with the university (École Polytechnique de Montréal) chilled water network. The heat exchanger capacity is sized to reject 100 kW with a ΔT of 7 °C.
- BT0 and BT1: storage tanks (974 L each).
- Hx01: heat exchanger between the two auxiliary loops (“0” and “1”). Standard tests imposing predefined (but possibly highly dynamic) inlet conditions on HVAC equipment to assess its performance and to develop or validate numerical simulation models. It is sized to exchange 100 kW with a ΔT of 4.5 °C.
- HP: variable capacity water-to-water heat pump (can be used as part of the auxiliary loops, or as the tested equipment). Operating limits: -10 °C on the evaporator side (with glycol), 55 °C on the condenser side (note that when bypassing the heat pump, the electric boiler can heat the auxiliary loops up to 85 °C). The heat pump has a capacity of 100 kW (cooling) and 140 kW (heating).
- P0 and P1: Variable speed pumps for the auxiliary loops. The design maximum flow rate in the loops is 4.7 L/s (75 GPM). The actual maximum flow rate depends on operating conditions because of pressure limits (e.g. with the “HP” heat pump in service, the maximum flow rate is about 3.8 L/s (60 GPM).
- Hx02 and Hx13: heat exchangers between the auxiliary loops and the test loops. These exchangers are designed to transfer 100 kW with a ΔT of 3 °C.
- P2 and P3: Variable speed pumps for the test loops. The design maximum flow rate in the loops (depending on the configuration because of minimum and maximum pressure limits) is 4.7 L/s (75 GPM).

8.2.2. Sensors, data acquisition and control

The laboratory is equipped with high accuracy temperature sensors and flowmeters, as well as power transducers:

- Pt 100 with 1/10 DIN accuracy in the test loop and Pt 100 with 1/3 DIN accuracy in the auxiliary loops. In addition, various thermopiles can be fitted in the test loops to measure temperature difference with a very high accuracy.
- Flowmeters with traceable calibration reports with an accuracy better than 1% of reading in their full operating range. Standard range is 1 L/s to 11 L/s (15 to 180 GPM), optional smaller flowmeters for test loops have a range of 0.06 L/s to 0.6 L/s (1 to 10 GPM).
- Power transducers with an accuracy (for voltage, current and power) better than 0.5% of full scale are available in 1-phase and 3-phase, for 120 V to 600 V and rated current between 5 A and 100 A. These transducers output voltage, current, VA, RMS power and power factor.

Data acquisition and control are performed by a modular high accuracy National Instrument CompactRIO system programmed in LabVIEW. As described above, the LabVIEW program can optionally communicate with TRNSYS for semi-virtual testing. Figure 52 shows a screenshot of the LabVIEW interface. In semi-virtual mode, T201_set, T301_set, FM201_set, and FM301_set come from the TRNSYS simulation through shared variables in LabVIEW.

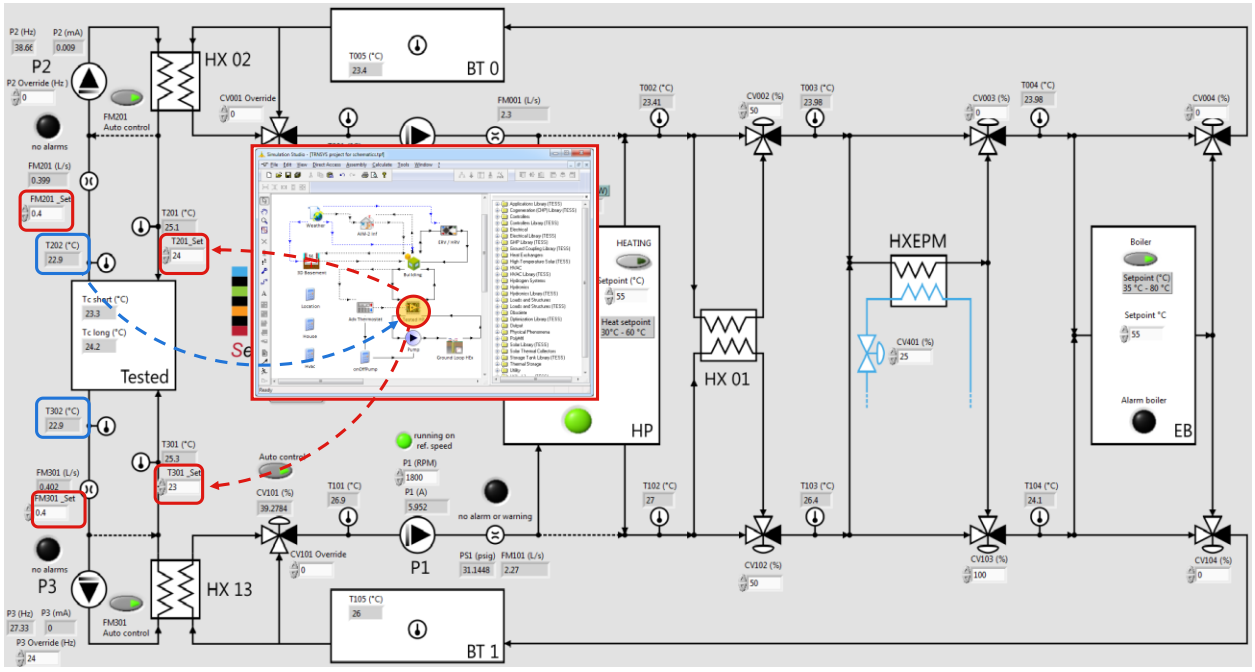

Figure 52 Screenshot of the LabVIEW interface showing the link with the TRNSYS simulation.

8.3. Example of previous studies

8.3.1. Development of a LabVIEW-TRNSYS bidirectional connection

In this project (Macdonald et al., 2014), a novel communication methodology was developed to allow rapid data exchange between the Data Acquisition software LabVIEW and the energy simulation program TRNSYS. The developed method uses data exchange through shared variables between the TRNSYS DLL and the LabVIEW executable, and does not require writing or reading data files. A procedure to properly initialize the simulation and the laboratory equipment was also developed and implemented. Changes to the TRNSYS code source are encapsulated in a newly developed component, named Type 131. The principle of the communication between the two programs is described in Figure 53.

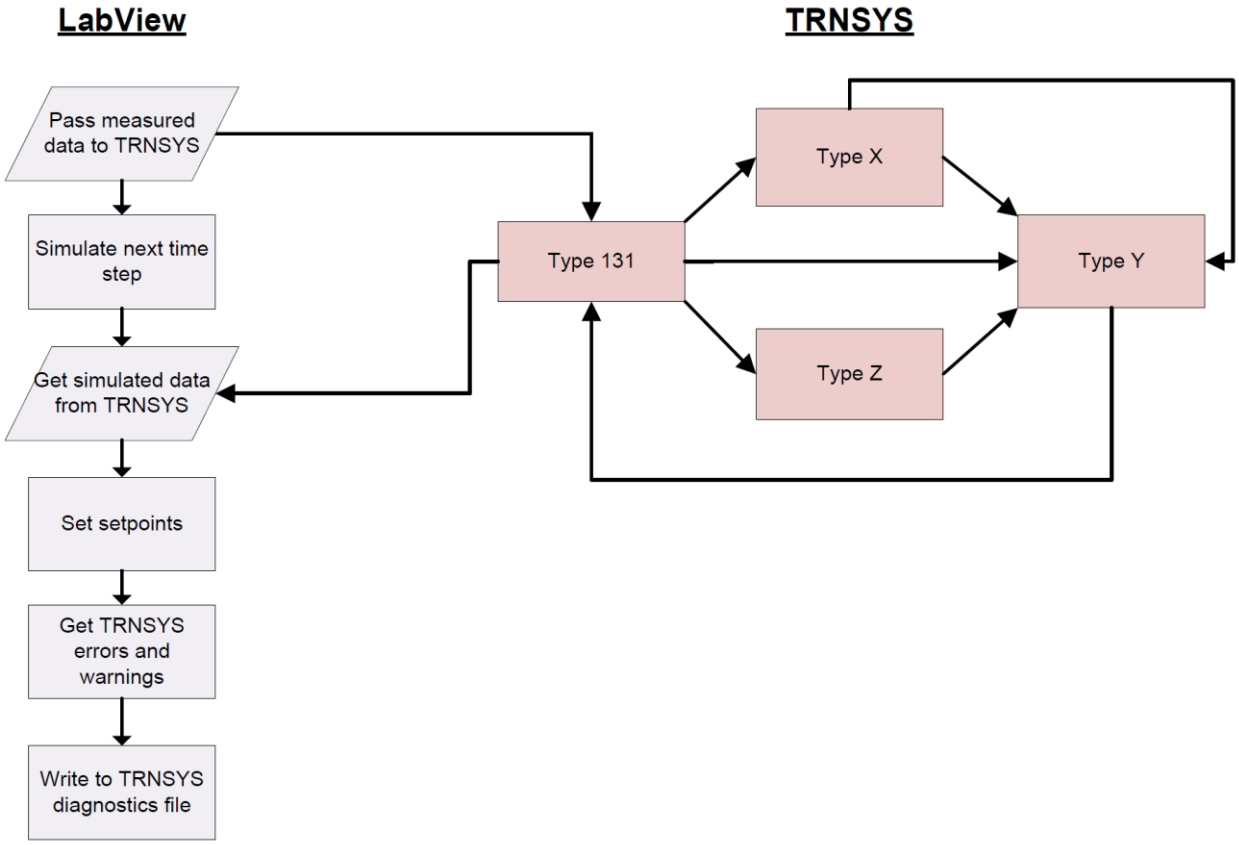

Figure 53: Principle of the LabVIEW interaction with TRNSYS.

8.3.2. Experimental Study of a Phase-Change Material storage tank

This project aimed at designing a storage tank with Phase Change Materials (PCM) and to test it in realistic operating conditions (D'Avignon and Kummert, 2013; D'Avignon and Kummert, 2016). The first objective was to integrate the newly designed PCM tank into the lab and adapt the data

acquisition environment to allow its detailed monitoring. A first series of tests was performed using predefined procedures, therefore without using the communication with TRNSYS. But the dynamic capabilities of the Semi-Virtual Laboratory were used to impose changing conditions to the tank and fully validate its detailed model.

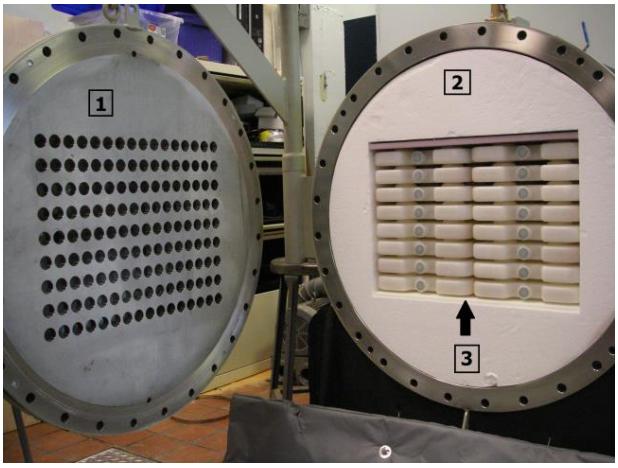

Figure 54: PCM tank viewed from the inlet, including 1) perforated plate, 2) capsule support and 3) PCM capsules.

Figure 55: Position of the instrumented PCM capsule in the tank as viewed from the outlet.

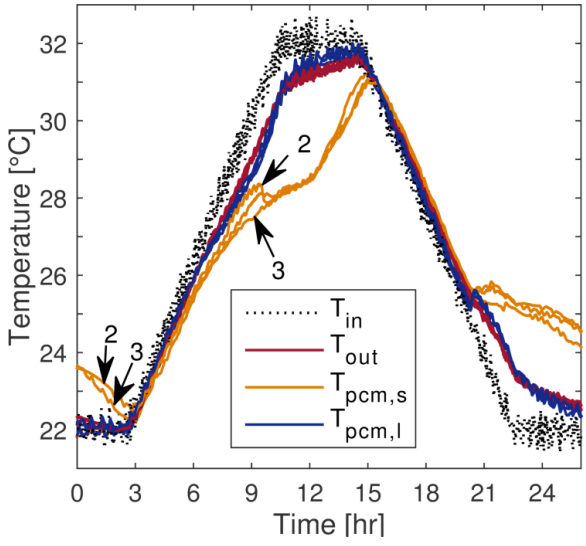

Figure 56: Example of results for a test with a fixed temperature change rate at the inlet of the tank.

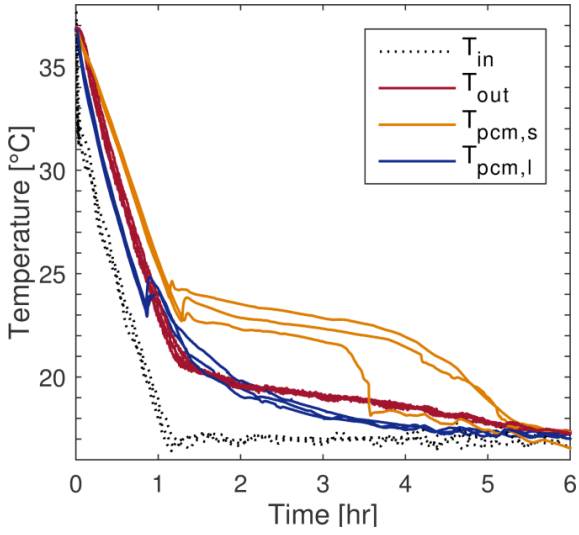

Figure 57: Example of results for a cooling step test.

Figure 54 to Figure 57 show the PCM tanks and some examples of results (Tin and Tout are the inlet and outlet temperatures of the tank, Tpcm,l and Tpcm,s are the PCM mass temperature at 2 different locations).

8.4. Test / experiment on energy flexibility

8.4.1. Objective

The PCM tank described above was tested in a semi-virtual environment. A TRNSYS simulation model was developed to represent a building with its heating system, consisting of decentralized heat pumps supplied by a warm water loop (see Figure 58). The warm water loop is heated by an electrical boiler and the PCM tank is piped in series with the boiler.

The simulation calculates the heating load on the water loop and simulates the boiler, and then imposes the inlet conditions to the PCM tank tested in the semi-virtual laboratory. The measured outlet conditions are then imposed on the simulation (as the supply temperature and flow rate to the building). The tested tank is relatively small, holding a total PCM mass of 185 kg, so the simulated building load was scaled down by artificially dividing the flow rate sent from the simulation to the laboratory. The experimental flow rate was set to 0.3 L/s for a peak heating load of about 4 kW. A steady-periodic simulation was performed, repeating a very cold day, which facilitated initializing the laboratory in the correct conditions. The boiler setpoint was set to 20°C in normal operation and 35°C when charging the tank, with a maximum power of 4 kW. These temperatures were selected to match the phase change temperature of the material within the tank (27°C with a relatively large hysteresis).

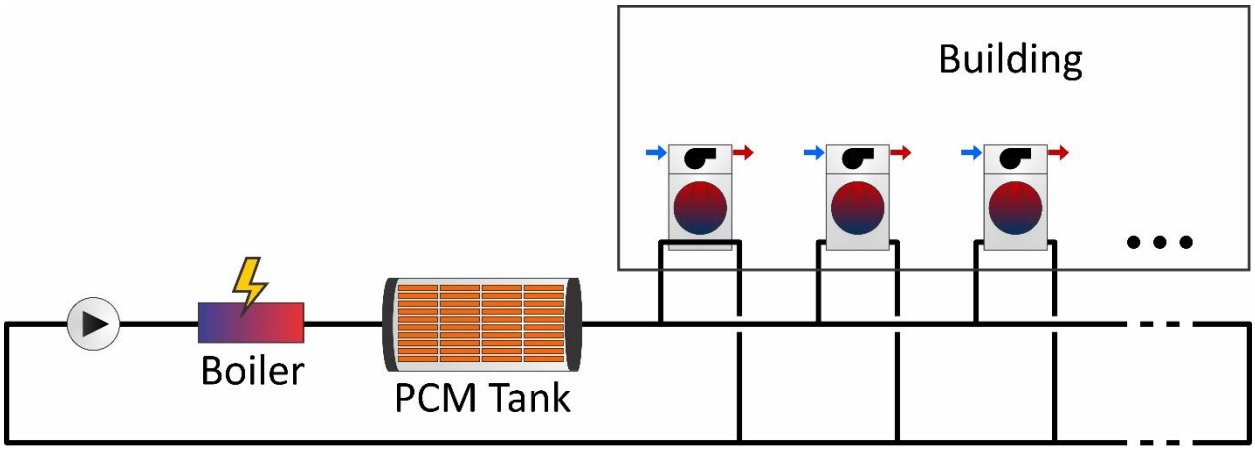

Figure 58: Simulated system for energy flexibility testing of a PCM tank in the semi-virtual lab.

8.4.2. Results

Figure 59 shows the reference system temperatures without PCM storage tank and applying a constant set point to the electrical boiler. The building set point, occupancy profile, and solar gains lead to a typical heating demand profile with a large morning peak. For the energy flexibility test, a downward flexibility event (i.e. an episode when electricity price or another penalty signal is

higher) is assumed from 5 AM to 9 AM (i.e. coincident with the morning peak in the reference profile).

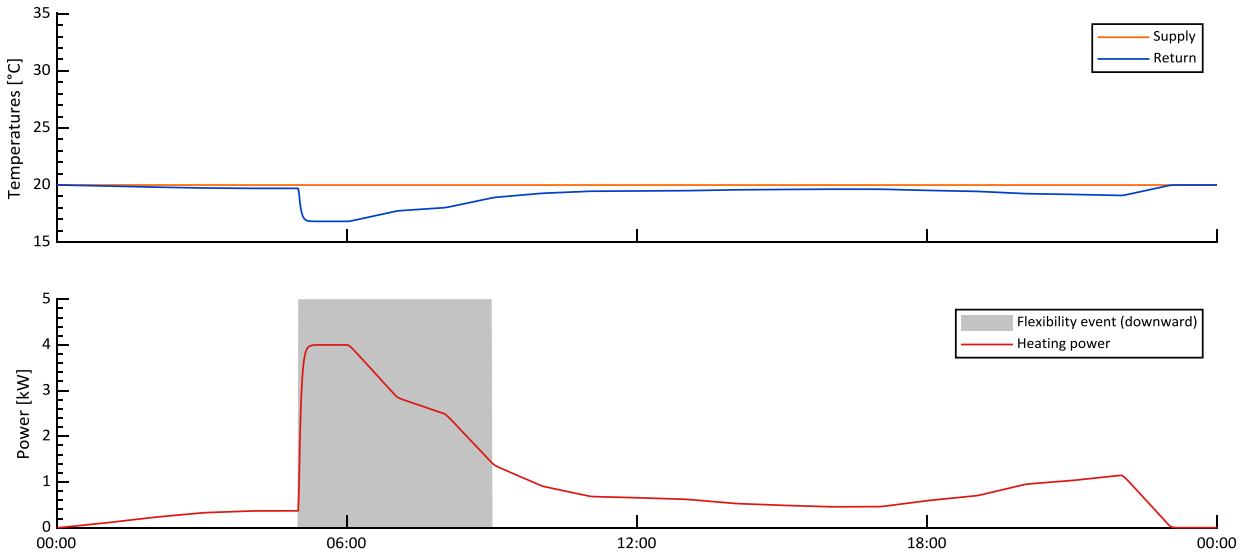

Figure 59: Heating power and temperature profiles for the reference scenario.

Figure 60 shows the temperature profiles and heating power with an energy flexibility strategy in place and with the PCM tank present in the system. The energy flexibility strategy consists in increasing the system set point to 35 °C before the downward flexibility event, in order to charge the PCM tank. The set point is returned to the normal value (20 °C) when the event starts and remains at that value until another “charging” episode occurs. In this simple test, a fixed preheating period of 5 hours (from 0:00 to 5:00) is assumed. The set point is raised to 35 °C but the PCM outlet temperature does not reach this temperature because of the limited boiler power (apparent for the first hour) and of the limited heat transfer rate to the PCM (apparent from 1:00 to 5:00, when the tank outlet temperature slowly increases but never reaches the inlet temperature). When the flexibility event starts, the tank is discharged and provides the full heating load for almost exactly one hour, but after that the limited heat transfer rate from the solidifying PCM results in some auxiliary heating being required. PCM discharging continues after the flexibility event and is still apparent at the end of the day, although with a smaller impact. This illustrates that in this particular case the limited heat transfer rate in the tank leads to a suboptimal response – if all the stored energy was recovered over the 4-hour flexibility event, the flexible energy would be higher.

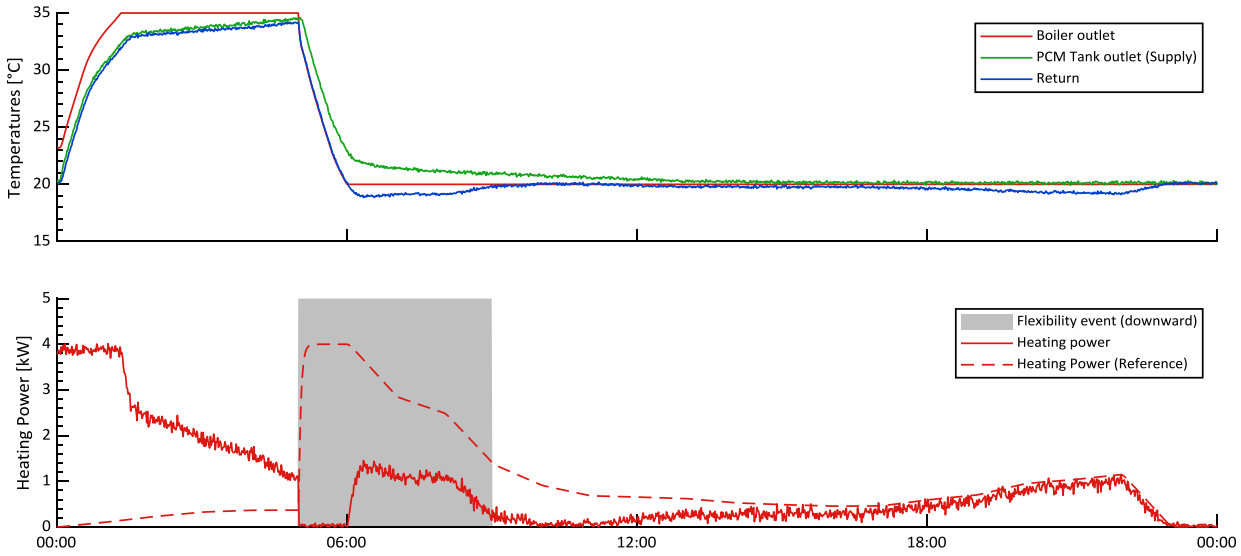

Figure 60: Heating power and temperature profile for the flexible scenario.

Figure 61 shows the flexible power. The positive value before 5 AM corresponds to a “prebound”, i.e. a rebound effect that occurs before the event because we assume a (simple) predictive control strategy. The negative values after 5 AM show the desired response to a downward flexibility event, although the useful flexible energy (occurring between 5 AM and 9 AM) is reduced by the limited heat transfer rate. The flexible energy (green area) is 12 kWh, of which 9 kWh are actually available during the event. The “rebound” energy (which actually happens before the event in this case: “prebound”) is around 12 kWh.

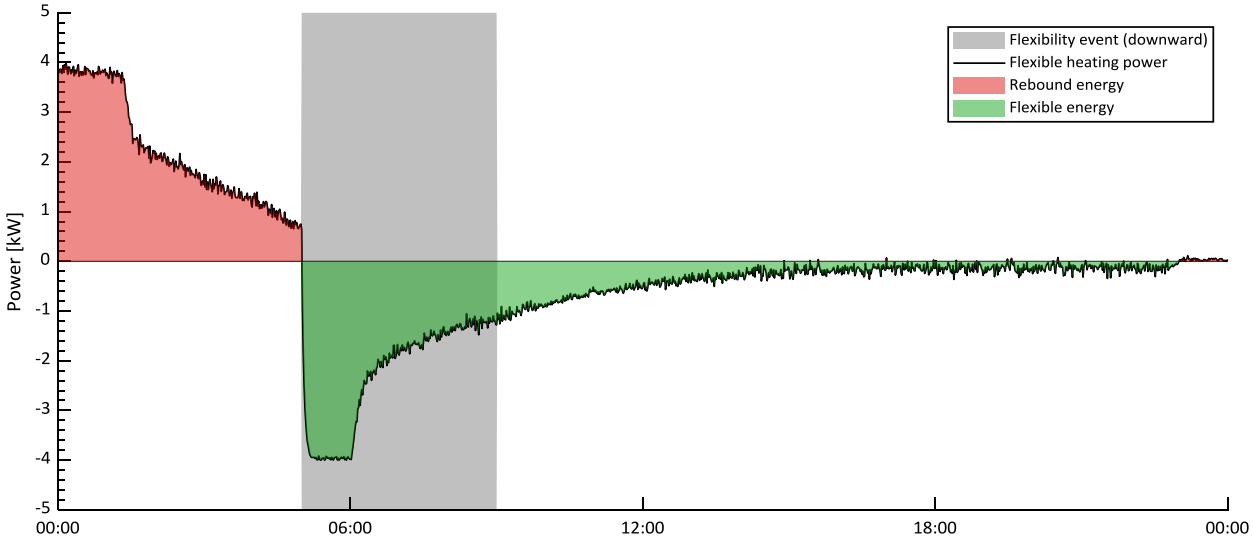

Figure 61: Flexible power and energy.

More details on the experimental tests and models are available in (D'avignon, 2015) and (Lessard, 2016). The Semi-Virtual environment allowed to further validate the developed model component in TRNSYS and demonstrate the usefulness of the laboratory to assess the storage tank behaviour in realistic operating conditions.

8.4.3. Lessons learned

Usefulness and design of the laboratory

The Polytechnique Montréal Semi-Virtual Lab was designed to perform hardware-in-the-loop tests of passive (e.g. storage tanks) and active (e.g. heat pumps) components.

One of the lessons learned is that a high flexibility (in the sense of offering many testing configurations) has a high price in terms of simplicity and robustness. The highly flexible configuration makes it more difficult to take care of practical aspects like maximum operating pressure, working fluids separation (e.g. glycol vs water). Although the auxiliary loops were designed to be fully exchangeable, only one configuration was used, so that several connections and 3-way valves were in fact never operated (but did present a challenge for fluid isolation and pressure levels, as pressure drops change dramatically with the configuration). The desire to allow testing small commercial equipment up to 100 kW also resulted in relatively large pipes, valves and heat exchangers, leading to control difficulties described in the next section when smaller component (sized for residential applications) were tested.

In the case of novel equipment such as the tested PCM tank, we also learned that conventional testing (with predefined set points, step responses, ramps, etc.) is necessary to understand how the component responds and develop/calibrate models, before moving on to the semi-virtual testing phase. A good semi-virtual testing laboratory should first be a good conventional testing laboratory.

The electrical side was given relatively little consideration during the design phase, focusing on power and voltage measurements. It is therefore not possible to assess the impact of the simulated component on the grid itself (e.g. voltage implications of a heat pump starting up).

Controllability

The simulated system is replaced with heat exchangers controlled by relatively simple PID controllers, and it proved difficult to avoid oscillations in the imposed inlet conditions, especially when the thermal load to be imposed was small. The 3-way valves have a large response time and the thermal mass of the heat exchangers often resulted in PID's overshooting and then oscillating. When only one connection was used, a workaround was to create a "ghost" thermal load and compensate it with the other heat exchanger, but this is not applicable when 2 connection ports are used, such as for heat pump testing. Real building systems often have a very large thermal mass and transport delays, so they do in fact oscillate and often have relatively

broad set point dead-bands, so typical hardware (e.g. control valves) are not necessarily “fast-acting” in a scientific testing context (even when so-called “fast-acting”).

Software maintenance

The semi-virtual environment combines the complexity of a data acquisition software (LabVIEW) with an energy simulation program (TRNSYS). Once a working configuration has been obtained, a “fear of touching the program” seems to be inevitable. This leads to skipping software upgrades, and can easily result in software issues (compatibility, unsupported software). The effort in maintaining the software environment was higher than anticipated, and certainly higher than the effort in maintaining the laboratory hardware.

The software complexity also increased the typical problem in a university context where there is a need for know-how transfer between successive students. The laboratory is a complex hydronic system to operate, and is controlled by a complex software program, which means that a considerable time investment is required to train incoming students.

9. Learnings and recommendations

9.1. Comparison of the different experimental studies

This report presents different experimental facilities and specific experiments that were performed at laboratory scale to assess how energy flexibility can be activated in buildings. The construction of these facilities has been motivated by the fact that energy flexibility strategies, usually developed through simulations, needs to be validated through test under dynamic, real (or as close as possible to real) operating conditions. This collection of laboratories represents therefore a necessary tool where researchers and industry can test, under controlled conditions, the performance of newly proposed systems before they are implemented in real buildings and/or field tests. Compared to field testing, dynamic tests in a controlled laboratory environment with a semi-virtual approach offer the flexibility of imposing well-controlled and repeatable boundary conditions on the equipment, without waiting for given conditions to occur in the real world. The same system can be tested in different environment (e.g. connected to different building types, or exposed to different climatic conditions) quickly by reconfiguring the simulation of the virtual parts. Unwanted interferences (e.g. from users) can be avoided and the accuracy of measured data is generally better in a controlled laboratory than in a field study. Of course, field tests are still necessary for a complete performance assessment, but semi-virtual testing allows going further than conventional lab tests at a fraction of the cost of a pilot project.

A common characteristic of typical tests in all the labs presented is that the experiments are short tests lasting from days to one-two weeks. Five of the six facilities presented in the report are conceived under the semi-virtual concept: this means that there is a dynamic interaction of some real devices (heat pumps, batteries, storage tanks, PV system, etc.) with a virtual building and/or additional parts of the system. The continuous dynamic interaction between the “real” part of the system and the “virtual” part is done based on the Hardware-in-the-loop (HiL) concept with a frequency of 1-6 minutes. In addition to predefined operating conditions (constant inputs, ramps, etc.), HiL allows testing realistic operating sequences imposed by the virtual building being tested, and the behavior of local controllers can be assessed at the same time as the performance of the equipment. The test facility consists of separate hardware and software parts that can be modified or updated separately, offering a wider range of experimental configurations. Related to the overall control of the test facilities, four out of the six laboratories described in the reports use LabVIEW as flexible high level interface.

The aim of two experiments carried out in two labs (the OPSYS test rig at DTI and the semi-virtual laboratory at PLYMTL) is to quantify the amount of energy flexibility can be derived from a building and a PCM tank respectively, comparing the performance of the system between a reference case and a case when energy flexibility is activated. The three experiments carried out in FHNW, Aalto and IREC aim to test how a certain flexible system behaves with an advanced control/management system in order to increase self-consumption or minimize energy costs or

CO_2 emissions in comparison with a reference case when energy flexibility is not activated. The facility which differs from the previous common approach is the ZEB Living Laboratory (see chapter 6) which is a real single family house with a heated floor area of approximately 100 m^2. However, the ZEB Living lab has the common characteristic with the others that it can be managed and be forced to act under pre-defined conditions, implemented in the controller of the building, for periods of time when tests are carried out. This of course excludes the outdoor boundary conditions, which are not controllable. Furthermore, the house can also be run in a "fully virtual" mode (i.e. mimicking the presence of users even if no one is really in the building). This is the case of the performed tests aimed at calibrating first-order reduced building models, which is a key aspect in the use of MPC to enhance energy flexibility in buildings. A distinctive aspect of ZEB Living Laboratory at NTNU/SINTEF is that allows studies of comfort perception and users flexibility acceptance when experiments with persons were designed. As a summary, Table 8 compares the main objective of the experiments developed in each of the labs, with the real elements controlled in the system and the length of the experiments which usually involves some warming-up days.

Table 8: Comparison between experiments on energy flexibility in the different labs.

Lab	Main objective	Real controlled devices	Activated flexibility sources	Test length
IREC	Test MPC strategies to minimize energy costs or CO_2 emissions	Heat Pump	Building thermal mass DHW water tank	4 - 5 days
Aalto	Test EMS to minimize energy costs in a NZEB	Battery Heat Pump Electric heater in tank	Battery DHW water tank	1 week
DTI	Quantification of energy flexibility and validation of simulation tool	Heat Pump Thermostat (Sim)	Building thermal mass	1 - 2 weeks
NTNU/SINTEF	Parameter identification of a building control oriented model	Single electrical emitter following PRBS	Building thermal mass	6 - 11 days
FHNW	Test EMS to increase PV self-consumption	Battery Heat Pump	Battery DHW water tank	4 days
POLYMTL	Quantification of energy flexibility	PCM tank	PCM tank	3 - 4 days

9.2. Recommendations for experimental tests on energy flexibility

In each of the previous chapters a section explaining the lessons learnt in each facility when developing experiments to investigate energy flexibility can be found. The take-home lessons derived are specific for each test and laboratory but quite a few common points exists as the laboratories have a common approach and the performed tests have strong similarities. A collaborative work among the researchers and the operators in charge of all the laboratories has lead to extract a set of practical reccommendations when planning or executing experiments with the objective to test energy flexibility in buildings. In addition, some reflections on more general aspects related to the planning and maintenance of the laboratories are also reported below.

9.2.1. Best practices for experiments

Experiments for testing energy flexibility are complex experiments that require close and dynamic interaction between the "real" hardware elements and the simulation of "virtual" elements. The lab setup not only involves the interaction of several hardware elements with the data acquisition, control and data storage system (i.e. LabVIEW), but also the data exchange and communication between different simulation environments (i.e. IDA-ICE, Modelica or TRNSYS), hardware/data acquisition and even control systems running on different platforms (i.e., embedded PLC or Matlab). Energy flexibility tests based on semi-virtual test rigs thus present an additional complexity in terms of the general software tools capable of handling not only all the hydronic and electrical systems, but also the different and specific software environments necessary to control the different elements of the test rig.

Planning and preparing the experiment

- Plan the length of the experiment carefully. The minimum duration is imposed by the time constant of the tested systems, and in the reported tests it amounted to a few days (3 - 4 days) including a pre-conditioning period to place the system in the desired initial conditions, especially when storage elements or high inertial systems are included in the test. Testing MPCs can require a longer test period depending on the prediction horizon. It is not recommended to extend the test duration much beyond the required length according to the objectives, thermal mass, and control horizon, in order to limit the time effort and reduce the likeliness of unwanted disturbances (hardware or software problems, loss of communication between elements, etc). Several problems can appear during the experiments due the complexity of hardware and software pieces and their intercommunication. Plan the tests as short as possible, while focusing on the scope and expected results, without jeopardizing its usefulness and objective.
- Evaluate whether or not experiments should be compared with a reference case. If yes, an experiment will often consist of at least two tests: one reference case and the case when energy flexibility is activated.

- The real and virtual components of the system should be chosen according to the goals of the test and kept the same for all tests composing an experiment. Modifying some aspects of the platforms during the course of a set of experiments can make difficult, if not impossible, to compare them.
- It is recommended not only to develop the numerical model of the virtual part of the test bed, but also to complete with a model of the real part of the system (even if this is simplified). This allows having a "digital twin" of the complete system, which is extremely useful to select representative test periods or to fine-tune important parameters of the experiment prior to the run of the tests. The model is also typically used to warm-up the simulation before the start of the actual testing period.
- Before starting a test period all the components of the system should be examined and debugged to minimize the potential for issues occurring during the actual test. Partial short tests on each subsystem are recommended before the complete experimental run takes place.
- Measure all the important values with a sufficient time resolution and accuracy. This is important for both the evaluation of the results from the hardware in the loop test and for a thorough comparison between measured and simulated results. Define and set control probes, and also consider to add additional sensors and/or double measurement of critical variables as they will help you to control if the experiments are running as they should.
- Check the stability and accuracy of the boundary conditions for the emulated variables (temperatures, flows, etc.) and fine-tune the control elements in the facility (i.e., PID) for a specific experiment, if needed.
- To evaluate the advantage gained when using a MPC, the results can be compared with implementing other simpler controller in the simulation (e.g. compare with a rule-based controller).

During the experiment

- It is important to monitor the tests very closely in order to quickly detect and correct any problems. This will prevent that valuable time is lost due to an otherwise necessary restart of a test. Regular visits to the lab and/or remote monitoring during tests and preliminary analysis of the results (at least daily) are strongly recommended.
- Enable remote visualisation (and if possible, control) of the main variables of the experiment from your office desk. When possible establish surveillance values to watch and alarms (e.g. e-mail messages) to warn the operator/researcher in case of anomalies.
- Perform a comprehensive check of the experiment during the first hours and react accordingly. Malfunctions can usually be detected at the very early stages of the experimental run.
- If a pre-warming method/period has been established to bring the storage elements (batteries, thermal storage) to a certain level of charge, check carefully that the initial conditions are reached. The same recommendation applies to for the virtual/simulated part of the system.

After the experiment

- Often, the aim of the experiment will be to develop or refine a model of the system being tested, so that other operating conditions can be assessed in simulation. In that case, the model should be carefully calibrated based on experimental results and its range of validity should be clearly assessed. This is not an easy task and it is advisable to plan enough time for that task after the tests are completed.
- Be sure to carefully record and document any permanent change done in the test rigs during the test and/or its preparation. Additionally, write down the lessons learnt when it comes to running of a test, so they will stay in the memory of the research group.
- Store the collected data and metadata in a structured repository, so they can used for further analysis. Consider to store in an open access repository to be shared with other researchers.

9.2.2. Best practices for test facilities

Laboratories presented here are among the first world-class facilities for allowing investigation of energy flexibility in buildings. They were designed as flexible facilities to test new components and their integration and management involving electrical and thermal systems. Five of the six laboratories presented here have the common feature that they can interact with at least a virtual building model and virtual weather conditions, greatly expanding their flexibility and the range of testing conditions they can provide. This potential comes hand in hand with a large complexity due to the hardware and software elements that need to be in place. Practical advices when designing or maintaining this kind of test facilities are:

- Look for a trade-off between flexibility of the elements in the lab and increased complexity according to the overall goals of the facility.
- Always calibrate and verify sensors and the entire acquisition chain thoroughly. A practical but effective approach is to acquire multiple values for the same physical quantity, especially for the important measured values during a test.
- Consider characterizing the elements and systems first in steady-state or predefined conditions before launching flexibility experiments. This provides a greater insight into the behaviour of the elements/systems and increases their controllability.
- As complex software environment is a key part of this type of test facilities, maintenance (software updates, etc.) and documentation, especially targeting new researchers, should be prioritized. Do not minimize the effort devoted to these tasks.

10. Acknowledgements

The authors of the report want to thank Hicham Johra, from the University of Aalborg (Denmark), and Roberto Lollini, from EURAC (Italy) the time they have dedicated for its extensive and exhaustive review.

The work conducted on the OPSYS test rig described in chapter 5 was financially supported by the Danish Energy Agency via the funding program EUDP under the contracts: 64014-0548 and 64014-0573.

The work conducted at Aalto University was partly funded by the Academy of Finland project “Advanced Energy Matching for Zero-Energy Buildings in Future Smart Hybrid Networks 2014-2018, decision no. 277680”.

The research conducted in IREC’s laboratory has received funding from the European Union’s Horizon 2020 research and innovation program under the Marie Skłodowska-Curie grant agreement No 675318 (INCITE). Dr. Jaume Salom acknowledge the financial support of the Ministry of Economy and Competitiveness of Spain under the GEIDI project (ref. TIN2016-78473-631 C3-3-R).

The ZEB Living Laboratory at NTNU/SINTEF has been developed by the Research Centre on Zero Emission Buildings (ZEB). Research activities carried out with this facilities have been carried out under the funding of the Research Centre on Zero Emission Buildings (ZEB) and the Research Centre on Zero Emission Neighbourhoods in Smart Cities (ZEN). The author from NTNU gratefully acknowledges the support from the ZEB/ZEN partners and the Research Council of Norway, and the other researchers involved in the activities reported in this manuscript: Pierre Vogler-Finck, Laurent Georges, Maria Justo Alonso, Ruth Woods, Kang Wen, Fredrik Håheim, Peng Liu, Magnar Berge, Martin Thalfeldt, Martin, Gabriele Lobaccaro, Arild Gustavsen, and John Clauß.

The SemiVirtual Laboratory at Polytechnique Montréal was funded by the Canada Foundation for Innovation (CFI), Leaders Opportunity Fund, Grant No 27766. Research projects were partly funded by the Natural Sciences and Engineering Research Council of Canada (NSERC), through Prof. Kummert's Discovery Grant RGPIN-2016-06643.

The research at the Energy Research Lab of the FHNW was supported financially by the Swiss Federal Office of Energy under the contract numbers: SI/501141 and SI/501240.

11.References

Bosch, 2017. http://dk.documents.bosch-climate.com/download/pdf/file/6720813696.pdf

Clauß, John; Vogler-Finck, Pierre JC; Georges, Laurent . 2018. Calibration of a high-resolution dynamic model for detailed investigation of the energy flexibility of a zero emission residential building. Proceedings of the Cold Climate HVAC Conference 2018, Kiruna (Sweden)

D'Avignon, K. and Kummert, M., 2013. 'Comparison of system-level simulation and detailed models For storage tanks with phase change materials', in Proceedings of Building Simulation 2013:13th Conference of International Building Performance Simulation Association, Chambéry, FRA, August 26-28, pp. 2940–2948.

D'Avignon, K. and Kummert, M., 2016. 'Experimental assessment of a phase change material storage tank', Applied Thermal Engineering, 99, pp. 880–891. doi: 10.1016/j.applthermaleng.2016.01.083.

D'Avignon, K., 2015. 'Modeling and experimental validation of the performance of phase change material storage tanks in buildings'. PhD thesis, Montréal, QC, CAN: Polytechnique Montréal, Dept. of Mechanical Engineering.

Dott, R, Ackermann, C, Koch, M, Messmer, C, Afjei, T & Eismann, R, 2018. LEWASEF: Leistungsgeregelte Wärmepumpenanlagen mit Solar-Eisspeicher und Fotovoltaik, Swiss Federal Office of Energy SFOE

Dott, R, Afjei, T, Winteler, C & Genkinger, A, 2016. SOFOWA: Kombination von Solarthermie, Fotovoltaik, Wärmepumpen und Eisspeicher, Swiss Federal Office of Energy SFOE

Finck, C, Beagon, P, Clauss, J, Péan, T, Vogler-Finck, P, Zhang, K, Kazami, H, 2018. Review of applied and test control possibilities for energy flexibility in buildings, techincal report IEA EBC Annex 67

Georges, Laurent; Justo Alonso, Maria; Woods, Ruth; Wen, Kang; Håheim, Fredrik; Liu, Peng; Berge, Magnar; Thalfeldt, Martin. 2017. Evaluation of Simplified Space-Heating Hydronic Distribution for Norwegian Passive Houses, ZEB Project report 39– 2017, ISBN 978-82-536-1558-5 (pdf)

Goia, Francesco; Finocchiaro, Luca; Gustavsen, Arild, 2015. The ZEB Living Laboratory at the Norwegian University of Science and Techonology: a zero emission house for engineering and social science experiments. Proceedings of 7PHN Sustainable Cities and Buildings. 21-21 Aug 2015, Copenhagen (Denmark).

Goia, Francesco; Gustavsen, Arild, 2017. Energy performance assessment of a semi-integrated PV system in a zero emission building through the periodic linear regression method. Proceedings

of NSB 2017 – The 11th Nordic Symposium on Building Physics. 11-14 June 2017, Trondheim (Norway).

Jensen et al, 2018. “Combined optimization of heat pumps and heat emitting systems". Danish Technological Institute and Aalborg University. May 2018. www.teknologisk.dk/39663

Kilpeläinen S, Delgado BM, Ruusu R, Hasan A., 2019. Real-time Optimization of Energy Flows in a Semi-virtual Nearly Zero-energy Building Emulator. The 9th International Conference on Sustainable Development in the Building and Environment (SuDBE2019). July 22nd-24th, University of Reading, Reading, UK.

Kilpeläinen S, Lu M, Cao S, Hasan A and Chen S., 2018. Composition and Operation of a Semi-Virtual Renewable Energy-based Building Emulator. Future Cities and Environment, 4(1): 1, pp. 1–14.

Kim, Y.J., Fuentes, E., and Norford, L.K., 2016. “Experimental Study of Grid Frequency Regulation Ancillary Service of a Variable Speed Heat Pump.” IEEE Transactions on Power Systems 31(4):3090–99.

Lessard, D. 2016. ‘Essais du Laboratoire Semi-Virtuel ‘d’Éqiupements CVAC’. MEng thesis, Montréal, QC, CAN: Polytechnique Montréal, Dept. of Mechanical Engineering.

Lobaccaro, Gabirele; Esposito, Simona; Goia, Francesco; Perino, Marco. 2017. Daylighting availability in a living laboratory single family house and implication on electric lighting energy demand. Proceedings of CISBAT 2017 - International conference on Future Buildings & Districts – Energy Efficiency From Nano to Urban Scale. 6-7 Sep. 2017, Lausanne (Switzerland).

Lu M, Kilpeläinen S, Cao S, Hasan A, Chen S., 2017. Performance Analysis of a Semi-Virtual Renewable Energy System and Building Operation. SET 2017 International Conference, Bologna, Italy, July 2017.

Macdonald, F., D’Avignon, K., Kummert, M. and Daoud, A., 2014. ‘A TRNSYS-LabVIEW bi-directional connection for HVAC equipment testing using hardware-in-the-loop simulation’, in Proceedings of SSB 2014: the 9th International Conference on System Simulation in Buildings, Dec 10-12. Liège, BEL, p. P65.1-P65.15.

Péan, T. and Salom, J, 2019, Laboratory facilities used to test energy flexibility in buildings, Catalonia Institute for Energy Research, IREC, Spain, 2nd Edtion, http://www.annex67.org/media/1708/laboratory-facilities-used-to-test-energy-flexibility-in-buildings-2nd-edition.pdf

Péan, T., Costa-Castelló, R., Fuentes, E., and Salom, J., 2019. "Experimental Testing of Variable Speed Heat Pump Control Strategies for Enhancing Energy Flexibility in Buildings," in *IEEE Access*, vol. 7, pp. 37071-37087. doi: 10.1109/ACCESS.2019.2903084

Pflugradt, N, 2015. LoadProfileGenerator, available at https://www.loadprofilegenerator.de/

Poulsen et al, 2017. The good installation of heat pumps (in Danish). Danish Technological Institute and Insero. 2nd edition. January 2017. www.teknologisk.dk/39663

Ruusu R. Cao S, Delgado BM, Hasan A., 2019. Direct quantification of multiple-source energy flexibility in a residential building using a new model predictive high-level controller. Energy Conversion and Management 180, 1109–1128.

Vogler-Finck, Pierre JC; Clauß, John; Georges, Laurent. 2017. A dataset to support dynamical modelling of the thermal dynamics of a super-insulated building. https://doi.org/10.5281/zenodo.1034819

Vogler-Finck, Pierre JC; Clauß, John; Georges, Laurent; Sartori, Igor; Wisniewski, Rafael. 2018 Inverse model identification of the thermal dynamics of a Norwegian zero emission house. Proceedings of the Cold Climate HVAC Conference 2018, Kiruna (Sweden).

Waddicor, D.A., Fuentes, E., Azar, M., Salom, J., 2016. "Partial Load Efficiency Degradation of a Water-to-Water Heat Pump under Fixed Set-Point Control." Applied Thermal Engineering 106:275–85. http://dx.doi.org/10.1016/j.applthermaleng.2016.05.193.

Woods, Ruth; Berker, Thomas; Korsnes, Marius. 2016. Making a home in Living Lab: the limitations and potentials associated with living in a research laboratory. Proceedings of the Demand Centre Conference 2016

www.iea-ebc.org

EBC

Energy in Buildings and Communities Programme